**Scuola Dottorale di Ateneo**
**Graduate School**

**Dottorato di ricerca**
**in Scienze e Gestione dei Cambiamenti Climatici**
**Ciclo 28**
**Anno di discussione 2015**

# *Impacts of global environmental changes on water: challenges for sustainable development*

**SETTORE SCIENTIFICO DISCIPLINARE DI AFFERENZA: AGR/02; SPS/10**
**Tesi di Dottorato di Fabio Farinosi, matricola 818050**

**Coordinatore del Dottorato**

**Prof. Carlo Barbante**

**Tutore del Dottorando**

**Prof. Carlo Giupponi**


**Co-tutori del Dottorando**

**Prof. Paul Moorcroft**
**Prof. Ian Sue Wing**
**Dr. Enrica De Cian**

# About the author

Fabio Farinosi is an environmental economist by training and a researcher in the fields of disaster risk reduction, climate change adaptation and mitigation strategies, and natural resource management. In the last few years, he has been involved in research projects about natural hazards impact assessment, integrated water resource management risk analysis, policy assessment and implementation. He worked as researcher at the Fondazione ENI Enrico Mattei and the Euro-Mediterranean Center for Climate Change. There, he was involved in several research projects including natural hazard risk and impact analysis, policy assessment and implementation, water management, and analysis of climate change adaptation strategies. Among the other experiences abroad, he spent a semester at the United Nations Environment Program - Regional Resource Centre for Asia and the Pacific in Bangkok, Thailand, where he carried out a study on community driven rural development and community based adaptation to climate change in Thailand.

In 2012, he joined the Science and Management of Climate Change PhD Program at the Ca' Foscari University of Venice under the supervision of Professor Carlo Giupponi. Fabio conducted part of the research leading to this dissertation as Giorgio Ruffolo Doctoral Research Fellow in the Sustainability Science Program at the Harvard University, where he collaborated with the initiative Sustainable Development in Amazonia: Land Use and the Hydrologic Cycle led by Professors Paul Moorcroft and John Briscoe. His dissertation focuses on the impacts of human induced environmental changes on water resources.

# *Impacts of global environmental changes on water: challenges for sustainable development*

*Fabio Farinosi*

# Acknowledgements

# Table of Contents

# List of figures

# List of tables

# Summary

This research aims to understand how human driven global environmental changes in terms of climate and land use are expected to affect the spatial and temporal distribution of water resources. The main questions that this thesis asks are: (1) how are global climate and land use change expected to impact the spatial and temporal distribution of the water resources, (2) how are human activities like hydropower and agricultural production likely to be impacted by global environmental changes, and (3) how can different socio-environmental systems be adapted to the changing conditions. The thesis is organized in a set of studies aimed at estimating the main practical consequences in terms of hydropower and agricultural production at different geographical scales. It does so by applying the most appropriate statistical or physical modeling tool to a series of case studies. A statistical model is utilized to assess the sensitivity of the global hydropower generation to variations in climate. A biosphere model integrated with a routing scheme is used to assess the impacts of climate and land use change on the hydrology of the Tapajos river basin, a portion of the Brazilian Amazon. A hydro-energy model is used to assess the possible implications of planned hydropower development in the river system. A crop model is used to analyze the expected impacts to agricultural productivity in the upper part of the Tapajos basin, one of the most important areas for this economic sector in Brazil. Results show how the global hydropower system is expected to be vulnerable to global changes with specific magnitudes linked to the spatial distribution of climate change and the specific characteristics of the power plants. The Tapajos river basin hydrology is expected to be seriously impacted by climate change, mainly through a delay in the beginning of the rainy season and a reduction of its duration. Land use change, specifically deforestation, is expected to partially offset the decreasing trends in river discharge caused by climate change, but at the same time to cause a consistent increase in flow variability. Moreover, the crop analysis confirmed the expected negative climate change

impacts on the agricultural sector in the upper part of the basin, creating the basis for a possible demand for irrigation: an adaptation strategy destined to increase the anthropogenic pressure on the water resources in the area. The project aims to provide policy makers with a better understanding of the expected future impacts and to enhance long-term adaptation strategies. The global hydropower analysis gives an idea of the patterns of vulnerability of this system of production. The basin scale analysis shows how the river flow could be modified by the combined effects of climate, land use change and alternative uses water demand. This confirms that an increasing level of uncertainty should be taken into consideration in case of infrastructural development in the area. This thesis provides a significant contribution to the debate about uncertainty and stationarity in water management. It proves, providing practical examples, how different socio-economic and ecological systems at different geographical scales are interconnected: the dynamics influencing one system affect, directly or indirectly, the connected systems causing a cascade effect. The thesis shows that accounting for the interconnections between water, food and energy production in the context of global environmental changes is necessary to achieve sustainable development.

# 1. Introduction

## 1.1. Motivation

Water, bloodstream of the planet, is considered the basis of nature and the living substance of the biosphere (Ripl 2003). The evolution of human history could be virtually identified with milestones progresses in water management. At first, humans prospered adapting to the spatial and temporal distribution of natural resources, mainly water (Ruddiman 2005). Then, starting from the middle Neolithic (10,200-3,300 BC), humankind developed strategies aimed at managing this important resource in order to meet the basic needs of water supply and food production. Ruddiman (2005) identified the discovery of irrigation as the main factor transforming nomad groups to stable and organized populations. Irrigation and agriculture, jointly with livestock production, are also identified as the first human modification on climate, with the first anthropogenic emissions of carbon dioxide and methane (Ruddiman 2005). All the greatest civilizations of the Bronze Age (3,300-1,200 BC) developed in the floodplains of large rivers: Mesopotamia in the Tigris-Euphrates system, name which in ancient Greek means "[land] between rivers" (*mesós*, "middle"; and *Potamoi*, "rivers"); Pharaonic Egypt in the Nile floodplain; The Harappan Civilization in the Indus-Ganges system; and the Chinese dynasties in the Yellow river floodplain. Recent studies (Langutt et al. 2013; Kaniewski et al. 2015) found evidence suggesting that the collapse of the biggest civilizations of the Minor Asia and North Africa (as for the Assyrian, Babylonian, Sumerian, Egyptian, and Akkadian) could have been driven by a series of intense drought events frequently occurring in a period of about 150 years around 1,200 BC. In addition, several other examples of how the fate of humans has always been linked to water

availability can be found in literature. For instance, Gleick et al. (1994; and 1998) offer a partial chronology of the conflicts related to water or having water management as military defense or offense strategy from 3,200 BC to date[1]. Climate variability and drought frequency are likely to have caused also the decline of the ancient Khmer empire between the 14th and 15th centuries (Buckley et al. 2010). Coming to more recent years, Werrell et al. (2013) linked the series of uprisings in 2011 turning upside-down the Middle Eastern and Northern African political establishment, generally called "Arab Spring", to the increasing food prices due to dryer conditions in the previous years. Correlations between changing climate conditions and the civil war in Syria were illustrated by Gleick (2014).

If it is certainly true, on the one hand, that water determines the human fate, it is also to be said that the anthropogenic activities are the main cause of impact on the water cycle. Vitousek (1997) offers a good representation of the interactions between human activities and the main biophysical processes (Figure 2-1). The consequences of these interactions are represented by modifications in the equilibrium of biophysical processes in direct or indirect response to human activities. Literature provides several examples of these interactions: Durack et al. (2012), for instance, used ocean observations to prove how in the period 1950-2000, could be highlighted a correlation between changes in climate and water cycle intensification rate. Another example is represented by infrastructural development. For instance, the installation of dams in unregulated rivers causes flow interruption as direct consequence (Liermann et al. 2012; Lehner et al. 2011). Indirectly, on the other hand, flow interruptions modify the sediment dynamics affecting river deltas and coastal areas (Syvitski et al. 2009; Syvitski 2005).

---

[1] A more updated list derived from the work of the same author is available at

http://www.oneonta.edu/faculty/allenth/WaterResourcesTracyAllen/Water%20Conflict%20Chronology.pdf
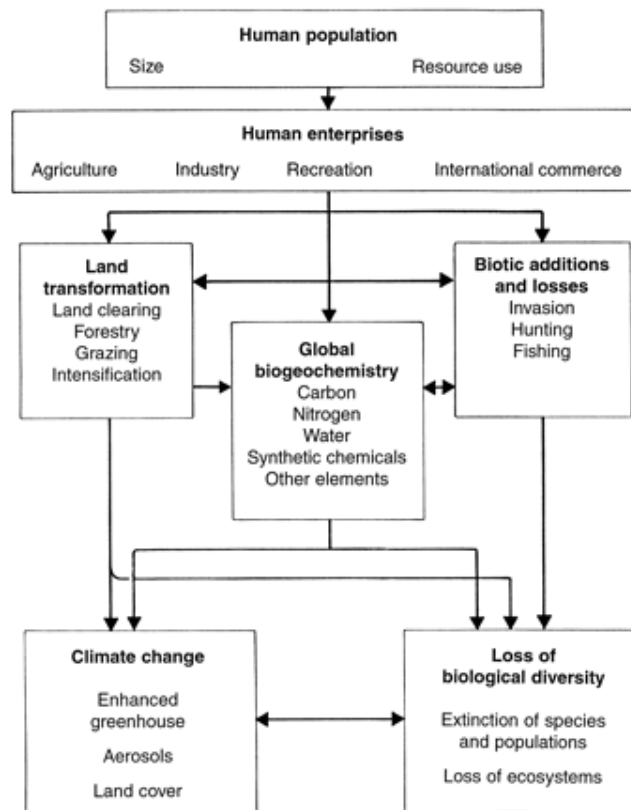
**Figure 2-1. Interactions between human activities and the Earth system (Vitousek 1997)**

Water flows through the center of the economy and humans well-being (SEI 2011). The contribution of water to food and energy production is remarkably important, to the point that water security is currently one of the main concerns in the discussions about climate change impacts, with water management being one of the biggest challenges for the XXI century (IPCC 2008; IPCC 2014). The impacts of climate change on the global spatial and temporal distribution of water resources is expected to be highly significant (IPCC 2012; IPCC 2014). The consequences of climate variations, in combination with the changes in land use and demography, are expected to substantially threaten water security, with tangible consequences for water supply and sanitation, health, food production, electricity generation, and extreme weather events (IPCC 2014). The global population, which was 7.2 billion in 2013, is expected to increase by more than 30%, reaching the threshold of 9.6 billion by 2050

(UN/DESA 2015). Considering that around 800 million people are actually in a condition of chronical undernourishment (FAO 2014), and 1.3 billion are without access to electricity (IEA 2013), nations around the world – in particular developing nations – will struggle to provide food and energy to more than 3 billion additional people in the coming decades. Hence, human pressure on water, vital element for food and energy production, is destined to rise significantly (McLaughlin & Kinzelbach 2015; IPCC 2014; Cosgrove & Loucks 2015). In particular, McLaughlin et al. (2015) estimated an increasing demand for cropland of about 30% by the year 2050 with respect to 2011, and a correspondent increase of green and blue water demand of about 60%. The increasing demand for water drives the increasing infrastructural development, vital strategy for achieving water security, especially in developing and least developed countries (Muller et al. 2015; Briscoe 2015). Grey et al (2006) analyzed the correlation between water insecurity and limitations in economic growth and development (Figure 2-2) showing how lack of water storage capacity affects the economic resilience of poor countries.
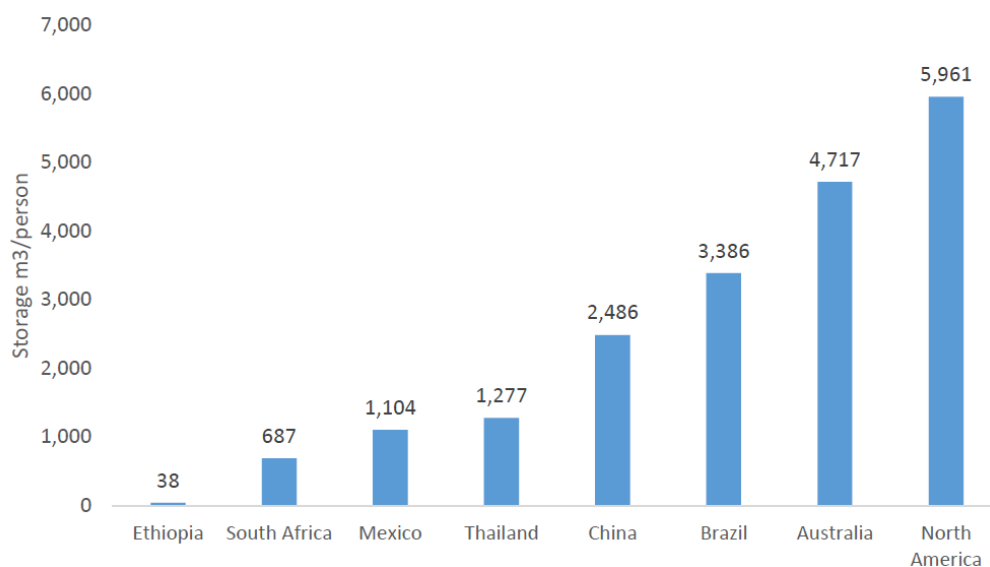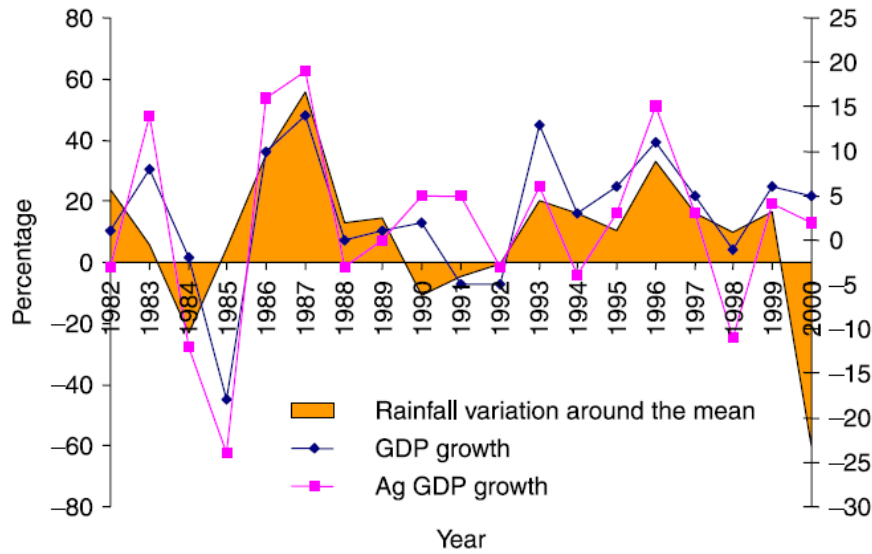
**Figure 2-2 Top: Reservoir storage per capita (m³/cap), 2003. Bottom: Rainfall, Gross Domestic Product (GDP) and Agricultural Gross Domestic Product (Ag GDP) growth for Ethiopia (Grey & Sadoff 2006).**

Water management around the world is highly depended upon large infrastructures, primarily reservoirs and dams, which aim at satisfying the multiple needs of water supply for urban and agricultural use, buffering the effects of drought/flooding, and generating electricity. The construction of infrastructures for water storage is extremely expensive, technically challenging, and severely impacting from a social and environmental point of view (WCD 2000). On the other hand, these infrastructures ensure continuous and reliable urban water supply, flood defense, and sustain the agricultural productivity (WCD 2000). Strobl et al. (2011) analyzed the distributional effects of large dams in Africa, concluding that about 12% of the calories consumed in the continent are produced through agriculture irrigated from large reservoirs. Moreover, dams are extremely important for navigation, recreational uses, and aquaculture (WCD 2000). Last but not least, flow regulation through dams and reservoirs allow the production of large amounts of electricity at a low marginal cost and, at least in the case of dams with large storage, available on demand (WCD 2000). As of 2012, hydropower produced about 16.9% of the total electricity worldwide (US EIA

2013). The International Energy Agency in the 2013 World Energy Outlook projected an increasing investment in hydropower by 2035 by more than 600 GW with respect to 2012 capacity (IEA - International Energy Agency 2013). Hydropower is expected to continue to be the largest source of renewable energy in the next two decades (Figure 2-3).
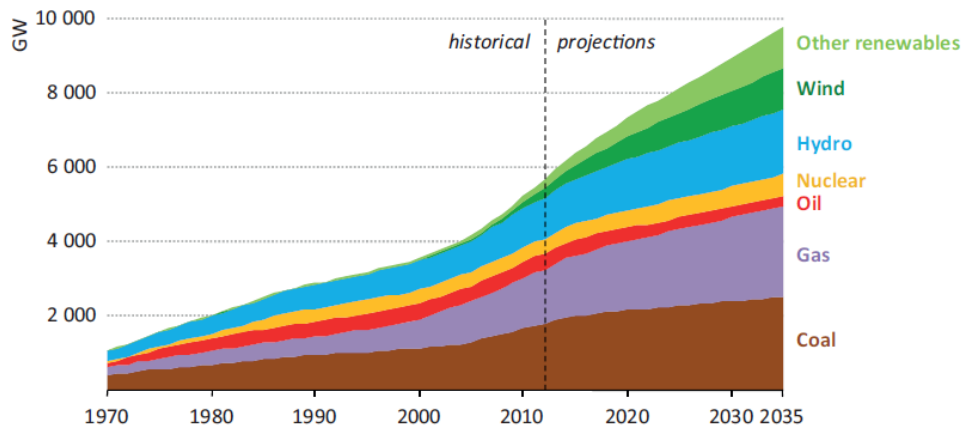
**Figure 2-3 Installed capacity by source, future scenario (IEA - International Energy Agency 2013).**

Although more than 50 per cent of the installed capacity is concentrated in only five countries – namely China, Brazil, United States, Canada and Russia – hydropower represents the main renewable source of electricity production for many countries in the world (US EIA 2013), representing the most important sector contributing to climate change mitigation in electricity production. Nowadays, the majority of new large projects in the implementation phase are located in developing countries, where the development of the hydropower sector is considered crucial to ensure cheap and reliable energy for emerging economies. This electricity production technology is one of the main pillars of the energy strategy of countries as China and Brazil for the next future (IEA - International Energy Agency 2013; EPE 2013). Despite the large mitigation potential hydropower has, this option is also strongly dependent on meteorological variability and climate trends. Growing concerns are animating the debate

about the vulnerability of hydropower technologies to climate change and the possibility for this important renewable source to sustain its future development (Mukheibir 2013). Moreover, the minimization of environmental and social impacts are driving the development of new projects towards the construction of reservoirs characterized by a relatively small size, a trend which is expected to significantly increase the vulnerability of the hydropower sector to climate change (IEA - International Energy Agency 2013). Highly controversial debates, in fact, surround the construction of new dams and hydropower plants in emerging economies where large rivers of high cultural and biological value have begun to be constructed. The social and environmental impacts of the new installation is quite significant and, very often, most feasible installation sites lay in areas extremely valuable for local communities and biodiversity. Local populations suffer for displacement, modification of the territory, loss of land, social structure disruption, and modification of the local ecosystem (Fleury & Almeida 2013). Emblematic is the recent case of Belo Monte in Brazil, where indigenous populations fiercely opposed to the construction of the dam in 2008. This protest resulted into violence bringing to the attack of the engineer responsible for the project, wounded with a machete[2]. Critics come from local populations, environmental activists and NGOs, but also from developed country, where the hydropower development was completed in the past century and there is no space for further profitable installations. An example of these critics could be found in an interesting conversation reported by the late Prof. John Briscoe (2014 Stockholm Water Prize Laureate):

*"You must understand", the Norwegian Minister of Development chided me "that Norway does not approve of the construction of dams". "But, Madam, your country was built on a platform of cheap and clean hydropower. You use 80% of your hydro potential, and you*

---

[2] http://arte.folha.uol.com.br/especiais/2013/12/16/belo-monte/en/

http://www.boston.com/bigpicture/2008/05/indigenous_brazilians_protest.html

*want Ethiopia, which has developed 1% of its hydro capacity, to forego a similar opportunity to develop?"* (Briscoe 2012).

The future of water management under a changing globe is bringing new challenges that require alternative and innovative scientific approaches. For instance, Vogel et al. (2015) proposed three alternatives for the future of water resource management: first, the urge of including the consideration of the coupled human-hydrologic system in hydrologic analysis; second, the integration of the human system dynamics into hydrologic design in order to include the impacts of human influence in the hydrologic system; third, the use of more advanced techniques for modeling of the coupled human-hydrologic system. Focusing on the first two points, the importance of understanding possible future strategies to be adopted in water management under changing global environmental conditions needs to be stressed. Not only water demand is expanding, but also water supply is likely to be affected by climate change, altering the temporal and geographical distribution of water resources throughout the globe (Figure 2-4; IPCC 2014). Moreover, the inclusion of feedbacks between human activities, climate and biophysical dynamics, still not embedded in their full complexity in global climate models, are expected to seriously increase the pressure of humans on the natural system, with possible catastrophic consequences (Bierkens 2015).
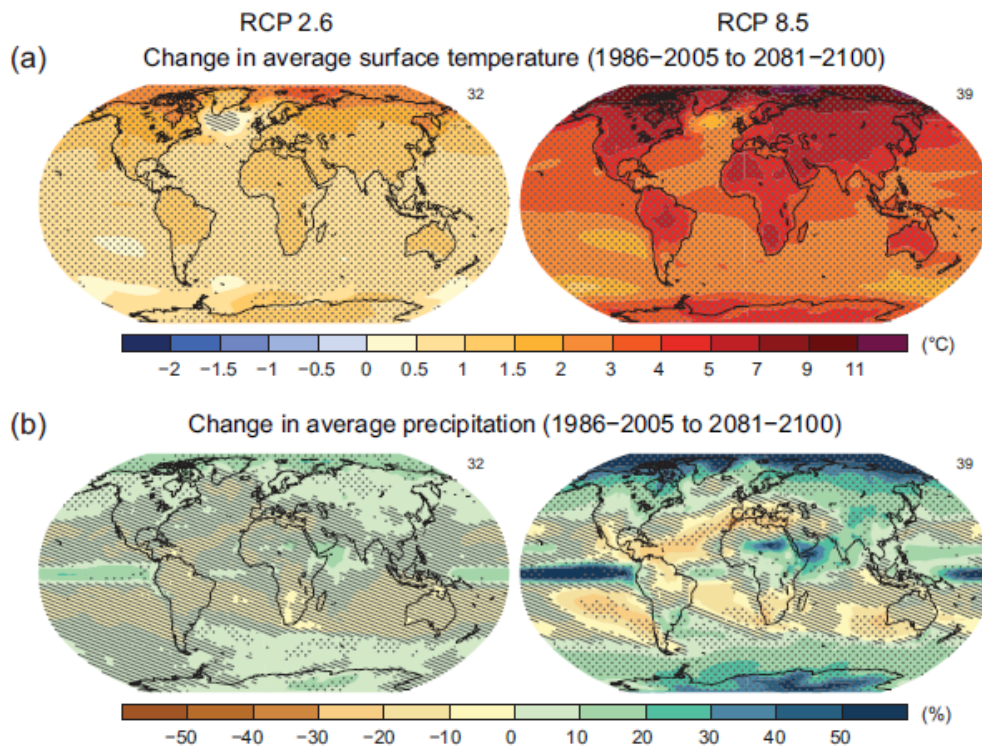
**Figure 2-4 Multi-model results for the scenarios RCP 4.5 and 8.5. Change in average surface temperature and precipitation (IPCC 2014).**

Changing climate conditions from long-term historical records represent a big challenge in water resource management. Hydraulic infrastructures have been historically sized and shaped using as reference past observations and assuming the stationarity over time of the hydrological conditions (Salas & Obeysekera 2014; Stakhiv 2011). The assumption of stationarity has been actively debated recently in literature (Milly et al. 2008; Milly et al. 2015; Galloway 2011; Montanari & Koutsoyiannis 2014; Salas & Obeysekera 2014) with the conclusion that a higher uncertainty should be taken into account while planning hydraulic infrastructures. To summarize, the main sources of uncertainty around water resource in a changing globe are: human pressure; ecological responses to anthropogenic modifications like climate and land use change; atmosphere-biosphere feedbacks; climate modeling; and flow projections (Franz & Hogue 2011; Paiva et al. 2012). The study of all the interlinked processes and dynamics mentioned above are necessary to correctly inform the decision

9

makers about the strategies to be adopted in water management plans. Appropriate information should be constructed analyzing the problems in a multidisciplinary way. This thesis provides an example of how different aspects of the combination of socio-hydrology, eco-hydrology (Sivapalan et al. 2012), climate science, agricultural science, and engineering are combined together to disentangle complex problems of water related systems at different geographical scales. It presents the analysis of the impacts of climate and land use change on complex water systems, and quantifies the potential impacts in terms of hydropower or agricultural losses. Depending on the scale of the analysis and the availability of data, it discusses the different methodological approaches potentially suitable for each of the specific problems taken into consideration. It investigated the positive and negative sides of each of them, and illustrates the main advantages of, for instance, the use of a statistical analysis in the context of global hydropower production or the biophysical and hydrological modeling of specific river systems. The final result is represented by a set of case studies in which tools characterized by different degrees of complexity are applied in different contexts. The stock of information produced represents an important contribution for the decision making process in water management, as well as climate change adaptation and mitigation.

## 1.2. Main questions addressed and thesis structure

This thesis aims at understanding how human driven global changes in terms of climate and land use are expected to impact on the spatial and temporal distribution of the water resources. It focuses on the analysis of physical changes in terms of water availability to understand the challenges for the sustainability of human water related activities in developing and developed countries.

The main questions this thesis is aimed to answer are:

- How will global climate and land use change impact the spatial and temporal distribution of the water resources?

- How will global climate and land use change impact on the human activities in terms of hydropower and agricultural production?

- What are the main adaptation options in the socio-environmental systems under consideration?

The thesis is organized in three studies aimed at estimating the main consequences of global changes (mainly land use and climate) in terms of hydropower production and agriculture at different geographical scales. In the first part of the dissertation, specifically in Chapter 2, a statistical model is utilized to assess the sensitivity of the global hydropower generation to the variability in seasonal averages as well as changes in extreme conditions of precipitation, runoff, and temperature. Climate projections from 5 different general circulation models were used to identify the expected future trends under two different climate scenarios.

In the second part of the dissertation, the analysis moves from a global to a regional and local geographical scale. A biosphere model (ED2.2) is utilized to assess the impacts of climate and land use change on the water cycle of a portion of the Brazilian Amazon. Chapter 3 presents a hydrological analysis, conducted using the land surface model (ED2.2) integrated with a routing scheme (ED2+R), aimed at understanding the expected impacts of the environmental changes on the rivers' discharge in the Tapajos river basin. A hydro-energy model (HEC-ResSim), was used to provide an example of how the computed river discharge scenarios could be translated in terms of disturbances to hydropower production in the area. Chapter 4 illustrates an analysis of the impacts of climate change to the agricultural sector in a specific portion of the basin analyzed in the previous chapter. A crop model (FAO-AquaCrop) was used to estimate the impacts of future climate projections to the rainfed

agriculture of the Upper Tapajos river basin in Mato Grosso, Brazil. Autonomous adaptation and the possible introduction of irrigation in a relatively large scale were analyzed, discussing also the possible complications caused by competitive uses of water in the basin. Last section (Chapter 5) summarizes the thesis findings, draws conclusions and policy implications of the work, and suggests directions for future research.

Each chapter is intended as an individual article. Therefore, some chapters may include repetitions of the prime definitions and case study description. In some cases the description of methodological approaches could partially overlap.

# 2. Vulnerability of Global Hydropower to Future Climate Change[3]

## Abstract

Historically hydropower has been an important driver of economic and social development by providing both energy and water management services that generate multiplier effects (Kumar et al. 2009; van Vliet et al. 2012). By offering low-carbon energy and climate-adaptation benefits, hydropower will play an increasingly important role also in the future in the context of greenhouse gas mitigation. In the context of climate change adaptation, reservoirs could be used for irrigation and flood risk management. Yet, future climatic conditions are likely to affect the potential of this source of energy with uncertain consequences for its adaptive and mitigation capacity. Here we analyze the sensitivity of storage hydropower with reservoirs of different size and assess the magnitude and uncertainty of its vulnerability under future climate at global scale. Results indicate that changes in seasonal runoff patterns as well as variations in frequency and intensity of wet and dry conditions are expected to affect hydropower. Significant heterogeneity across unit size is found and the response varies with the ability of the hydropower facilities to cope with inter- and intra-annual variability by using their storage capacity. Globally, climate change impacts on hydropower resulting from our estimates appear equivocal and substantial variations existing even within countries. Yet, clear patterns can be identified for particular hydropower plants size in certain regions such as Southern Europe, North America, and Asia.

---

[3] *This Chapter is based on*:

Farinosi, F., De Cian, E., Sue Wing, I. (*in preparation*). "Vulnerability of Global Hydropower to Future Climate Change"

## 2.1. Introduction

The international debate about greenhouse gases emission has set the stage for increased investments in renewable energy sources. Hydropower represents an important renewable source in many countries in the world, and it represents one of the main pillars of the near future energy strategy of countries like China and Brazil (IEA 2013). The share of renewables in global electricity generation approached 21% in 2012 and although wind and solar grew the most between 2005 and 2012, hydropower supplied 16.9% of world electricity (Bruckner et al. 2014). Storage hydropower can offer side benefits that could facilitate adaptation. Even in facilities primarily dedicated to electricity generation, reservoirs can serve multiple purposes such as flood control, water storage for agriculture and water supply, recreation, and aquaculture (Kumar et al. 2009; Schaeffer et al. 2012).

Hydro-generation primarily relies on water availability, which depends on a complex function of sources with their specific dynamics (ground water, snowpack, stream flows, and reservoir storage) and is affected by alternative competitive uses, such as irrigation, industrial cooling and heating. Therefore, hydropower generation is linked to meteorological variability and trends both directly and indirectly, and it responds to human and climate-induced variations in connected sectors. For instance, climate change could affect hydropower through changes in energy demand or through stresses posed to alternative power sources, as in the case of thermoelectric power in case of droughts (van Vliet et al. 2012).

In the specific case of hydropower, future climatic risk as defined in the Fifth IPCC Assessment (Oppenheimer et al. 2014) will arise from the interaction between the spatial distribution of future hazards and exposure, and the different vulnerability by type of hydropower facility. The impacts of changes in precipitation patterns and temperature is expected to interact with the implications those changes will have on ground water, snowpack accumulation, as well as with the characteristics of the hydropower facility. While run-of-the

river dams may be more vulnerable to changes in runoff and precipitation in the short term, larger reservoir dams may be more sensitive to longer term climate variations, including evaporation and temperature effects.

This paper explores the vulnerability of global hydropower generation to the variability in seasonal averages as well as changes in extreme conditions of precipitation, runoff, and temperature. A statistical model (Chambwera & Heal 2014) is used to estimate the elasticity of hydroelectricity generation to the historical variations (1980-2010) in precipitation and runoff, while controlling for temperature changes and other potential confounding factors at the global scale. We then illustrate how the estimated response function of hydropower to meteorological variations can be used to assess the future vulnerability of generation from hydropower sources in 82 countries. We combine the estimated elasticities with future changes in exposure to runoff, extreme wet and dry periods, high and low temperature around 2050 in two warming scenarios (Representative Concentration Pathways –RCP- 4.5 and 8.5, van Vuuren et al. 2011) simulated by five different Global Circulation Models (GCMs), which have participated to the CMIP5 modelling comparison exercise (Taylor et al., 2012).

The work offers three contributions to the existing literature on climate change impacts on energy supply. First, by combining a statistical approach with high resolution data, the paper develops scenarios of the potential risk that climate change could pose to future hydro generation worldwide with a high spatial resolution. Heterogeneities within the same basin or countries are therefore highlighted globally. Only a few studies have analyzed the vulnerability of hydropower supply on a global scale (Blackshear et al. 2011; Hamududu and Killingtveit 2012), while most assessments have focus on specific regions (Northern Europe, Bye 2008; Nordic regions, Beldring et al. 2006) or basins (Barnett et al. 2004; Van Rheenen et al. 2004). Hamududu and Killingtveit (2012) develop a GIS-based analysis aimed

15

at exploring the linkage between changes in runoff and hydropower supply. The relationship between these two variables is not empirically-based and, other factors, such as temperature, extreme dry and wet conditions, are not considered. Moreover, the analysis does not consider seasonal variability and focuses on the national geographical scale characterizing the median country changes. Blackshear et al. (2010) present a very useful framework that can be used to identify the main factors affecting hydropower generation, discussing also how the response and sensitivity varies with the type of facility (run-of-the river, pumped systems, reservoir dams). However, the paper does not provide actual estimates of the sensitivity of different types of dams. Basin-specific studies generally rely on hydrogeological models (Van Rheenen et al 2004), and only a few regional analyses have adopted statistical approaches (Blasing et al. 2013). Blackshear et al. (2011) use the existing literature and geographic databases to develop a framework aimed at assessing hydropower vulnerability at global scale. Their approach relies on the spatial comparison between climate data and the geographic location of hydropower facilities. The study identifies and discusses the main mechanisms through which climate change could affect hydropower generation, indicating how different types of hydropower facilities (reservoir-based, run-of-the-river, pumped-storage) would be differently affected by the various mechanisms.

Second, the paper explores the vulnerability of global hydropower not only to the variability in seasonal averages, which is in line with most of the existing assessment in literature (van Vliet et al. 2012), but also in changes in extreme conditions of precipitation, runoff, and temperature.

Third, geospatially referenced data on 8,689 dams used for hydropower generation from the International Commission On Large Dams database (ICOLD-CIGB) allow us to stratify the combined impact of both runoff, and dry/wet spells by reservoir size, with high

geographical resolution. Therefore, we can characterize the vulnerability of differed units with reservoirs of different sizes.

The remainder of this chapter is organized as follows. Section 2.2 describes the data and explains the statistical model. Section 2.3 presents the empirical findings and the results on the impacts of future climate change on hydropower generation. Section 2.3 discusses the main findings and section 2.5 concludes.

## 2.2. Methodology and Data

We use a statistical model to explore the historical sensitivity of hydropower to changes in both average and seasonal runoff, describing the flow effect of water availability, as well as in the frequency of dry and wet periods of different intensity, describing the stock effect due to variations in the water volume stored in the reservoirs. By using two Representative Concentration Pathway (RCP) of high (RCP 8.5) and medium (RCP 4.5) emission scenarios from five General Circulation Models participating to the CMIP5 project (Vuuren et al. 2011; Taylor et al. 2012) we analyze the risk posed by future changes in runoff as well as in exposure to extreme dry and wet conditions in the decade around 2050 (2046-2055). Dry and wet conditions are defined using Standardized Precipitation Indices (SPI, McKee et al. 1993). This index describes the number of standard deviations cumulative precipitation calculated over a predefined period, in this specific case over 6 or 24 consecutive months, is below or above the long-term median for the same period. The statistical analysis controls for time-invariant country-specific heterogeneity by including a country fixed-effect and for unspecified exogenous influences affecting all countries and units by including a time trend. The confounding effect of the electricity generation mix is also considered. Indirect demand effects are controlled for by including the number of cold and hot days, which could affect energy use for heating and cooling.

It is important to clarify that statistical and process models are characterized by two completely different approaches. The first one takes into consideration the historical records to study the elasticity of the energy production to the various inputs. The second approach studies the physical conditions of the hydrological system to estimate the potential ability to generate power. Although process models are probably more accurate in assessing the potential generation at dam level given water availability, they have a limited geographic coverage and very often do not account for operating strategies. The few global-scale studies have mostly focused on the direct impacts of changes in future runoff on the physical capability of power generation (Hamududu & Killingtveit 2012). Hydropower production is not only function of water availability and dam technical characteristics, but it also depends on the country energy system, its strategic management, other supply sources, water competitive uses, and electricity demand. By using historical data, our approach partially manages to take into consideration socio-economic factors influencing the peculiarity of the operating rules used to manage the country energy system and the specific reservoir.

### 2.2.1. Data Description

We match the global country-level annual data on power generation (World Bank n.d.) with high-resolution meteorological data from the Global Land Data Assimilation System (GLDAS) dataset (Rodell et al. 2004) and the data on reservoir dams from the International Commission On Large Dams database (ICOLD-CIGB). Of the reservoirs associated with the about 37,000 units included in the database we selected only those used for hydropower generation (8,689). The units were geospatially referenced using as a proxy the name of the reservoir or, with a reasonable approximation, the name of the nearest town (Kahle et al, 2013). The ICOLD database is used to spatially select the grid cells of the GLDAS database (1 degree x 1 degree) located in the neighborhood of dams. The dataset

indicates the year of construction and therefore allows developing time series at the country level by aggregating storage capacity by country and accumulating over time, starting from zero if no capacity was reported in 1960. Table 2-1 summarizes the data used in the analysis and the source.

We tested a number of variables and indicators characterizing changes in seasonal average conditions as well as changes in variability, such as extreme wetness and aridity. Changes in seasonal average conditions are controlled for by including seasonal cumulative precipitation or runoff. We stratify seasonal precipitation or runoff with the size of reservoir capacity at each point in time (weights are time-varying) in any given hydropower plant location. We scaled precipitation or runoff at each site with the volume of the reservoir to obtain volume-scaled runoff and precipitation and add together the sites stratified into three reservoir groups (small, medium, large) to the country level. Volume-scaled runoff is obtained by: 1) stratifying seasonal runoff with the size of reservoir capacity at each point in time in any hydropower plant location; 2) scaling runoff at each dam site with the volume of the reservoir; 3) adding together the sites stratified into three groups, small, medium, large at national level. We define the following categories:

- Small reservoirs: water storage capacity < 1 million cubic meters;

- Medium reservoirs: 1 < storage capacity <100 million cubic meters

- Large reservoirs: storage capacity > 100 million cubic meters.

The underlying prior is that a given amount of precipitation or runoff has a different effect on total power generation depending on whether it affects dams with large, small, or medium reservoirs. The use of the reservoir volumes in this study has to be considered as a proxy for the characteristics of the reservoir catchment areas, data not available for the majority the entries of the ICOLD Database. By scaling the meteorological variables with the volume we obtain an indicator of electricity production potential. The use of volume-scaled

runoff and precipitation allows differentiating marginal effects of runoff and precipitation for hydropower plants with different storage capacity. Table 2.1 summarizes the descriptive statistics for the three groups of units. Figure 2.1 shows the geographic distribution of all dams included in the ICOLD database.

| Variable | Obs | Mean ('000) | Std. Dev. ('000) | Min ('000) | Max ('000) |
|---|---|---|---|---|---|
| Total | 8,266 | 1,738,368 | 9,308,336 | 1 | 181,000,000 |
| Small-sized units | 889 | 368 | 288 | 1 | 993 |
| Medium-sized units | 4,851 | 22,095 | 24,087 | 1,000 | 99,913 |
| Large-sized units | 2,526 | 5,646,018 | 16,200,000 | 100,000 | 181,000,000 |

**Table 2-1 Summary statistics of the dam units in the ICOLD database. Volume of the reservoir in cubic meters.**
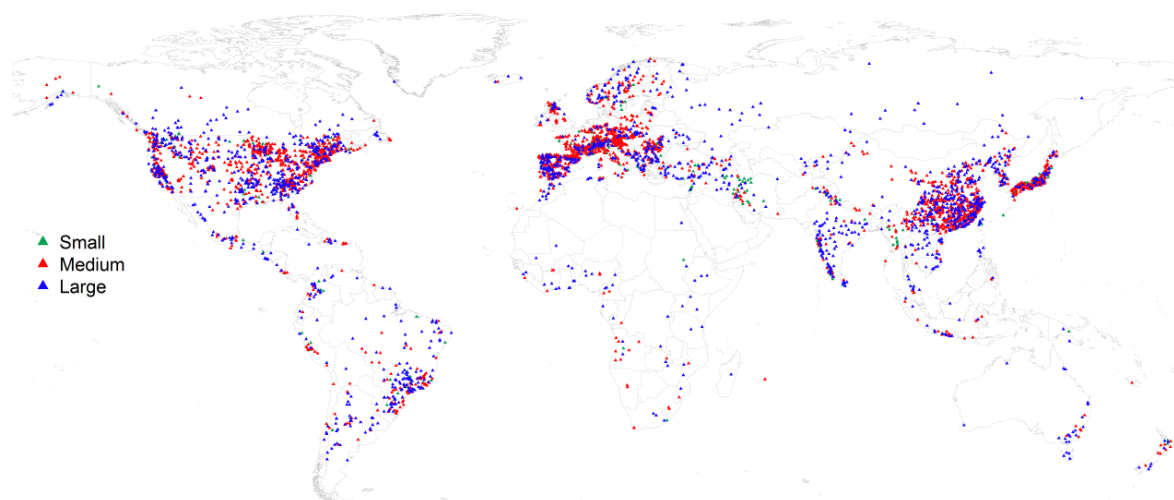


| | Reservoir facilities (#) | | | | Reservoir facilities (Share) | | |
|---|---|---|---|---|---|---|---|
| | Total | Small | Med | Large | Small | Med | Large |
| Africa | 149 | 10 | 51 | 88 | 7% | 34% | 59% |
| North America | 2312 | 107 | 1064 | 1141 | 5% | 46% | 49% |
| South America | 490 | 47 | 201 | 242 | 10% | 41% | 49% |
| Asia | 2872 | 362 | 1776 | 734 | 13% | 62% | 26% |
| Oceania | 178 | 15 | 86 | 77 | 8% | 48% | 43% |
| Europe | 2688 | 348 | 1673 | 667 | 13% | 62% | 25% |
| World | 8689 | 889 | 4851 | 2949 | 10% | 56% | 34% |

Cumulative seasonal precipitation and runoff data capture the flow effect of water available for electricity production in a given year, but, especially in the case of large dams, it does not inform about the stock effect due to variations in the volumes stored in the reservoirs. We model changes in inter-annual variability by using the Standard Precipitation Index (SPI) (McKee et al. 1993). The SPI is a widely-used drought indicator (McKee et al., 1993; Núñez et al. 2014; Orlowsky et al., 2013). The index represents the number of standard deviations that the cumulative precipitation over a desired time scale deviates from the long-term median (Guttman 1994). A long-term record of precipitation for the desired periods, in our case obtained from the GLDAS historical data (1960-2010), is fitted to a Pearson type III distribution (Guttman 1999; Kumar et al. 2009; WMO 2012; Núñez et al. 2014; Beguería & Vicente-Serrano 2014) and then transformed into a normal standardized distribution so that the mean SPI for the location and desired period is zero (Edwards and McKee, 1997). Different duration periods can be used to analyze the effect of precipitation anomalies of different persistency. Depending on the problem at stake, the SPI can be defined for durations between 3 and 24 months. For example, in the context of agriculture, a key indicator is soil moisture, which, at least for the most superficial layer, is sensitive to precipitation anomalies over relatively short time scales, between 1 and 6 months (agricultural drought) (Beguería et al, 2014). Groundwater and large reservoirs tend to be more resilient and therefore are sensitive to longer time scale anomalies, between 6 and 24 months (hydrological drought) (WMO 2012). Since the SPI is a normalized value, it is a valuable indicator both for wet and dry periods (WMO 2012). Positive SPI values indicate greater than median precipitation, and negative values indicate less than median precipitation. The intensity to be chosen as representative has been widely discussed in literature (McKee et al. 1993; WMO 2012;

Guttman 1999; Kumar et al. 2009) with the conclusion that values of plus and minus 1.5 represent reasonable thresholds to identify very wet and dry periods respectively. To examine the impact of hydrological drought, we use the 6 and 24 month SPI.

Since the effect of seasonal average temperature through evapotranspiration and melting is already captured by the seasonal average runoff variables, as temperature covariates, we here focus on the impact of the extremes by including the number of cold and hot days.

Table 2-2 provides the complete list of the variables used in the analysis. Table 2.3 summarizes the descriptive statistics of the main variables used in the statistical model. Table 2.4 summarizes the distribution of dams by size, along with national 2010 hydropower generation (World Bank, n.d.), and with the maximum number of months with severe drought between 1981-2010.

The dataset is a balanced panel of 82 countries observed over the period 1981-2010. Given the length of the time series, we test for the presence of unit roots by using the panel data unit root tests Harris-Tzavalis (1999), which is more suitable for panel with N>T, 82>29 in this case. The null hypothesis of the test is that all panels contain a unit root. In econometrics the presence of a unit root in time series data indicates that the underlying process is nonstationary. Nonstationarity has implications for inference and can lead to spurious correlation (e.g. correlation between two variables simply due to the fact that the move along the same trend). We find that the logarithmic transformation makes the series used in the model stationary. Basically, we tested whether hydropower generation was stationary or not, and we found that the logarithm of generation is stationary (e.g. does not have a unit root). Hence our preferred model uses the log transformed variables, with the exception of the SPI and hot days, which are counts of days or months and are already

stationary. Note that, since some of the variables take the zero value (runoff and precipitation), in order to enable the logarithmic transformation we add a unit to all of them.

| Variable | Data Source | Unit | Temporal scale | Spatial resolution |
|---|---|---|---|---|
| Hydroelectricity generation | World Bank | TWh | Annual | Country |
| Total runoff | GLDAS | mm/day | Daily | 1 degree x 1degree |
| Total precipitation and snow | GLDAS | mm/day | Daily | 1 degree x 1degree |
| Temperature | GLDAS | °C | Daily | 1 degree x 1degree |
| Volume of reservoir capacity | ICOLD | cubic meters | Annual | 35,764 georeferenced units |
| Share of nuclear power electricity | World Bank | 0-1 | Annual | Country |
| Share of coal power electricity | World Bank | 0-1 | Annual | Country |
| Share of gas power electricity | World Bank | 0-1 | Annual | Country |

**Table 2-2 Data source**

| Variable | Obs | Mean | S.Dev. | Min | Max |
|---|---|---|---|---|---|
| lnelygen (ln electricity generation) | 2490 | 22.28 | 2.00 | 16.76 | 27.31 |
| elygen_twh (electricity generation) | 2490 | 26.16 | 64.11 | 0.02 | 722.00 |
| Log annual runoff, medium sized units | 2407 | 13.99 | 7.63 | 1.39 | 23.52 |
| Log spring runoff, medium sized units | 2490 | 12.25 | 7.57 | 0.00 | 22.47 |
| Log summer runoff, medium sized units | 2407 | 12.43 | 7.57 | 0.00 | 22.86 |
| Log winter runoff, medium sized units | 2490 | 12.08 | 7.45 | 0.00 | 21.98 |
| Log annual runoff, small sized units | 2407 | 7.63 | 6.16 | 1.39 | 17.95 |
| Log spring runoff, small sized units | 2490 | 6.01 | 6.10 | 0.00 | 16.73 |
| Log summer runoff, small sized units | 2407 | 6.03 | 6.07 | 0.00 | 17.41 |
| Log winter runoff, small sized units | 2490 | 5.90 | 5.98 | 0.00 | 16.03 |
| Pop. Weighted Days Av. Temp<5 | 2490 | 37.94 | 57.95 | 0.00 | 242.85 |
| Pop. Weighted Days Av. Temp>27.5 | 2490 | 68.32 | 76.95 | 0.00 | 350.80 |
| Months w/. 6-month SPI < -1.5 | 2490 | 0.82 | 1.66 | 0.00 | 11.00 |
| Months w/. 6-month SPI > 1.5 | 2490 | 0.76 | 1.56 | 0.00 | 10.00 |
| Months w/. 24-month SPI < -1.5 | 2490 | 0.86 | 2.49 | 0.00 | 12.00 |
| Months w/. 24-month SPI > 1.5 | 2490 | 0.70 | 2.21 | 0.00 | 12.00 |
| Share of nuclear ely | 2490 | 0.06 | 0.14 | 0.00 | 0.80 |
| Share of coal ely | 2490 | 0.17 | 0.26 | 0.00 | 0.99 |
| Share of gas&oil ely | 2490 | 0.34 | 0.31 | 0.00 | 1.00 |
| **Unscaled runoff and precipitation variables** | **Obs** | **Mean** | **S.Dev.** | **Min** | **Max** |

| | | | | | | | | |
|---|---|---|---|---|---|---|---|---|
| Log summer&spring runoff | 2550 | 8.43 | 1.82 | 2.21 | 12.53 |
| Log fall&winter runoff | 2465 | 8.36 | 1.72 | 3.31 | 12.74 |
| Log summer runoff | 2550 | 7.70 | 2.15 | 0.93 | 12.35 |
| Log spring runoff | 2550 | 7.24 | 1.79 | 1.76 | 11.87 |
| Log winter runoff | 2550 | 7.07 | 1.69 | 2.07 | 11.37 |
| Log fall runoff | 2465 | 7.73 | 2.03 | 1.07 | 12.54 |
| Log summer precipitation | 2550 | 8.89 | 2.15 | 0.00 | 13.14 |
| Log spring precipitation | 2550 | 8.72 | 1.47 | 3.14 | 12.52 |
| Log winter precipitation | 2550 | 8.02 | 1.74 | 0.00 | 12.15 |
| Log fall precipitation | 2465 | 8.95 | 1.50 | 3.60 | 13.03 |

**Table 2-3 Descriptive statistics of the main variables used in the statistical model.**

| | Reservoir facilities (#) | | | | Reservoir facilities (Share) | | | | |
|---|---|---|---|---|---|---|---|---|---|
| country | Hydro generation (Twh) total | small | med | large | small | med | large | SPI24 <-1.5 | SPI6 <-1.5 |
| Canada | 326.7 | 876 | 26 | 226 | 624 | 3% | 26% | 71% | 10 | 15 |
| USA | 277.1 | 1346 | 80 | 814 | 452 | 6% | 60% | 34% | 16 | 23 |
| Brazil | 258.6 | 296 | 29 | 126 | 141 | 10% | 43% | 48% | 19 | 23 |
| China | 239.4 | 1678 | 133 | 1136 | 409 | 8% | 68% | 24% | 14 | 22 |
| Norway | 115.1 | 240 | 11 | 144 | 85 | 5% | 60% | 35% | 0 | 7 |
| Japan | 84.2 | 637 | 144 | 441 | 52 | 23% | 69% | 8% | 32 | 27 |
| India | 75.3 | 240 | 26 | 94 | 120 | 11% | 39% | 50% | 35 | 28 |
| Sweden | 67.0 | 170 | 19 | 82 | 69 | 11% | 48% | 41% | 6 | 14 |
| France | 64.3 | 325 | 60 | 239 | 26 | 18% | 74% | 8% | 29 | 22 |
| Venezuela | 51.0 | 10 | 0 | 2 | 8 | 0% | 20% | 80% | 21 | 22 |
| Italy | 41.1 | 329 | 95 | 215 | 19 | 29% | 65% | 6% | 33 | 36 |
| Austria | 35.5 | 170 | 40 | 120 | 10 | 24% | 71% | 6% | 28 | 21 |
| Paraguay | 34.9 | 4 | 0 | 0 | 4 | 0% | 0% | 100% | 3 | 17 |
| Switzerland | 34.4 | 145 | 59 | 71 | 15 | 41% | 49% | 10% | 29 | 23 |
| Colombia | 30.2 | 40 | 5 | 13 | 22 | 13% | 33% | 55% | 36 | 28 |
| Turkey | 29.4 | 76 | 10 | 23 | 43 | 13% | 30% | 57% | 25 | 27 |
| Spain | 28.5 | 358 | 0 | 199 | 159 | 0% | 56% | 44% | 33 | 27 |
| Mexico | 26.1 | 73 | 1 | 21 | 51 | 1% | 29% | 70% | 20 | 23 |
| Argentina | 25.3 | 51 | 2 | 15 | 34 | 4% | 29% | 67% | 26 | 24 |
| New Zealand | 23.1 | 50 | 7 | 22 | 21 | 14% | 44% | 42% | 19 | 18 |
| Pakistan | 20.5 | 4 | 1 | 1 | 2 | 25% | 25% | 50% | 33 | 26 |
| Germany | 19.5 | 116 | 8 | 97 | 11 | 7% | 84% | 9% | 3 | 16 |
| Chile | 16.9 | 15 | 2 | 7 | 6 | 13% | 47% | 40% | 38 | 27 |
| Romania | 14.7 | 156 | 18 | 114 | 24 | 12% | 73% | 15% | 28 | 31 |
| Australia | 14.7 | 88 | 4 | 45 | 39 | 5% | 51% | 44% | 15 | 31 |
| Peru | 13.7 | 37 | 6 | 24 | 7 | 16% | 65% | 19% | 28 | 29 |
| Finland | 13.1 | 45 | 0 | 32 | 13 | 0% | 71% | 29% | 4 | 16 |
| Korea N. | 12.6 | 44 | 0 | 29 | 15 | 0% | 66% | 34% | 5 | 12 |
| Egypt | 11.6 | 3 | 0 | 0 | 3 | 0% | 0% | 100% | 23 | 18 |
| Viet Nam | 11.4 | 23 | 0 | 3 | 20 | 0% | 13% | 87% | 22 | 25 |

**Table 2-4 Distribution and dimension of reservoirs for hydropower generation and maximum number of months with severe drought between 1981-2010.**

| country | Reservoir facilities Hydro generation (Twh) | total | small | med | large | Reservoir facilities small | med | large | SPI24 <-1.5 | SPI6 <-1.5 |
|---|---|---|---|---|---|---|---|---|---|---|
| Portugal | 9.7 | 68 | 5 | 40 | 23 | 7% | 59% | 34% | 30 | 32 |
| Zambia | 8.7 | 4 | 1 | 2 | 1 | 25% | 50% | 25% | 36 | 27 |
| Iran | 8.2 | 62 | 30 | 13 | 19 | 48% | 21% | 31% | 40 | 27 |
| Indonesia | 7.6 | 33 | 2 | 18 | 13 | 6% | 55% | 39% | 39 | 34 |
| Uruguay | 6.6 | 4 | 0 | 0 | 4 | 0% | 0% | 100% | 25 | 20 |
| Philippines | 6.6 | 14 | 1 | 5 | 8 | 7% | 36% | 57% | 39 | 35 |
| Ecuador | 5.9 | 5 | 1 | 2 | 2 | 20% | 40% | 40% | 22 | 22 |
| Iceland | 5.9 | 28 | 0 | 16 | 12 | 0% | 57% | 43% | 6 | 6 |
| Mozambique | 5.6 | 5 | 0 | 2 | 3 | 0% | 40% | 60% | 47 | 33 |
| Thailand | 5.5 | 15 | 0 | 3 | 12 | 0% | 20% | 80% | 27 | 24 |
| Ghana | 5.3 | 2 | 0 | 0 | 2 | 0% | 0% | 100% | 36 | 34 |
| Czech Republic | 5.2 | 39 | 1 | 31 | 7 | 3% | 79% | 18% | 38 | 31 |
| Nigeria | 5.2 | 5 | 0 | 2 | 3 | 0% | 40% | 60% | 27 | 22 |
| Malaysia | 5.1 | 19 | 2 | 6 | 11 | 11% | 32% | 58% | 53 | 35 |
| United Kingdom | 4.6 | 88 | 6 | 65 | 17 | 7% | 74% | 19% | 5 | 12 |
| Costa Rica | 4.6 | 9 | 1 | 6 | 2 | 11% | 67% | 22% | 31 | 29 |
| Albania | 4.1 | 9 | 1 | 0 | 8 | 11% | 0% | 89% | 25 | 29 |
| Greece | 3.5 | 25 | 2 | 10 | 13 | 8% | 40% | 52% | 37 | 33 |
| Zimbabwe | 3.3 | 1 | 0 | 0 | 1 | 0% | 0% | 100% | 48 | 24 |
| Sri Lanka | 3.2 | 15 | 4 | 4 | 7 | 27% | 27% | 47% | 34 | 23 |
| Cameroon | 3.0 | 7 | 0 | 2 | 5 | 0% | 29% | 71% | 40 | 39 |
| Syria | 2.9 | 3 | 0 | 2 | 1 | 0% | 67% | 33% | 41 | 27 |
| Bulgaria | 2.8 | 38 | 3 | 20 | 15 | 8% | 53% | 39% | 48 | 27 |
| Kenya | 2.6 | 6 | 0 | 2 | 4 | 0% | 33% | 67% | 14 | 25 |
| Guatemala | 1.9 | 4 | 1 | 0 | 3 | 25% | 0% | 75% | 22 | 28 |
| Myanmar | 1.9 | 23 | 16 | 7 | 0 | 70% | 30% | 0% | 30 | 25 |
| Poland | 1.9 | 45 | 1 | 32 | 12 | 2% | 71% | 27% | 25 | 24 |
| Honduras | 1.8 | 6 | 0 | 0 | 6 | 0% | 0% | 100% | 23 | 14 |
| Tanzania | 1.7 | 2 | 0 | 0 | 2 | 0% | 0% | 100% | 18 | 24 |
| Iraq | 1.7 | 5 | 0 | 0 | 5 | 0% | 0% | 100% | 43 | 35 |
| Ethiopia | 1.7 | 6 | 0 | 0 | 6 | 0% | 0% | 100% | 36 | 32 |
| Bolivia | 1.6 | 2 | 0 | 1 | 1 | 0% | 50% | 50% | 19 | 22 |
| South Africa | 1.4 | 11 | 1 | 6 | 4 | 9% | 55% | 36% | 29 | 28 |
| Nepal | 1.4 | 3 | 0 | 3 | 0 | 0% | 100% | 0% | 17 | 26 |
| El Salvador | 1.4 | 5 | 0 | 0 | 5 | 0% | 0% | 100% | 19 | 21 |
| Angola | 1.3 | 10 | 1 | 7 | 2 | 10% | 70% | 20% | 43 | 30 |
| Sudan | 1.2 | 3 | 1 | 0 | 2 | 33% | 0% | 67% | 46 | 34 |
| Morocco | 1.1 | 23 | 1 | 9 | 13 | 4% | 39% | 57% | 27 | 28 |
| Dominican Republ | 1.1 | 9 | 0 | 3 | 6 | 0% | 33% | 67% | 0 | 11 |
| Bangladesh | 0.9 | 1 | 0 | 0 | 1 | 0% | 0% | 100% | 19 | 19 |
| Ireland | 0.8 | 10 | 0 | 7 | 3 | 0% | 70% | 30% | 0 | 10 |
| Gabon | 0.8 | 1 | 0 | 0 | 1 | 0% | 0% | 100% | 30 | 30 |
| Lebanon | 0.7 | 5 | 4 | 0 | 1 | 80% | 0% | 20% | 34 | 38 |
| Nicaragua | 0.4 | 3 | 0 | 2 | 1 | 0% | 67% | 33% | 13 | 11 |
| Belgium | 0.3 | 10 | 0 | 10 | 0 | 0% | 100% | 0% | 14 | 16 |
| Congo | 0.3 | 1 | 0 | 1 | 0 | 0% | 100% | 0% | 42 | 33 |
| Haiti | 0.3 | 1 | 0 | 1 | 0 | 0% | 100% | 0% | 15 | 17 |
| Algeria | 0.3 | 4 | 0 | 0 | 4 | 0% | 0% | 100% | 33 | 34 |
| Togo | 0.1 | 2 | 1 | 0 | 1 | 50% | 0% | 50% | 38 | 31 |
| Cuba | 0.1 | 1 | 0 | 0 | 1 | 0% | 0% | 100% | 5 | 17 |
| Tunisia | 0.1 | 5 | 0 | 3 | 2 | 0% | 60% | 40% | 37 | 30 |
| Denmark | 0.0 | 7 | 1 | 5 | 1 | 14% | 71% | 14% | 17 | 9 |

'cont. **Distribution and dimension of reservoirs for hydropower generation and maximum number of months with severe drought between 1981-2010.**

### 2.2.2. Statistical model

Most studies (Hamududu & Killingtveit 2012; Prudhomme et al. 2013) on climate change impacts and hydropower rely on process-based models or simulation approaches. Only a few studies have adopted statistical approaches in the context of energy supply (Blasing et al. 2013), an alternative method (Chambwera & Heal 2014) that has been used extensively to analyze climate change impacts in other sectors (Deschênes & Greenstone 2007; Lobell & Burke 2010; De Cian et al. 2013).

We use a panel regression model to estimate a reduced-form relationship between annual hydropower generation at national level ($Y_{i,t}$), a set of meteorological variables ($M_{i,t}$), and number of other covariates controlling for time-invariant country-specific heterogeneity (country effect, $\mu_i$), unspecified exogenous influences affecting all countries and units (time effect, $\tau_t$), and the electricity generation mix, $Z_{i,t}$:

$$Y_{i,t} = \mu_i + \tau_t + F[M_{i,t}] + Z_{i,t}\gamma + \varepsilon_{i,t} \tag{2.1}$$

where $\varepsilon_{i,t}$ is a random disturbance term. Coefficients in Equation (2.1) are identified from the inter-annual variations and, therefore, they represent a short-term response to annual variation in the meteorological variables considered. Therefore, it represents the adjustments along the intensive margin, given the existing stock of storage hydropower capacity.

The specific form of model described in Equation (2.1) is described in Equation (2.2):

$$ln\,G_{i,t} = \mu_i + \tau_t + Z_{i,t}\gamma + \sum_k^K \beta_1^k SPI_{i,t}^k + \sum_v^V \beta_2^v lnRO_{i,t}^v + \sum_j^J \beta_3^J T_{i,t}^{\ j} + \varepsilon_{i,t} \tag{2.2}$$

where $\ln G_{i,t}$ is the logarithm of electricity generation from hydropower in country i, year t, $SPI_{i,t}^k$ is frequency of positive and negative SPI for the long and medium term (6 and 24 months) above or below the threshold (-1.5 for negative SPIs and +1.5 for positive SPIs), $\ln RO_{i,t}^v$ is the logarithm of annual or seasonal volume-scaled runoff with reservoir size *v*, $RO_{i,t}^v = \sum_{v \in \{sm,med,la\}} RO_{v,t} Vol_{v,t}$. $T_{i,t}^j$ is the frequency of population-weighted cold (average daily temperature <5°C) and hot (average daily temperature >27.5°C) days. The set of variables $Z_{i,t}$ control for the electricity mix.

The main model specification uses seasonal volume-scaled runoff and SPI stratified by dam size, but results are robust to a number of alternative specification. All estimated specifications include a fixed effect that controls for the unobserved heterogeneity ($\mu_i$i) and year dummies ($\tau_t$) and are estimated using the panel fixed effect estimator with robust standard errors.

### 2.2.3. Future projections

Expected future climate change impacts are calculated by combining the estimated parameters from Equation (2.2) describing the response of hydropower generation (G) to changes in the frequency of positive and negative SPIs[4] and to changes in average seasonal runoff with Representative Concentration Pathway (RCP 4.5 and 8.5) trajectories (Vuuren et al. 2011) simulated using five GCM models. The model taken into consideration are: the Centro Euro-Mediterraneo sui Cambiamenti Climatici Climate Model CMCC-CM (Scoccimarro et al. 2011), a coupled atmosphere-ocean general circulation model developed from the Scale Interaction Experiment SINTEX-G (SXG) model (Gualdi et al. 2008; Bellucci

---

[4] The calculation of SPI indices using the CMIP5 projections has already been applied in literature, see for example (Orlowsky & Seneviratne 2013).

et al. 2008) and from the CMCC Carbon Cycle Model (Fogli et al. 2009; Vichi et al. 2011); the National Aeronautics and Space Administration Goddard Institute for Space Studies NASA GISS E2-H, a combination of the Model E atmospheric code coupled with the HYCOM ocean model (Lee et al. 2013; Miller et al. 2014; Nazarenko et al. 2015; Schmidt et al. 2011; Schmidt et al. 2014); the National Center for Atmospheric Research Community Climate System Model NCAR-CCSM4 (Gent et al. 2011), a couple Earth System Model simultaneously simulating the earth's atmosphere, ocean, land surface and sea-ice; the Max Planck Institute for Meteorology Earth System Model MPI-ESM (Raddatz et al. 2007; Marsland et al. 2003), a coupled atmosphere, ocean and land surface model; and the Institute of Numerical Mathematics coupled atmosphere-ocean general circulation model INM CM4 (Volodin et al. 2010).

We define current and future climate as the decadal mean of the meteorological variables between 2006-2015 and 2046-2055, respectively. We combine the decadal mean of the meteorological variables with the fitted response from model (5) in Table 2-5 to obtain the ratio of future to current electricity supply at dam level:

$$\frac{G_{d\in i}^F}{G_{d\in i}^C} = exp\left\{\sum_k^K \hat{\beta}_1^k \Delta SPI_{d\in i}^k\right\} exp\left\{\sum_v^V \hat{\beta}_2^j \ln \frac{RO_{d\in i,F}^v}{RO_{d\in,C}^v}\right\} \tag{2.3}$$

Future impacts will depend on the interplay between:

- hydropower sensitivity to average seasonal runoff, positive and negative SPI frequency by unit size $(\widehat{\boldsymbol{\beta}}_1^k, \widehat{\boldsymbol{\beta}}_2^v, \widehat{\boldsymbol{\beta}}_3^j)$

- change in climate exposure $(\Delta \boldsymbol{SPI}_{i,t}^k, \boldsymbol{log}\frac{\boldsymbol{SRO}_{i,F}^j}{\boldsymbol{SRO}_{i,C}^j},)$

- how this interacts with the spatial distribution of small, medium, large dams.

Although some studies (Zarfl et al. 2015; IEA - International Energy Agency 2013) have recently tried to depict a future scenario of hydropower installations, we decided not to include information about the future hydropower development in 2050. We calculate future impacts considering the current (2010) distribution and dimension of dam reservoirs. Our analysis therefore assess the potential vulnerability of existing hydropower generation based on dam reservoirs to future climate.

## 2.3. Results

### 2.3.1. Empirical results. Main model specifications

Table 2.5 summarizes the results from the specification that uses volume-scaled runoff (2.1). Specification (1) only includes volume-scaled annual runoff, specification (2) adds the contribution of short- and long-term SPIs (6 and 24 months). Specification (3) stratifies the effect of SPI by unit size. Specifications (4) and (5) analyze the impact of seasonal runoff by unit size .

Model (1) shows that total annual runoff has a significant impact on the annual generation of hydropower. Medium-sized units are the most sensitive because they account for most generation in the majority of countries and because they have a lower buffer capacity relative to large-sized units. In medium-sized units an increase in total runoff by 1% increases electricity generation by 0.08%. Small-sized units are less sensitive to inter-annual variations in runoff, and the same percentage change in total runoff (1%) increases electricity generation by 0.02%. The smaller coefficient is due to the fact that small-sized dams account for a minor share of the annual generation in most countries, and data on electricity production do not distinguish generation by unit size.

Changes in annual or seasonal runoff capture the flow effect of water availability for electricity generation in a given year, but it does not inform about the stock effect due to variations in the volume stored in reservoirs. The longer term stock effect can be captured by the SPI indicators.

When SPI indicators are included in Model (2) and (3) the marginal effects to inter-annual variation in total runoff remain significant, but are smaller in magnitude. SPIs, especially the 24-month, inform about the stock effect due to potential variations in volumes stored in reservoirs over longer time periods due to prolonged wet or dry periods. The 6-month and 24-month negative SPIs (e.g. taking values below -1.5 indicating severely dry conditions) are significant and negatively signed, indicating that persistent droughts reduce average annual hydropower generation.

Positive SPIs are positively signed and significant only for a medium intensity of wet periods (6 month). The increased flows that would occur during wetter seasons or spells are usually stored in the reservoirs and transformed in electricity over a longer time period, or released through the spillways if the accumulated water exceeds the storage capacity. Mostly run-of-the-river small- and medium-sized hydropower plants are positively impacted from extended wet periods, if processing in real time the excessive amount of water, with an impact on the national annual hydropower production. This pattern is shown in model (3), where positive 6-month SPI is statistically significant only when affecting small-sized units. It is important to note that in the database used for the present analysis, even small-sized units have a relatively large storage capacity (only few of them have a reservoir capacity lower than 100,000 cubic meters). In case of extreme events, the larger reservoirs are used for flood risk mitigation and the run-of-the-river plants are usually shut down, either to prevent damages, or because of non-optimal difference between the water level upstream and downstream the dam (head).

Models (4) and (5) show that medium- and large-sized units are more sensitive to changes in winter and spring runoff, whereas small-sized units are sensitive to changes in summer runoff, probably because those would coincide with periods of peak demand.

Temperature has also a significant impact. A greater exposure to cold and hot days has a positive effect on hydropower supply, but only cold days have a significant impact in the full-sample specification shown in Table 2-5, probably through supply-side mechanism of favoring snowpack accumulation. In contrast, hot days have two opposite effects that might cancel out. On the demand side, more frequent hot days can also increase hydropower supply through the induced change in electricity demand. Warm days are characterized by highly volatile electricity demand, with high peaks during the warmest part of the day. The excess of demand is often satisfied by increasing hydropower production, mainly due to its intrinsic characteristics, immediate availability and almost negligible marginal cost. On the supply side more frequent hot days can increase the evaporation of the water stored during the summer period and water losses could be particularly important in case of reservoirs characterized by large surface. Blasing et al. (2013), in a study focusing on California, show that higher spring temperatures cause a faster melting of the snowpack, leading to earlier snowmelt and increased spillage because the oversupply of water do not match the timing of when demand peaks.

| | (1) | (2) | (3) | (4) | (5) |
|---|---|---|---|---|---|
| 24SPI<-1.5 | | -0.00386* | | | |
| | | (2.0296e-03) | | | |
| 24SPI>1.5 | | 0.00263 | | | |
| | | (2.1000e-03) | | | |
| 6SPI<-1.5 | | -0.00521** | | | |
| | | (2.5877e-03) | | | |
| 6SPI>1.5 | | 0.00402* | | | |
| | | (2.2433e-03) | | | |
| 24SPI<-1.5 Large-sized units | | | -0.00978** | -0.01054** | -0.01023** |
| | | | (4.8762e-03) | (4.6913e-03) | (4.5877e-03) |
| 6SPI<-1.5 Med-sized units | | | -0.00250 | -0.00012 | 0.00106 |
| | | | (7.5991e-03) | (7.5339e-03) | (7.4955e-03) |
| 6SPI>1.5 Med-sized units | | | 0.00417 | 0.00529 | 0.00370 |
| | | | (7.1482e-03) | (7.3249e-03) | (7.1976e-03) |
| 6SPI<-1.5 Small-sized units | | | -0.01606* | -0.01709* | -0.01542* |
| | | | (9.1783e-03) | (9.0569e-03) | (9.1663e-03) |
| 6SPI>1.5 Small-sized units | | | 0.01294** | 0.01265** | 0.01240* |
| | | | (6.2150e-03) | (6.2803e-03) | (6.2838e-03) |
| Tot RO Med-sized units | 0.07643*** | 0.06000*** | 0.06352*** | | |
| | (2.461e-02) | (2.0771e-02) | (2.1977e-02) | | |
| Tot RO Large-sized units | 0.03278** | 0.02924** | 0.02917** | | |
| | (1.402e-02) | (1.2997e-02) | (1.3425e-02) | | |
| Tot RO Small-sized units | 0.01986** | 0.01648* | 0.01599 | | |
| | (9.969e-03) | (9.6758e-03) | (9.6516e-03) | | |
| Winter RO Large-sized units | | | | 0.01662** | 0.01730** |
| | | | | (8.0248e-03) | (8.0093e-03) |
| Winter RO Med-sized units | | | | 0.04221*** | 0.04093*** |
| | | | | (1.4159e-02) | (1.4339e-02) |
| Summer RO Small-sized units | | | | 0.01925* | 0.01899* |
| | | | | (9.7099e-03) | (9.7122e-03) |
| Spring RO Large-sized units | | | | 0.01027* | 0.00963* |
| | | | | (5.1712e-03) | (5.1842e-03) |
| Spring RO Med-sized units | | | | 0.01789 | 0.01838 |
| | | | | (1.3263e-02) | (1.2949e-02) |
| #Days AVT<5°C | 0.00280** | 0.00297** | 0.00299** | 0.00316*** | |
| | (1.199e-03) | (1.1732e-03) | (1.1770e-03) | (1.1665e-03) | |
| #Days AVT>27.5°C | 0.00070 | 0.00119 | 0.00116 | 0.00125 | |
| | (1.006e-03) | (1.0178e-03) | (1.0207e-03) | (1.0255e-03) | |
| Nuclear Share | -3.27997*** | -3.27698*** | -3.28287*** | -3.31387*** | -3.38356*** |
| | (7.541e-01) | (7.5393e-01) | (7.5362e-01) | (7.5202e-01) | (7.7780e-01) |
| Coal Share | -1.89951*** | -1.86788*** | -1.88261*** | -1.91993*** | -1.91138*** |
| | (6.901e-01) | (6.9520e-01) | (6.9139e-01) | (6.8507e-01) | (6.9167e-01) |
| Gas&oil Share | -1.74647*** | -1.72125*** | -1.73433*** | -1.75203*** | -1.72553*** |
| | (4.279e-01) | (4.3056e-01) | (4.2862e-01) | (4.2503e-01) | (4.2044e-01) |
| Constant | 20.90087*** | 21.16754*** | 21.13529*** | 21.39249*** | 21.59240*** |
| | (5.047e-01) | (4.4790e-01) | (4.6993e-01) | (3.9405e-01) | (4.2874e-01) |
| Observations | 2,460 | 2,460 | 2,460 | 2,460 | 2,460 |
| R-squared | 82 | 0.456 | 0.456 | 0.456 | 0.453 |
| Number of id2 | 0.452 | 82 | 82 | 82 | 82 |

Robust standard errors in parentl
*** p<0.01, ** p<0.05, * p<0.1

**Table 2-5 Estimation results. Model with volume-scaled annual surface and subsurface runoff. While the main paper report the estimated models including all variables, here we reported the models that only include the most statistically-significant variables.**

### 2.3.2. Empirical results. Robustness check and alternative model specifications

Our preferred estimated model is model (5) in Table 2-5 because it characterizes the seasonality of hydropower response to changes in runoff. In order to check whether the seasonal dimension significantly amplifies climate projection uncertainty, Figure 2-2 compares the impacts computed using preferred model (5) with the impacts resulting from the response estimated in model (3), which instead considers the sensitivity to average annual runoff.

Figure 2-2 reports the estimated response of hydropower generation to the historical inter-annual variation in total and seasonal runoffs, and to the changes in extreme precipitation conditions described by the 6 and 24 month positive and negative Standardized Precipitation Indices (SPI) (McKee et al. 1993). Results indicate that hydropower is sensitive to changes in runoff patterns as well as to prolonged dry and wet conditions. Response varies significantly with the ability of hydropower facilities to cope with the observed changes by using their storage capacity. Large-sized units are more able to buffer inter-annual variability in seasonal runoffs, whereas facilities with medium and small reservoirs, as well as run-of-the-river units, are the most sensitive to short term runoff variations. SPIs inform about the stock effect due to potential variations in volumes stored in reservoirs over longer time periods due to prolonged wet or dry periods. The occurrence of one additional month classified in a long-term dry event (24-month SPI lower than the standard deviation threshold defining severe dry events, -1.5) reduces hydroelectricity generation from large units by 1%, while the occurrence of one additional medium-term dry event (6-months SPI<-1.5) reduces generation from small units by 1.5%. The need for water release for agricultural uses, in combination with the management rules regarding environmental or minimum flow during more persistent dry conditions, could explain the lower sensitivity of annual generation to changes in the frequency of negative 24-month SPI when affecting large units. The practices

of imposing water release from reservoirs for minimizing drought impacts in agriculture are widely used especially in areas where agriculture has a higher value added. Temperature has also a significant impact. A greater exposure to cold and hot days has a positive effect on hydropower supply, but only cold days have a significant impact in the full-sample possibly through supply-side mechanism of favoring snowpack accumulation.

**SPI, Total runoff (Model 3 in Table 2-5)**
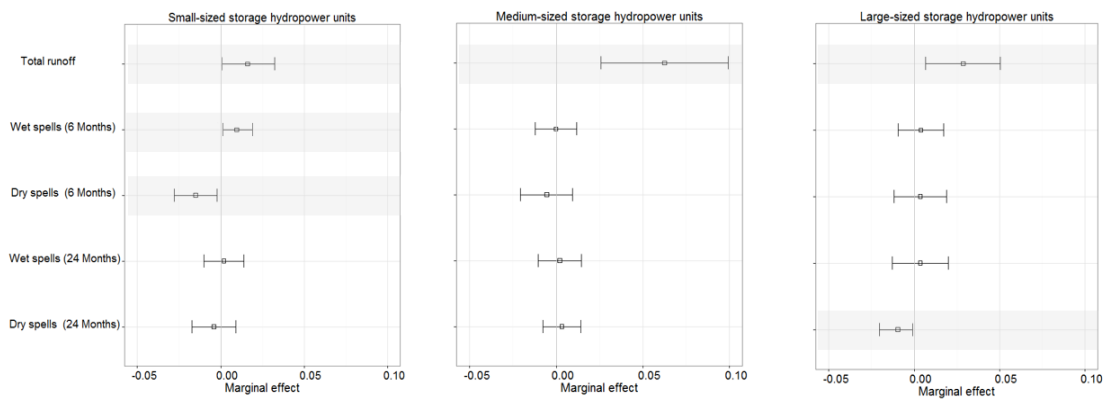


**SPI, Seasonal runoff (Model 5 in Table 2-5) – Preferred model for our analysis**
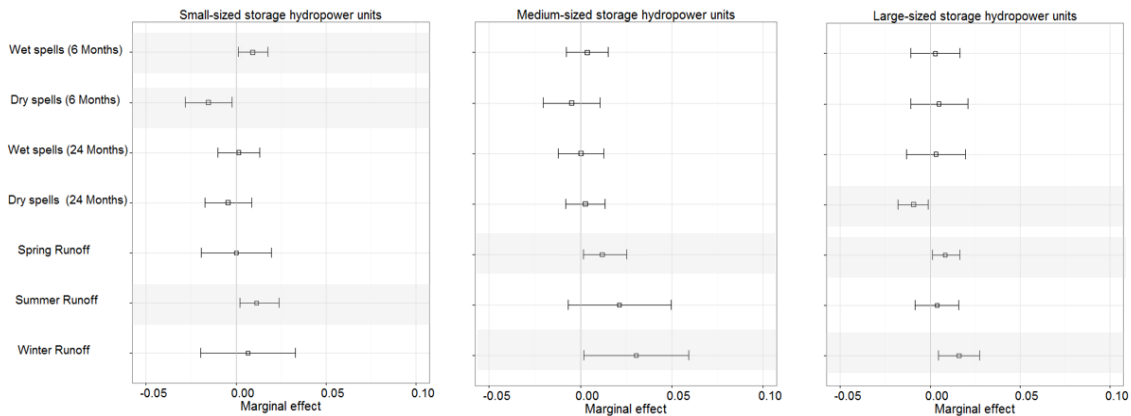


**Figure 2-2 Historically-estimated sensitivity of national hydropower generation to changes in dry (SPI24<-1.5; SPI6<-1.5) and wet spells (SPI24>1.5; SPI6>1.5), total, and seasonal runoffs. Gray areas highlight the variables remaining significant after cleaning the model from the variable statistically not significant. See Table 2-5 for the full empirical results of the clean models.**

### 2.3.3. Future projections

As illustrated in the methodological section, we used the estimated coefficients to project the impacts of future climatic conditions to the global hydropower production. Figure 2-3 illustrates the median changes projected by the 5 GCMs in the sites where the dams under consideration are located for the statistically significant variables of the formulation (5) in Table 2-5.
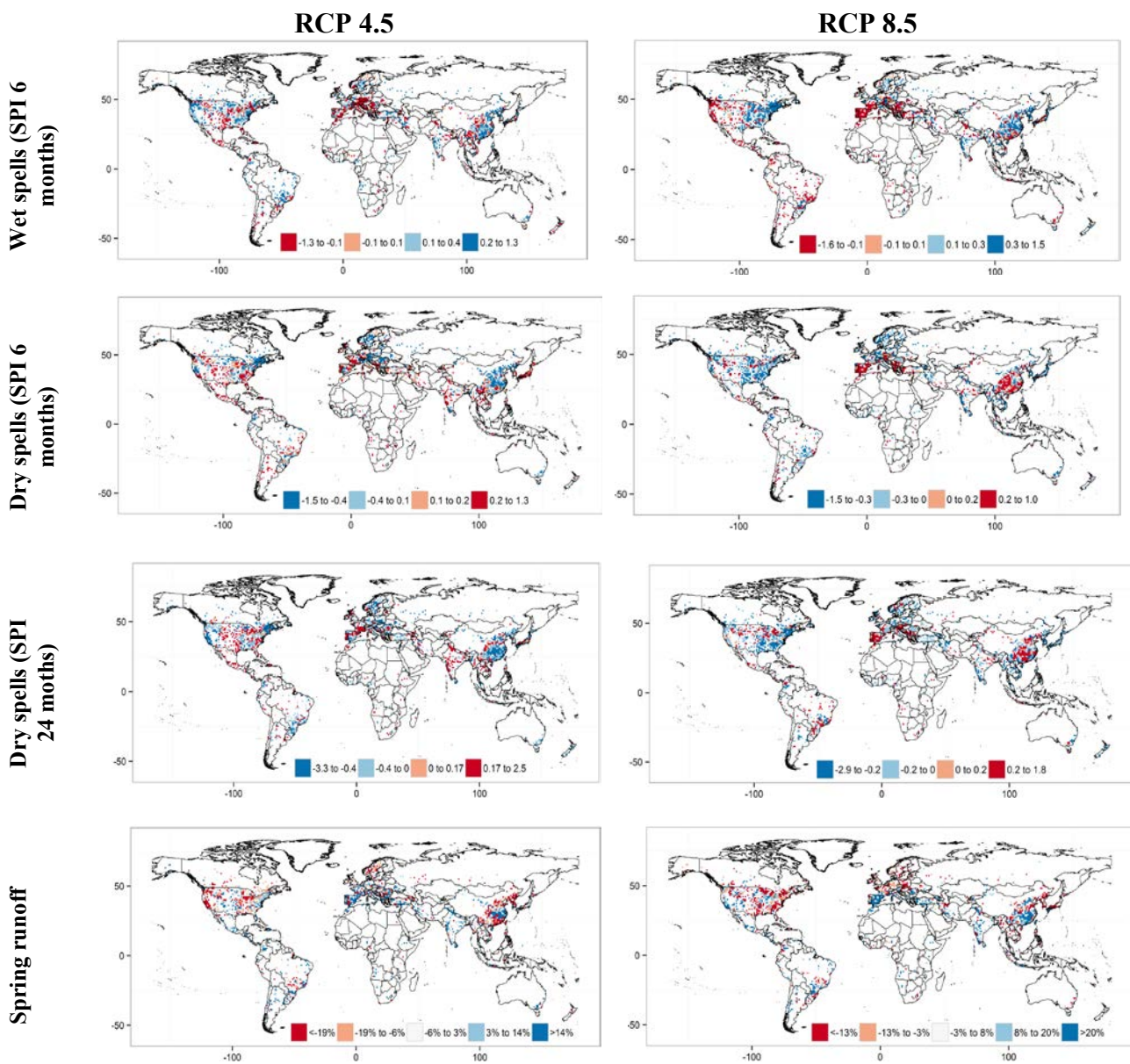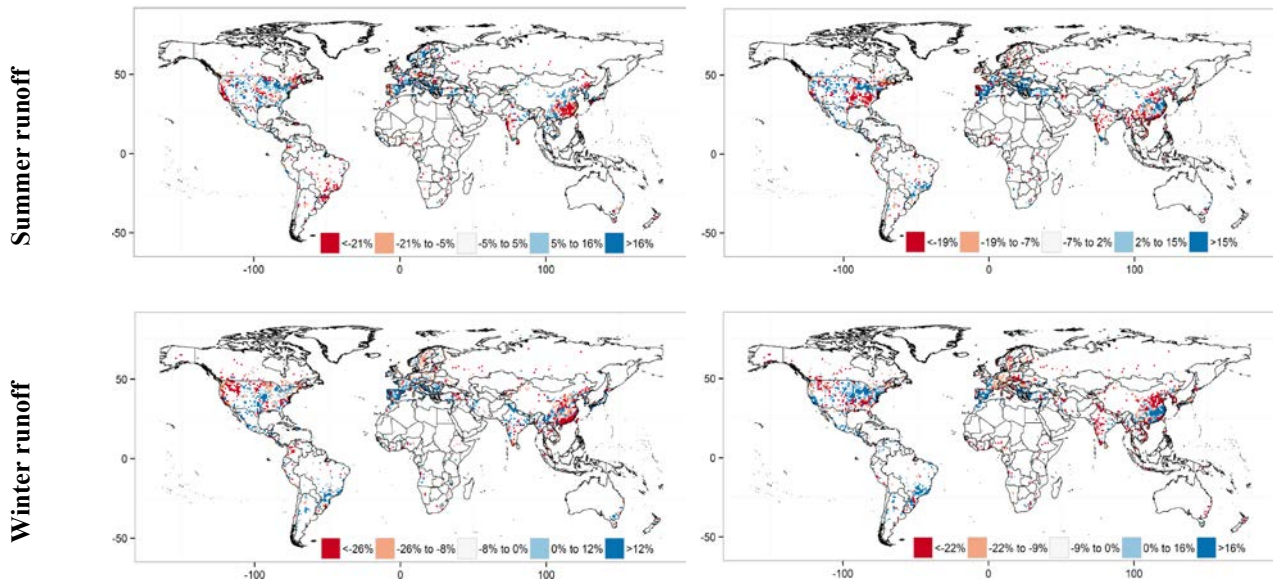
**Figure 2-3 Change (2050 vs 2010 - Median of the 5 models) in seasonal runoff (expressed in %) and wet/dry spells (expressed in months).**

Figure 2-4 visualizes the distribution of hydropower percentage changes around 2050 computed at the multi-model median climatic conditions for the main basins across the world. Substantial variation exists across different plants located within the same basin and vulnerability varies with the ability of hydropower facilities to cope with inter- and intra-annual variability by using their storage capacity. Divergent results in the same basins depend mainly on the specific characteristics of the individual reservoirs and its specific vulnerability to climate variations described in Table 2-6.

| Scenario | Continent | Generation (TWh), 2010 | Median Change (TWh) | # GCMs Negative impacts | # GCMs Positive impacts |
|---|---|---|---|---|---|
| **RCP4.5** | Africa | 99 | 0.07 | 2 | 3 |
| | America N. | 656 | 2.17 | 3 | 2 |
| | America S. | 681 | -1.00 | 3 | 2 |
| | Asia | 1297 | 7.29 | 0 | 5 |
| | Europe, North | 391 | 0.79 | 2 | 3 |
| | Europe, South | 234 | -0.42 | 3 | 2 |
| | Oceania | 55 | -0.07 | 2 | 3 |
| | World | 3414 | 8.83 | 1 | 4 |
| **RCP 8.5** | Africa | 99 | 0.97 | 2 | 3 |
| | America N. | 656 | 7.30 | 0 | 5 |
| | America S. | 681 | -3.99 | 3 | 2 |
| | Asia | 1297 | 2.24 | 1 | 4 |
| | Europe, North | 391 | 1.43 | 1 | 4 |
| | Europe, South | 234 | -1.25 | 5 | 0 |
| | Oceania | 55 | 0.08 | 3 | 2 |
| | World | 3414 | 6.78 | 1 | 4 |

**Table 2-6 Global- and continent-wide potential impacts on hydrogenation around 2050 as simulated by 5 different GCM models. Dam level Multi Model Median and impact sign agreement among GCMs. Changes at the Median climate are relative to 2010 generation.**

General trends can be identified in large river basins where hydropower potential has been already substantially developed. Small-sized hydropower units, more sensitive to intra-annual or in general shorter term variations, show prevailing negative impacts in Latin America, China, Japan, and South-East Asia, Middle East, and Southern Europe under both climate scenarios, with several units reporting agreement between scenarios and GCMs in Asia. Medium- and large-sized units, more sensitive to inter-annual variability, show agreement between the five GCMs for a number of units in the high warming scenario (RCP 8.5).
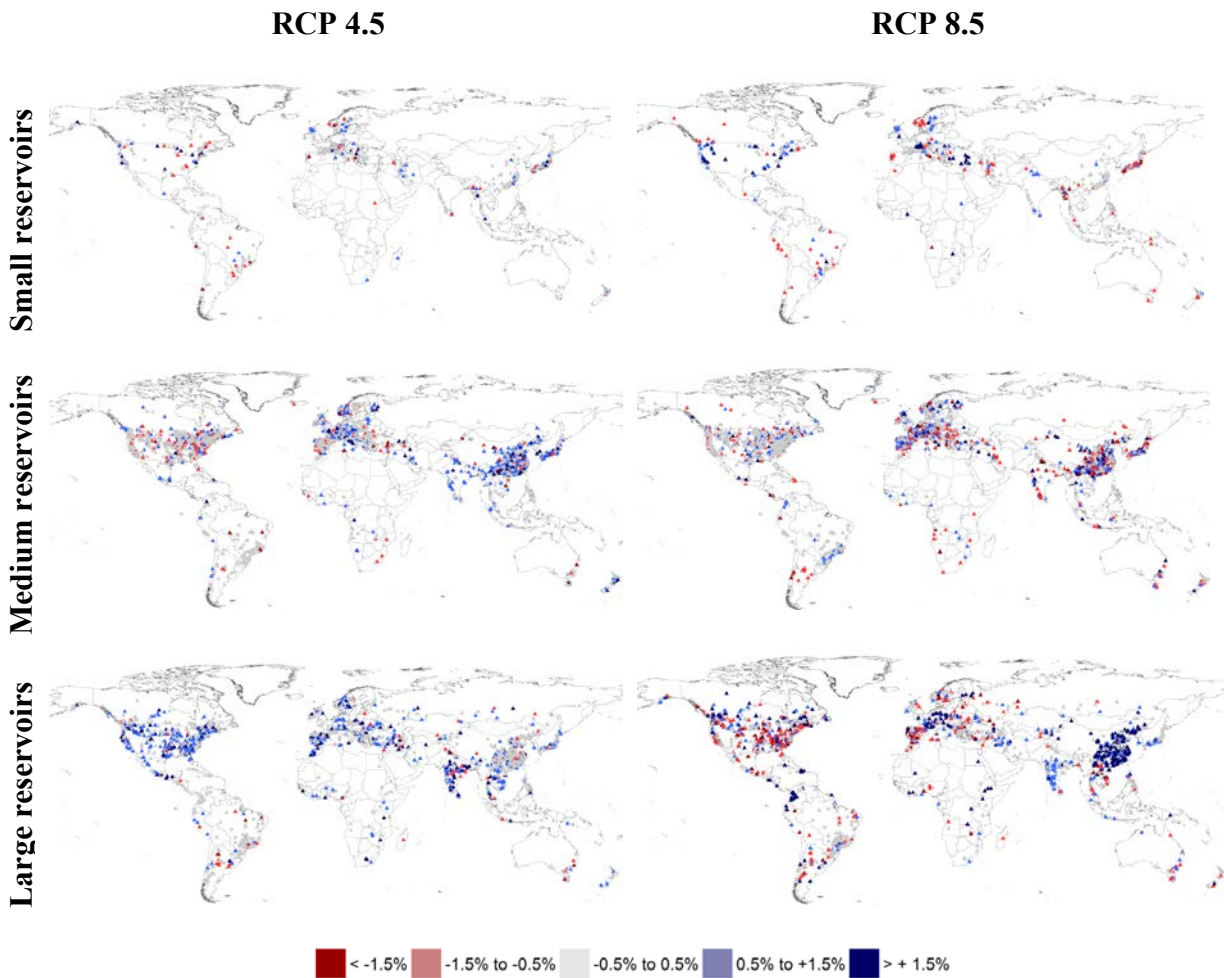
**Figure 2-4 Climate change impacts (as % change) in 2050 RCP 4.5 and RCP 8.5 as simulated by 5 different GCM models. Dam level Multi Model Median of the results calculated using the different climate models.**

Figure 2-5 visualizes the percentage changes in hydropower generation for the main river basins across the world. This analysis is extremely important especially taking into consideration the hydropower future installation plans that are being implemented in this period in particular in developing countries. Divergent results in the same basins depend mainly on the specific characteristics of the individual reservoirs and its specific vulnerability to climate variations. Nonetheless, it is possible to identify general trends in the large river basins where hydropower potential has been already substantially developed. The results calculated using different climate projections converge and design clear trends in some areas of Europe and North America, as for instance Mediterranean and continental Europe and

Eastern United States. The production is expected to be substantially declining in the southern part of Europe and in the Alpine region, with different intensities depending on the climate scenarios.

**RCP 4.5** **RCP 8.5**
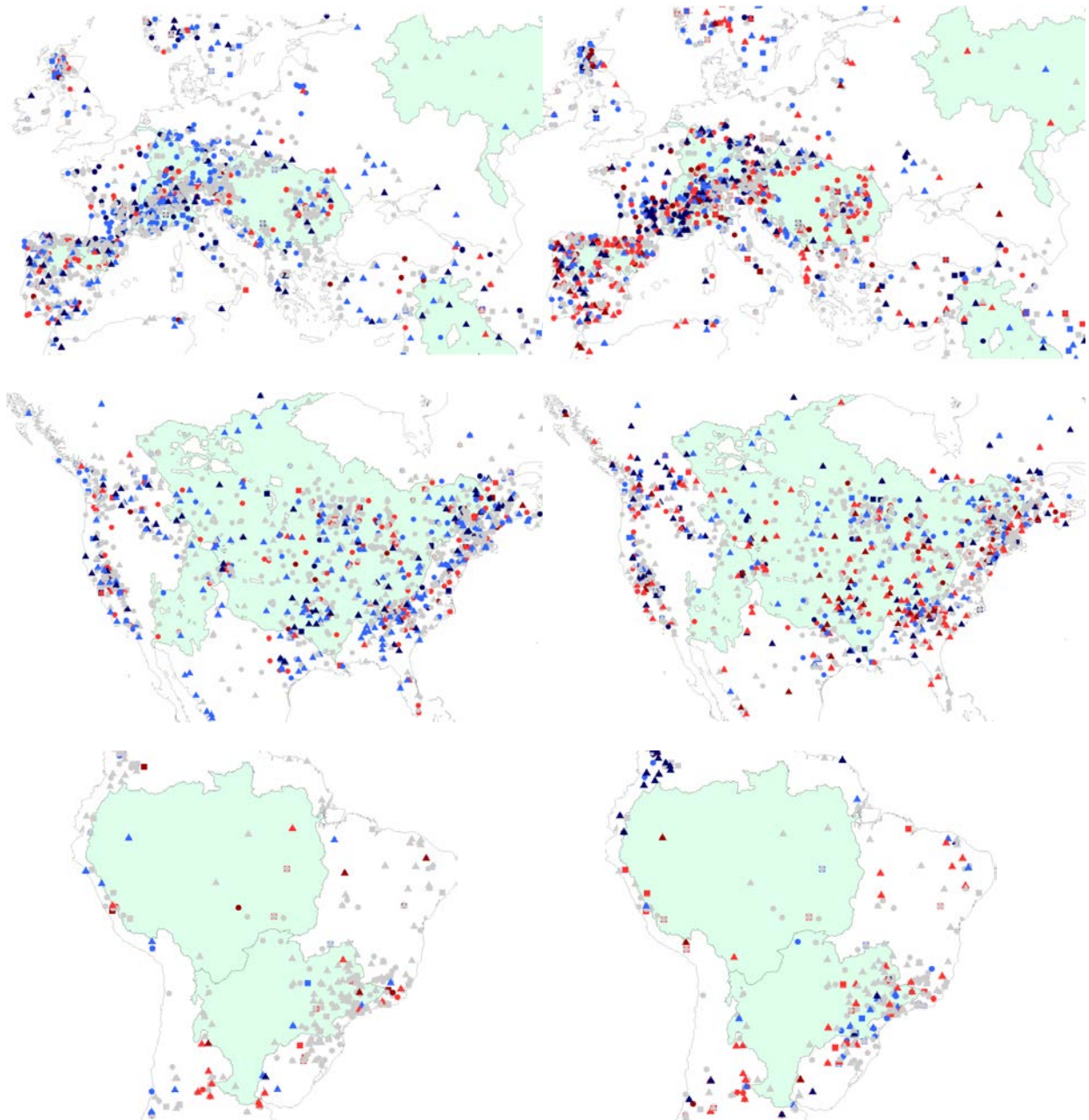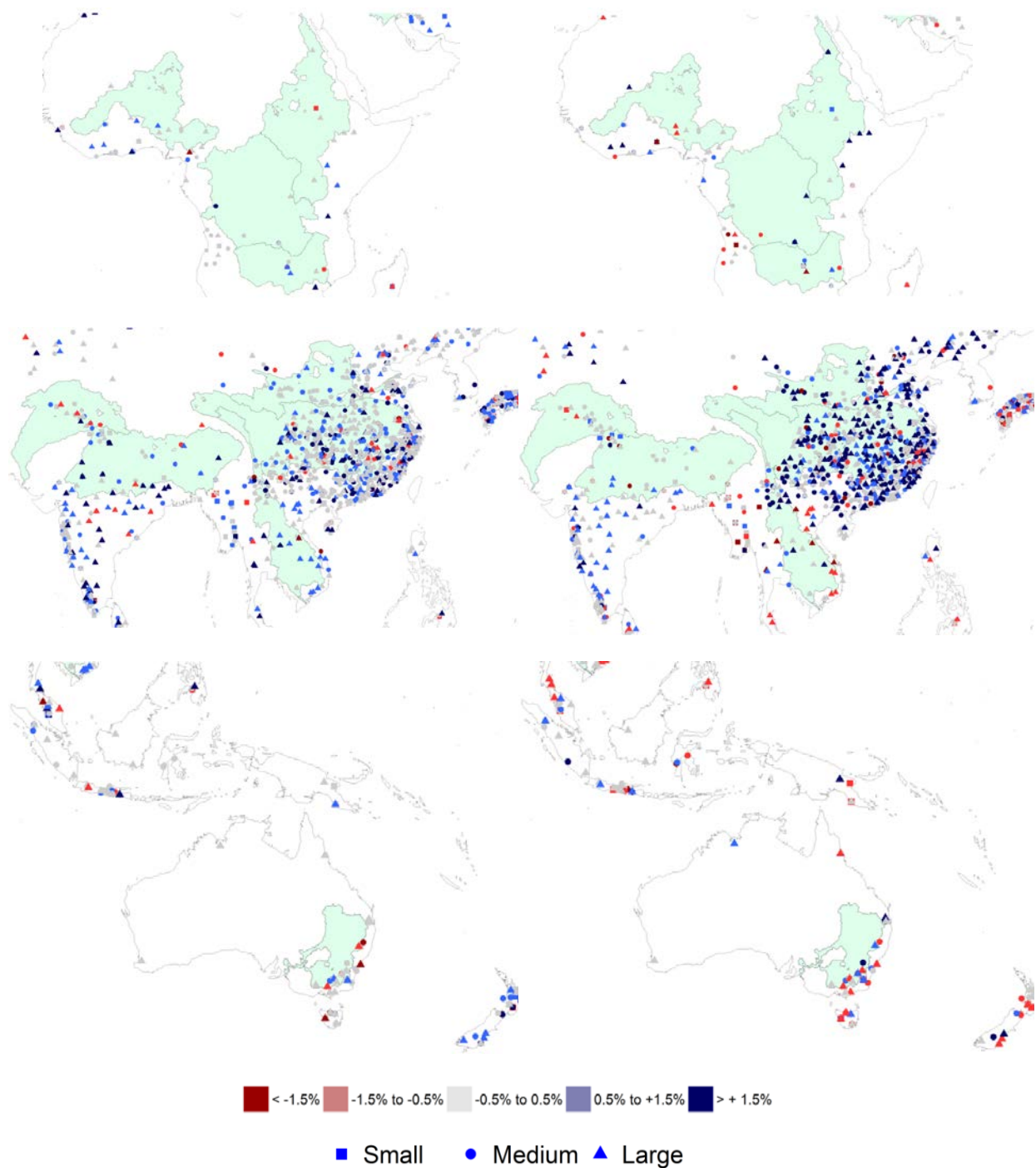
**Figure 2-5 Climate change impacts in 2050 RCP 4.5 (left) and 8.5 (right) as simulated by 5 different GCM models for the main river basins across the world. Dam-level Multi Model Median, reservoir size group, and convergence in sign of the results calculated using the different climate models (3 to 5 GCMs agreement).**

In the Eastern part of United States, the analysis shows a slight decline, with some exceptions in the Southern part, where the model estimates an increase in production, but with a high uncertainty among the climate projections from different GCMs. High

40

uncertainty is showed in the area of the Colorado river basin, where the hydropower potential production is expected to decrease especially with the less extreme climate scenario (RCP 4.5).

Figure 2-6 summarizes the impacts of climate change on hydropower generation in 2050 in the two climate scenarios, RCP 4.5 and 8.5, for the main hydropower producing countries grouped by geographic areas. The uncertainty range reflects both the GCMs uncertainty for a given dam, as well as the spatial distribution in a given country.

Decreasing projections and high uncertainty are reported for the African and South American river basins where ambitious hydropower development plans have been developed in the recent past (Figure 2-5). Clear patterns are, instead, designed for the Eastern Asian River Basins, where a clear decreasing trend is highlighted, especially associated with the most pessimistic climate scenario (RCP 8.5). Negative trends also for the Murray-Darling river basin in Australia.
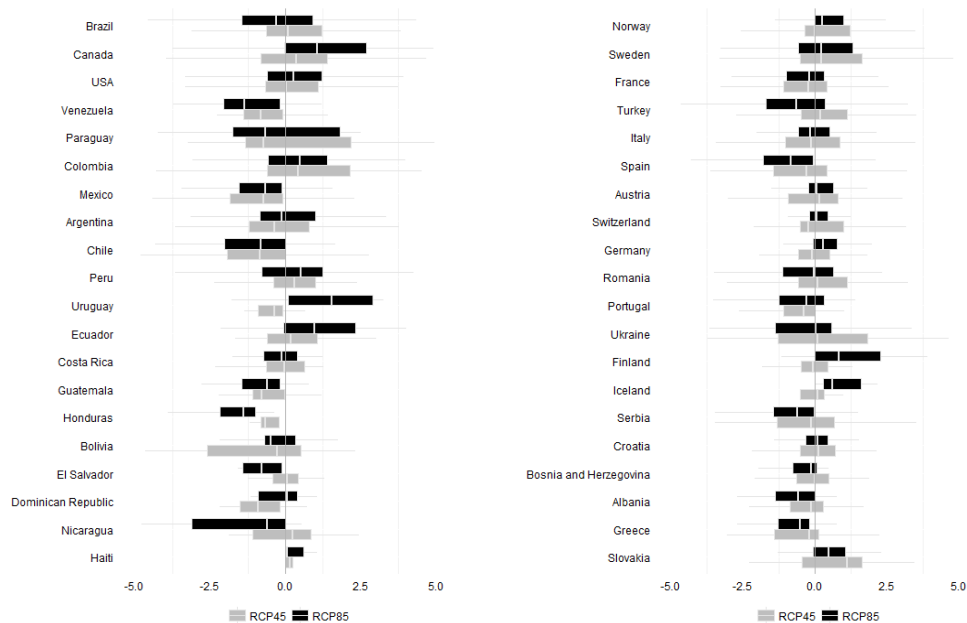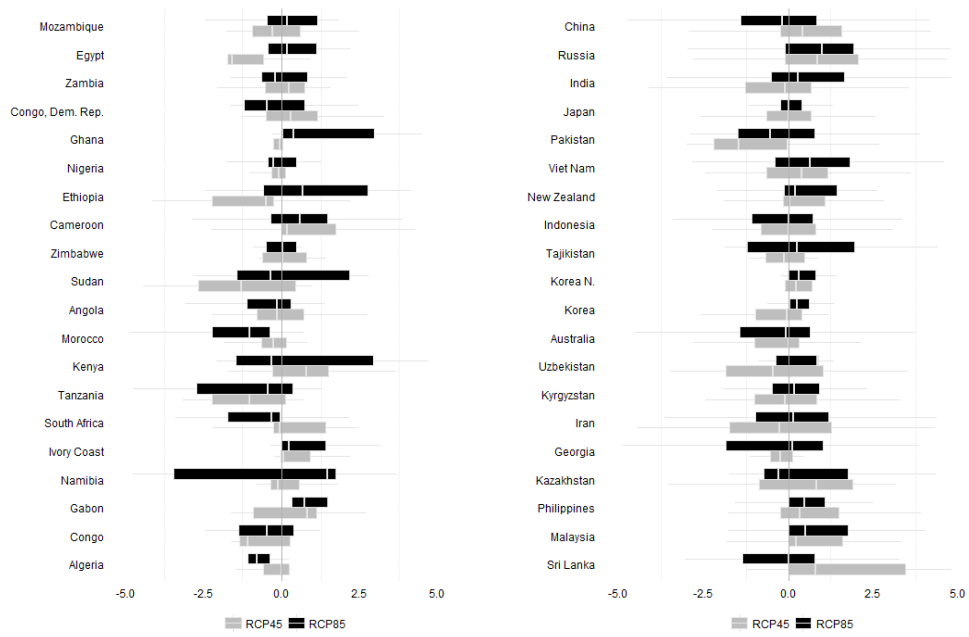
**Figure 2-6 Spatial distribution and GCMs uncertainty of climate change impacts on hydropower generation around 2050 in RCP 8.5 and RCP 4.5. Percentage changes in electricity generation relative to current levels (2006-2015 annual average).**

Figure 2-7 shows the spatial distribution of impacts computed at the median climate across the 5 GCMs. It is evident how the results converge in some geographic areas and diverge in others. This is mainly due to the uncertainty linked to the climate projections from different GCMs. Experiments run with different models provide aligned results in some areas of the world (mainly temperate and continental areas of Europe, Asia and North America), and substantially divergent in other areas (like Africa, South America, Central Asia, and Pacific). A number of large hydropower-producing countries in the north (Canada, US) and parts of Europe (France, Germany, Switzerland and Northern European countries) are expected to have an increased generation, while hydropower generation is expected to generally decrease in Mediterranean and Southern countries (e.g.. Australia, India, Spain, Italy, Northern Africa, Pakistan, Venezuela, Chile).
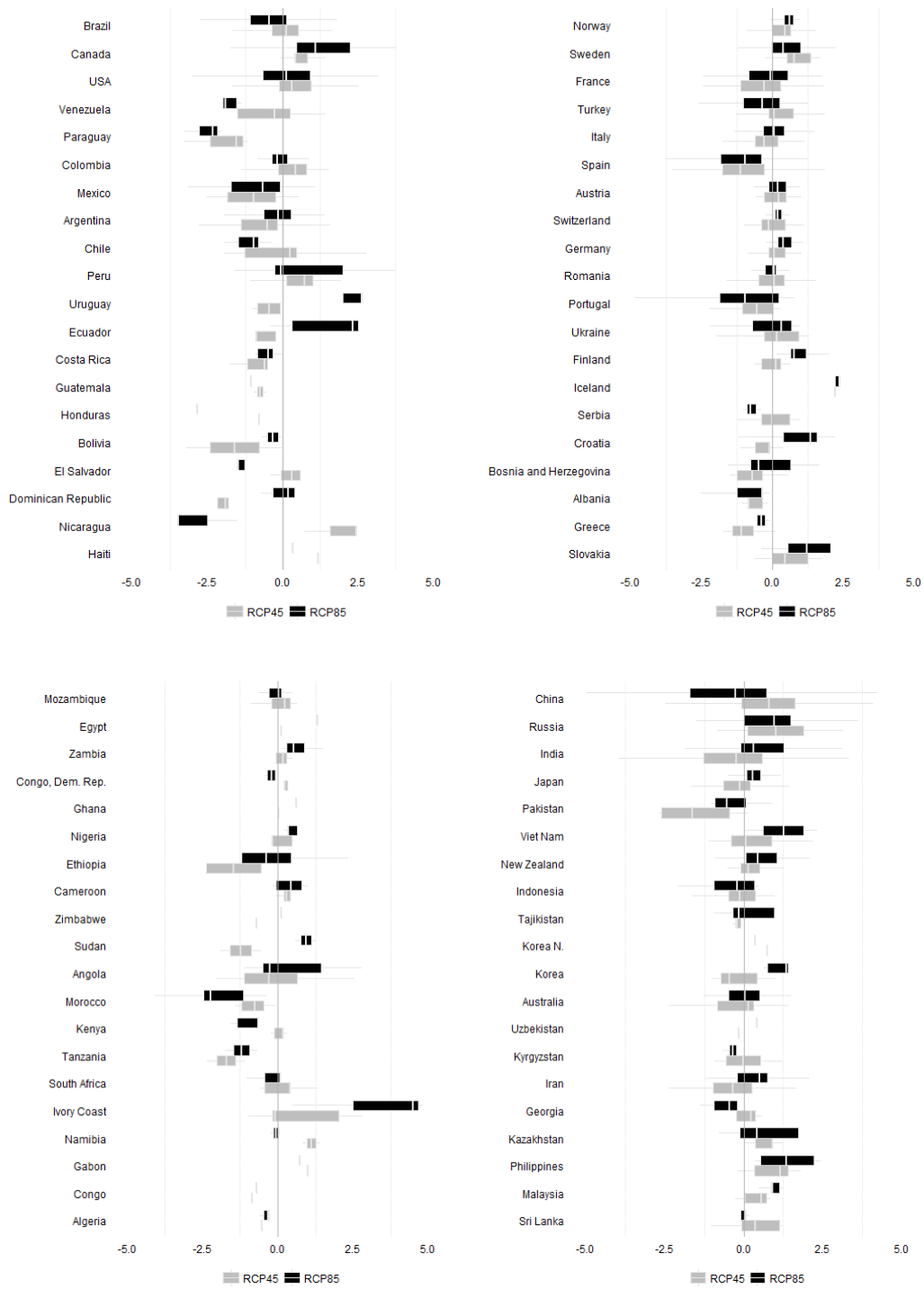
**Figure 2-7 Spatial distribution at median climate of climate change impacts on hydropower generation around 2050 in RCP 8.5 and RCP 4.5. Percentage changes in electricity generation relative to current levels (2006-2015 annual average).**

When looking at the weighted average impacts at the country level (Figure 2-7, and in Annex A - Figure A-1 and Figure A-2), our results are in line with previous studies using a similar scale. Hamududu and Killingtveit (2012) have also highlighted the increase in the Northern region and in Northern Europe and the decrease in Southern Europe and several Middle East countries.

Figure A-3, Figure A-4, and Figure A-5 in Annex A highlight the agreement in sign of future climate change impacts at dam level among GCMs at global scale. The value presented is the median of the impacts calculated using the 5 different climate models.

## 2.4. Discussion

Building on the historically-estimate hydropower response function, we illustrate the potential future vulnerability of hydropower generation by considering the current distribution of hydropower facilities as of 2010, and holding everything else (e.g. prices, technology, demand, policy) equal. We compare the expected climatic conditions for the decadal mean conditions centered around 2050 (2046-2055) to the current situation centered around 2010 (2006-2015). We generate future patterns of the potential risk (Oppenheimer et al. 2014) climate change could pose to hydropower by combining its sensitivity estimated using the statistical model with the current exposure (e.g. current location and distribution of hydropower units) and with the change in climatic conditions around 2050 relative to the current climate.

Globally, climate change impacts on hydropower are expected to be relatively small in magnitude, between 0.2 and 0.3% of total generation, and positive in sign, with four out of five models agreeing on the sign (Table 2-6). Continent-wide impacts are equivocal in sign across GCMs in most regions, but clear patterns can be identified for North America (positive

impact) and South Europe (negative impact) in the high warming scenario (RCP 8.5), and for Asia (positive impact) in the moderate warming case (RCP 4.5).

Negative impacts emerge in most of the units located in China, India, Russia, United Stated and Latin America. In the Eastern Asian River Basins a decreasing trend is highlighted, especially in the most pessimistic climate scenario (RCP 8.5). Negative trends can be detected also for the Murray-Darling river basin in Australia. Results are mixed for Europe, though the multi-model median tends to suggest a reduction in hydropower in the South and an increase in the North. Potential negative impacts and higher uncertainty are reported for the African and South American river basins where ambitious hydropower development plans have been developed in the recent past. In the Amazon and Congo River basins, in particular, controversial hydropower future installation have been planned and are currently under development (IEA 2013).

Figure 2-8 highlights the consequences of future climate on country-level generation. On the left it shows the share of units experiencing negative impacts, on the right those with positive impacts for the major 20 world producers. Countries are ordered by impact size, from positive (top) to negative (bottom). Although aggregate impacts on national generation are generally clear, the subnational distribution is highly diverse. Hydropower units facing positive and negative countries coexist in most countries. Paraguay, Venezuela, Pakistan, and Mexico in the RCP 4.5 show a prevailing negative impact, with more than 80% of the hydropower units experiencing a decline in generation. Therefore, the benefits of GHG reduction when moving from the RCP 8.5 to the more moderate scenario RCP 4.5 are also highly dispersed within countries. We can say that in Paraguay, Venezuela, Pakistan, and Mexico GHG mitigation would reduce impacts only marginally. In Spain, Turkey, China, and Brazil the share of negatively affected units drops significantly from 82 to 47%, from 29 to 0%, from 37 to 3%, and from 31 to 11%, respectively.

**RCP4.5**
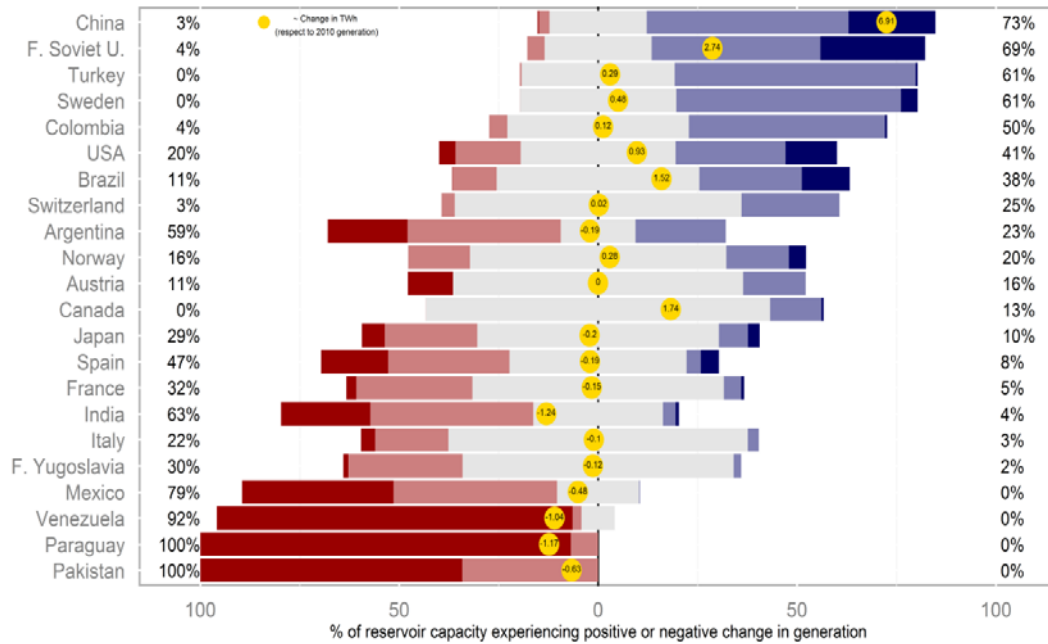
**RCP 8.5**
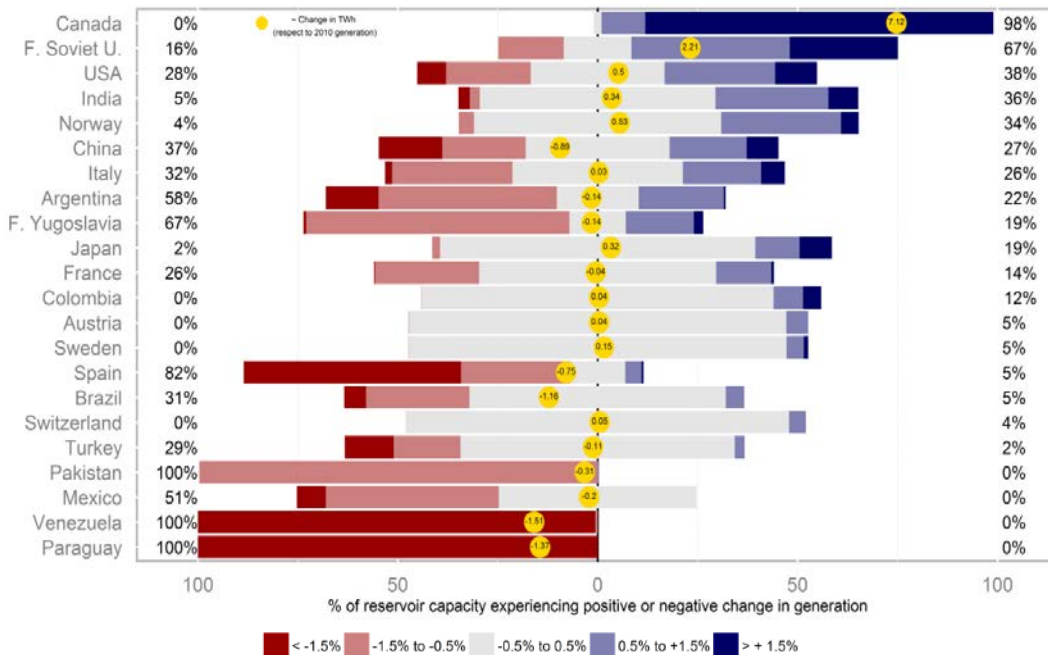
Figure 2-8 Climate change impacts (as % change) in 2050 RCP 4.5 and RCP 8.5 as simulated by 5 different GCM models in the main hydropower producers in the world. Dam level Multi Model Median of the results calculated using the different climate models. Absolute numbers in the yellow circles provide changes relative to 2010 generation.

## 2.5. Conclusions

Rising concerns have stirred the debate about the future vulnerability of hydropower to climate change and of its sustainable development as renewable source of energy. Although storage hydropower could help to mitigate climate change and cope with water scarcity and flood events, climate change is expected to modify the future conditions in which the hydropower operators are called to manage the storage capacity. Moreover, attempts to minimize environmental and social impacts of hydropower facilities has led to an increased development of relatively smaller sized reservoirs, mainly run-of-the-river, which are actually the most sensitive to changes in average seasonal runoffs as well as in extreme dry and wet conditions. Our results suggest that regional pattern of future climate as well as the sensitivity of facilities with reservoirs of different size should be considered when planning these long-lived, less adaptable hydraulic infrastructure.

This paper also points at the potential bias that might exist in the state-of-the art literature on mitigation scenarios reviewed in the IPCC Working Group III (Clarke & Jiang 2014), which so far has not considered the linkages between impacts, adaptation, and mitigation. Current mitigation scenarios, which do not account for the climate change feedback on the potential of renewable energy sources, such as hydropower, could underestimate or overestimate mitigation costs, and provide a biased picture of future possible energy mix through possible interactions with competing mitigation options. More research to address this gap is warranted, and future work in this direction will need to incorporate the local character of empirically-based climate impacts at the global level.

# 3. Future Climate and land use change impacts on river flows in the Tapajos Basin in the Brazilian Amazon[5]

## Abstract

Land use conversion and the changing climate are expected to significantly alter the tropical forest hydrology. In this study, we used a land surface model (ED2.2) integrated with a routing scheme (ED2+R) to analyze the hydrological alterations expected in the Tapajos river basin, a large region of the Brazilian Amazon, caused by the two main environmental drivers: climate and land use. We used two representative atmospheric carbon dioxide pathways, moderate – RCP 4.5, and severe – RCP 8.5, estimated by the Earth System Model HadGem2-ES. Human land use disturbance effects on vegetation were simulated using two scenarios with different degrees of deforestation: one limited, and the other extreme. Climate change is predicted to consistently reduce river flows throughout the year, bringing a considerable shift in flow seasonality towards later onset, and increasing overall variability. Land use change is expected to partially counter-act the diminishing trend in flow, with increasing impact on the inter- and intra-annual variability. Overall reduction of river flows, combined with the shift and the shortening of the wet season, could seriously impact the productivity of the large hydropower system planned in the region. These predictions were

input into a hydro-energy model (HEC-ResSim) parameterized to simulate the operation of the largest dam planned for the basin, Sao Luiz do Tapajos. The theoretical productivity of the hydropower facility follows the hydrological trends, stressing how the designed hydropower system, due to the general lack of storage capacity, is unable to buffer the increased flow variability, making the hydropower system extremely vulnerable to the hydrological alterations caused by the combined effect of climate and land use change.

## 3.1. Introduction

Tropical basins have been subject to exponentially increasing human pressure in the past decades. The largest tropical forests, Amazon, Borneo - Indonesia, and Congo, have heavily shrunk and large portion of their original territory has been replaced by agricultural areas (Lewis et al. 2015). Majority of these forests lie in developing countries where the economic development is boosting the demand for the full exploitation of the natural resources they offer, in terms of land, water, wood and minerals. Moreover, climate change is expected to further impact the delicate equilibrium of tropical forests (Trumbore et al. 2015; Millar & Stephenson 2015). The Amazon is the largest of the remaining tropical forests, but the increasing economic activity in the area, mainly agriculture and livestock production, have significantly modified the historical relation between humans and nature in this area. For example, Lemos & Silva (2011) estimated that about 16% of the 4.2 million square kilometers of forest in the Brazilian Amazon were lost in the period 1970-2009. The majority of this forest loss occurred in the period 1990-2005, the period of major expansion of agriculture in the Brazilian states of Mato Grosso, Rondonia, and Para' (Davidson et al. 2012; Soares-Filho et al. 2006; Lemos & Silva 2011). In the first decade of the 21st century, the Brazilian government took action to minimize the deforestation rates through new regulations and monitoring strategies (Nepstad et al. 2014), strategy which have proved to be

substantially effective. Although the rate of deforestation sensibly declined in the past decade, the demand for land and natural resources in the Amazon area is still high and could increase if governance measures are not maintained. Brazil is amongst the top world producers of soybean, corn, and cattle, with substantial low efficiency in terms of relation between production and area used (Cohn et al. 2014; FAO n.d.). Moreover, Brazil is largely dependent on natural sources for its energy security. With approximately 83 GW of installed capacity, Brazil has the world's second largest hydropower installed capacity after China (IEA 2013; REN21 2013; US EIA 2013). As of 2011, about 69% of the almost 120 GW installed capacity in the country come from hydropower plants. In the same year, electricity generated by these plants accounted for about 80% of the total energy produced (~424 of ~530 TWh) (IEA, 2013; US EIA, 2013). As of 2012, Brazil has developed only one third of its estimated hydropower potential (~245 GW, IEA, 2013). According to the Ten Years Development Plan developed by the Brazilian Energy Research Bureau (EPE), the hydropower installed capacity is expected to increase from 85 to 119 GW (about 40%) in the period 2013-2022 (EPE 2013). The IEA estimates that 42 GW of the additional installed hydropower capacity will be developed in the period 2021-2035 (IEA, 2013).

The Tapajos, basin studied in this chapter, is one of the Amazonian river tributaries, and has the highest agricultural production concentrated in its southern portion, region lying in the state of Mato Grosso (IBGE 2015). Moreover, this basin is home to one of the most ambitious hydropower development plans in South America: a system of more than forty large and medium dams is planned for this basin, representing one of the largest portions (about 20% of the installed capacity) of the planned Brazilian future investments in electricity production (EPE 2013).

Both land transformation and climate change threaten the environmental integrity of the Tapajos and the broader Amazon region. The combined effects of agricultural expansion,

forest logging and climate change is expected to affect the region's environment in a number of ways, including: reducing water available for human consumption, disrupting river navigation and hydropower generation; increasing frequency and magnitude of extreme events, floods and dry spells; augmenting forest fragmentation, drought frequency and altering fire frequency; and decreasing the overall agricultural and economic productivity (Davidson et al. 2012; Coe et al. 2013). Future scenarios for this important region are various and dependent on local and global mitigation strategies (Soares-Filho et al. 2006; Kruijt et al. 2014; Nepstad et al. 2014). The natural response of the biome to climate and land use change already is not fully understood, as this depends on the complex biosphere atmosphere feedback mechanisms with the region's climate that has been the focus of numerous studies (e.g. Cox et al. 2004; Zhang et al. 2015; Swann et al. 2015).

The main objective of this paper is to understand how anthropogenic disturbances in climate and land cover dynamics are expected to impact the river flows in the Tapajos river basin in the next decades. We do so by performing a number of model experiments with different combination of climate and land use change scenarios using the Ecosystem Demography Model 2.2 (Medvigy et al. 2009) coupled with a flow routing simulation model (ED2+R). The use of terrestrial biosphere models, such as ED2.2, able to capture the biosphere dynamics is crucial to understand the implications of land cover change for the main variables representing the water cycle (Knox et al. 2013). Terrestrial biosphere models are able to reproduce the modification of the vertical water balance within climatological grid cells over time, including water uptake by different plant functional types found within the ecosystem and the resulting dynamics of evapotranspiration, soil moisture, percolation, and surface and sub-surface runoff. A hydrological routing scheme is needed to simulate the propagation of the calculated water budget for each of the grid's components in the simulated domain. Land surface models, initially created for improving climate simulations, are often

used for computing hydrological fluxes at large scales (Zulkafli et al. 2013). The main advantage of their use is represented by the possibility to reproduce the different land surface processes, as for instance surface energy balance, hydrological cycle, carbon cycle, and vegetation dynamics, to understand the feedbacks between biosphere and atmosphere. In order to reconstruct the river flow dynamics from the land use modeled water budget, the estimated water flows need to be routed taking into account the specific topographic and characteristics of the domain into consideration (Arora et al. 1999).

In this experiment, our objective was to understand the marginal contribution and cumulative effects of two contrasting drivers: global climate change, expected to reduce river flows (Malhi et al. 2008; Joetzjer et al. 2013; Cox et al. 2004), and deforestation, expected to increase surface runoff (Bosch & Hewlett 1982; Andréassian 2004; Brown et al. 2005; Bruijnzeel 1990; Sahin & Hall 1996). The specific questions investigated are:

1.     How do future scenarios of climate and land use affect the magnitude and variability of river flows in the Tapajos river basin?

2.     What are the dominant trends of future variability in the river flows in the Tapajos river basin? Is the increased local runoff caused by land transformation or, instead, the climate-induced reduction in precipitation?

Answering these questions is directly relevant to the scientific debate centered on the concept of stationarity in the context of hydraulic infrasture design (Milly et al. 2015; Milly et al. 2008; Galloway 2011). In addition to the scientific insights gained from this study, the answers to these questions are extremely relevant to the improvement of water resources management and development planned in the Tapajos and the broader Amazon region.

The remainder of the Chapter is organized as follow: the following section describes the physical characteristics and the hydrology of the Tapajos basin. The subsequent section describes data, experimental setup, model calibration, and flow bias correction used in the

analysis. The main results will be presented and discussed both for the hydrological evolution and the implications for hydropower. A final section will summarize the study and highlight the main conclusions.

### 3.1.1. Description of the case study area

The Tapajos river basin is a large basin draining an area of 476,674 square kilometers in center-north Brazil. The river system is the fifth largest tributary of the Amazon flowing northward on the territories of the States of Mato Grosso, Para' and Amazonas (Figure 3-1). Main rivers in the basin are Rio Tapajós, Rio Jamanxim, Rio Teles Pires, and Rio Juruena.
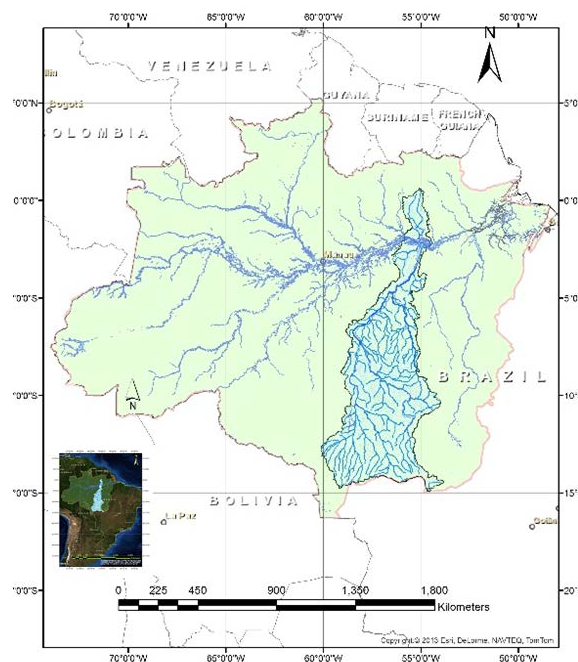


**Figure 3-1 Tapajos River basin (Light blue) and Amazon River basin (light green) geographical location.**

The basin's elevation goes from about 800 meters asl in its southern part, to about 7 meters at the confluence with the Amazon river. The geological conformation of the soils goes from deep soils within the Brazilian shield in the south to soft alluvial deposits typical of

54

the plains in the northern part, closer to the Amazon River. The region has a tropical climate with a long rainy season in the period September – May and a dry season in June-August. The precipitation is abundant, ranging from about 1,500 in the south to 2,900 mm/year in the northern part of the basin (ANA 2011; Hales & Petry 2013). Land cover varies from typical Cerrado dry vegetation in the south to tropical rainforest in the north. The portion of the basin laying in Mato Grosso State have been heavily deforested in the past to open space for agriculture (Figure 3-2), with different consequences for the local hydrological and atmospheric circulation as shown in other studies in the focused on the Amazon area (Hayhoe et al. 2011; van der Ent et al. 2010; Vergara & Scholz 2011). The northern part of the basin in the states of Para and Amazonas are largely protected for social (indigenous lands) or environmental reasons (state and national parks; ANA 2011). The Tapajos river basin economy is mainly based on agribusiness and related services.
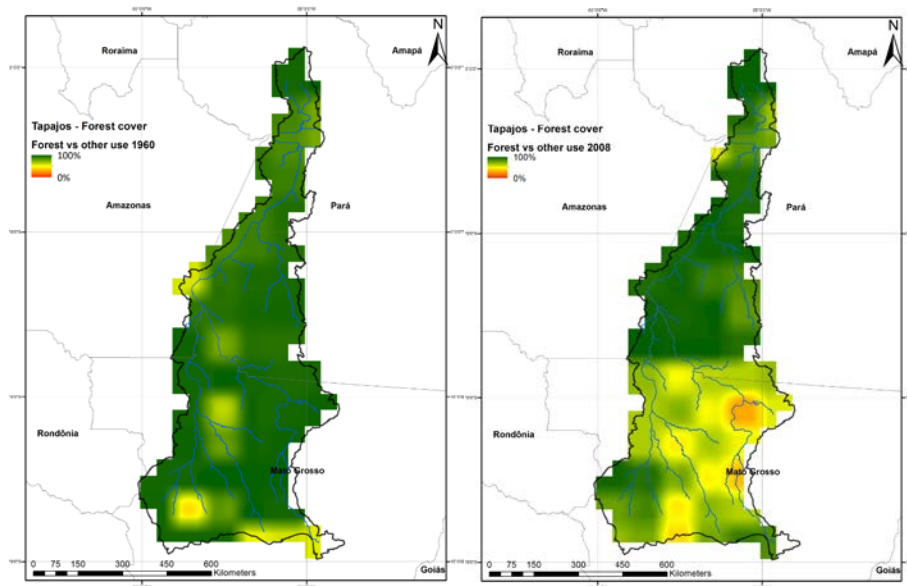


**Figure 3-2 Tapajos River basin land cover 1960 (left) vs 2008 (right). Green indicates full forest cover, red full deforestation. Author's own elaboration based on (Hurtt et al. 2011; Hurtt et al. 2006; Soares-Filho et al. 2006) data.**

## 3.2. Methodology and Data

### 3.2.1. Model description

ED2.2 terrestrial biosphere model was used to simulate vertical water fluxes through the biosphere. ED2.2 simulates ecosystem structure and dynamics as well as the corresponding carbon, energy, and water fluxes (Hurtt et al. 2013; Medvigy et al. 2009; Moorcroft et al. 2001). ED2.2 simulates the dynamics of four different tropical plant functional types: early successional trees (fast growing, low wood density, and water-needy); mid-successional trees; late-successional trees (slow growing, shade tolerant, high wood density); and $C_4$ grasses (comprehending also pasture and agriculture) (Medvigy et al. 2009; Swann et al. 2015). Each grid cell is subdivided into a series of dynamic tiles that represents the sub-grid scale heterogeneity within each cell. This characteristic of the ED2.2 model makes it suitable for a more efficient simulation of domains characterized by a mixture of natural and anthropogenically modified landscapes. ED2.2 simulates the biosphere dynamics taking into consideration natural disturbances, such as forest fires and plant mortality due to changing environmental conditions, and man-made disturbances, such as deforestation and forest harvesting (Medvigy et al. 2009; Albani et al. 2006). Disturbances are expressed in the model as annual transitions between primary vegetation, secondary vegetation, and agriculture (cropland and pasture) (Albani et al. 2006). A natural disturbance, as, for instance, wildfire, is represented in the model by the transition from primary vegetation (forest in the case of the Amazon) to grassland-shrubland and subsequently to secondary vegetation (forest re-growth); the abandonment of an agricultural area is represented with the conversion from grassland to secondary vegetation, while forest logging by the transition from primary or secondary vegetation to grassland. The model is composed of several subroutines operating at multiple temporal and spatial levels, including plant mortality, plant growth, phenology, biodiversity, soil biogeochemistry, disturbance, and hydrology (Medvigy et al. 2009; Longo

2014). It computes the fluxes of water, carbon, and energy through the vegetation, air-canopy space, and soils, which results in daily estimates of subsurface and surface runoff from each grid cell. The number of soil layers and their thickness influence the level of detail with which the model represents the soil moisture gradients. Groundwater exchange is function of the hydraulic conductivity, soil temperature and terrain topography. Water percolation is limited in the bottom layer by the subsurface drainage, determining the bottom boundary conditions. For a more complete description of the model, we refer the reader to the literature available (Moorcroft et al. 2001; Medvigy et al. 2009; Longo 2014; Zhang et al. 2015).

Daily runoff estimates from ED2.2 were computed for each specific grid cell independently, and therefore a hydrological routing scheme was linked to the model in order to estimate flow accumulation and attenuation as water moves through the landscape towards the basin outlet. The flow routing scheme was adapted from IPH-MGB, a rainfall-runoff model that has been extensively used in large river basins in South America (Collischonn et al. 2007). The native IPH-MGB model is composed of four different sub-models: soil water balance, evapotranspiration, intra-cell flow propagation, and inter-cell routing through the river network. Only the latter two sub-models were utilized as the first two are estimated with ED2.2. The resulting ED2+R model computes the daily total volume of water passing through any given grid cell in the resulting drainage network in two separate steps: first, ED2.2 estimates of daily surface and subsurface runoff from each grid cell are divided into three linear reservoirs with different residence times in order to represent overland flow (surface reservoir), interflow (intermediate reservoir) and groundwater flow (base reservoir) (Figure 3-4). This first step allows for a better representation of flow attenuation or propagation through the climatological grid cells that are relatively large (0.5°, corresponding to approximately 55 km). Water then moved from each cell into the drainage network computed from a digital elevation model (DEM) using the algorithm of Reed (2003), and

enhanced with a parameter that accurately assign flow directions to DEM grid cells over regions with meandering rivers. Each DEM grid cell therefore becomes part of a flow path, which then accumulates water to a final downstream drainage network outlet. A complete description of the technique for defining drainage networks from DEMs employed in this study can be found in Paz et al. (2006). Once water reaches the drainage network, ED2+R solves the Muskingum-Cunge equation of flow routing using a finite-difference method and as a function of river channel length and width, terrain elevation slope, and terrain roughness. Multiple groups of grid cells with common hydrological features, or hydrological response units, can be created in order to parameterize and calibrate ED2+R. In our approach, hydrological traits associated with soil and land cover are primarily computed in ED2.2, thus we calibrated ED2+R at the subbasin level as delineated from the DEM.

### 3.2.2. Parameterization and calibration of the model

ED2+R was tested in the Tapajos, one of the largest river basins discharging into the Amazon. For calibration purposes the basin was divided in seven sub-basins, each of them with a corresponding gauge for which historical daily river flow observations were available (Figure 3-3).
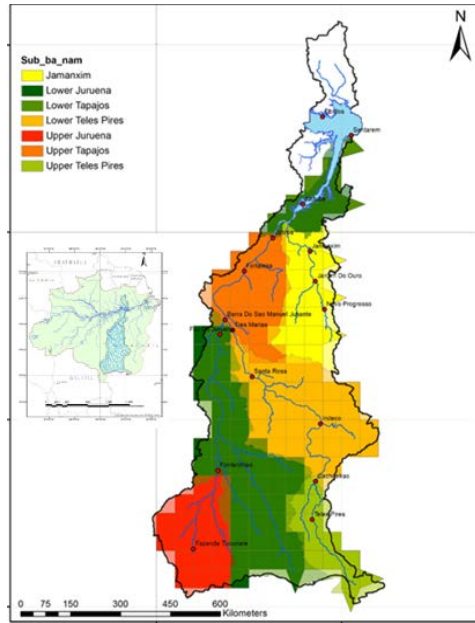
**Figure 3-3 Organization of the Tapajos basin into seven sub-basins. The domain is subdivided in cells with 0.5° resolution.**

Simulations were carried out for the period 1970-2008. ED2.2 model was forced using reconstructed climate (Sheffield et al. 2006) and land use (Hurtt et al. 2006; Soares-Filho et al. 2006) data at 1 degree spatial resolution. The meteorological data has a 3 hours temporal resolution that was downscaled to hourly resolution. Surface and subsurface runoff calculated for each cell by the ED2.2 model are connected with the three linear reservoirs of the routing scheme (Figure 3-4). Two steps of calibration were executed: a first step adjusted the flow partitioning between the native ED2.2 surface and subsurface reservoirs and the ED2+R surface, intermediate and base reservoirs (parameters $\alpha$ and $\beta$ in Figure 3-4). The second step of calibration adjusted the residence time of the flow between the ED2+R reservoirs of different grid cells in the domain (CS, CI and CB in Figure 3-4) and the base flow (QB in Figure 3-4).
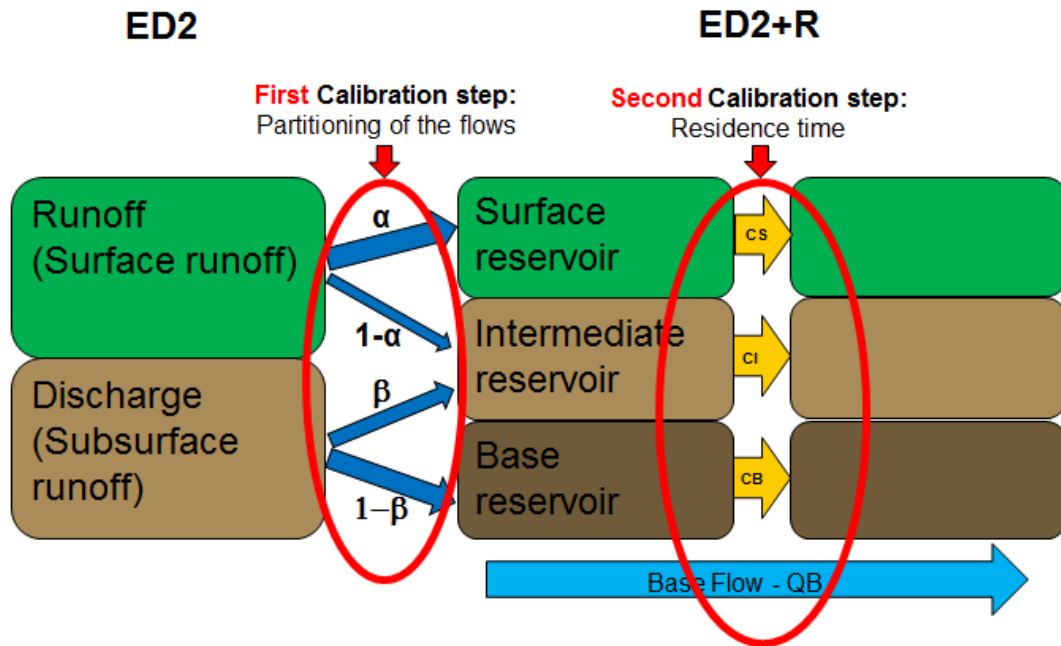
**Figure 3-4 Schematic representation of the connection between the biosphere model and the hydrological routing scheme.**

Residence times characterizing overland, intermediate and groundwater flows from a cell to another (respectively CS, CI and CB in Figure 3-4) in each of the sub-basins were calibrated using gauge observations (HYBAM and ANA) spanning a period of 17 years, from 1976 to 1992. The period 1993-2008 was used for validation, while the period 1970-1975 was not considered in order to avoid models' spin-up effects. Missing observations in the streamflow time series were filled via linear spatial and temporal interpolation between the series in neighboring gauge stations:

$$Obs_y(t) = K + \beta_1 \cdot Obs_z(t) + \beta_2 \cdot Obs_q(t) + \beta_3 \cdot Obs_y(t - 365) + \beta_4 \cdot Obs_y(t + 365)$$

$$(3\text{-}1)$$

Where $z$, $y$ and $q$ are three gauge stations with timeseries highly correlated (Pearson's r $\geq 0.85$), and $t$ expresses time in days. The estimated $\beta$ coefficients were used for the estimation of the missing observations in the site $y$.

Comparison between observations and simulated flows were carried out using Pearson's R correlation coefficient (Pearson 1895), volume ratio, and the Nash-Sutcliffe coefficient (Nash & Sutcliffe 1970).

### 3.2.3. Scenario descriptions

ED2+R model was forced using past and future climate data derived from the coupled Earth System Model (ESM) HadGem2-ES of the UK Met Office Hadley Centre (Collins et al. 2011; Collins et al. 2008; Bellouin et al. 2007; Johns et al. 2006; Martin et al. 2006; Ringer et al. 2006) for the CMIP5 project (Taylor et al. 2012). HadGem2-ES has been widely analyzed in literature (Good et al. 2013; Joetzjer et al. 2013; Sillmann et al. 2013) and found effective in reproducing the climate in the area under consideration improving the performances of the previous models (Good et al. 2013; Sillmann et al. 2013). Moreover the earth system component of this ESM was developed in collaboration with the Brazilian National Institute for Space Research (Instituto Nacional de Pesquisas Espaciais - INPE). Baseline scenario was obtained using HadGem2-ES historical simulations for the period 1985-2005; future simulation were computed using two distinct climate change Representative Concentration Pathways (RCP 4.5 – moderate, and RCP 8.5 – extreme climate change) (Vuuren et al. 2011).

Land use data were retrieved from two widely used datasets: historical data were taken from Hurtt et al. (2006 and 2011); future scenarios are based on two different simulations of deforestation, Governance and Extreme Deforestation scenarios, from Soares-Filho et al. (2006) (Figure 3-5).
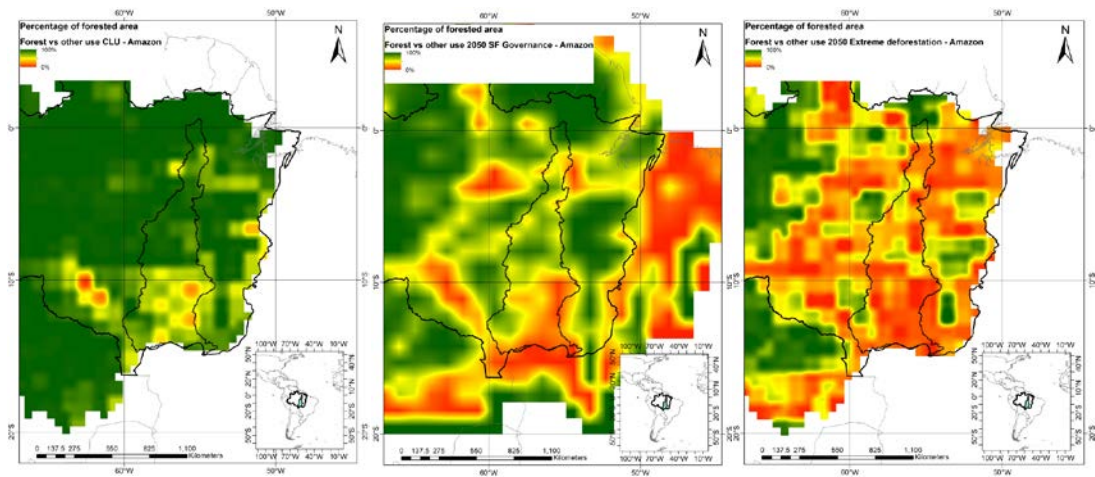
**Figure 3-5 Tapajos River basin land cover 2005 (left) vs two different 2050 scenarios: Governance (center) and Extreme Deforestation (right). Green indicates 100% forest cover, red 0%. Author's own elaboration based on Hurtt et al. (2006) and Soares-Filho et al. (2006) data.**

Different combinations of the different scenarios described above were simulated with ED2+R in order to assess the marginal contribution and cumulative effects of climate change and land use conversion. Rather than considering an exhaustive number of scenarios, the experimental setup was designed to appropriately assess the marginal contributions and cumulative effects of the two drivers of change. A total of six climate and land use scenarios were simulated (Table 3-1). All of them were simulated for a total of 20 years at daily time steps. The choice of the simulation length was made in order to efficiently balance the tradeoff between the simulation results and the constrained time and computing capacity resources.

1. Historical land use and historical climate – 1985-2005 (hereafter Baseline);

2. Constant land use (no change after 2005) and moderate climate change – 2025-2045 (noLU_rcp45);

3. Constant land use (no change after 2005) and severe climate change – 2025-2045 (noLU_rcp85);

4. Moderate land use and moderate climate change – 2025-2045 (GOV_rcp45);

5. Moderate land use and severe climate change – 2025-2045 (GOV_rcp85);

62

6. Severe land use and severe climate change – 2025-2045 (EXT_rcp85).

| Land use — Climate | 2005 Land use | 2050 Governance | 2050 Extreme Deforestation |
|---|---|---|---|
| 1986-2005 HadGem Historical | Baseline | | |
| 2026-2045 Moderate (rcp 4.5) | noLU_rcp45 | GOV_rcp45 | |
| 2026-2045 Extreme (rcp 8.5) | noLU_rcp85 | GOV_rcp85 | EXT_rcp85 |

Table 3-1 Climate and land use change scenarios produced for the flow analysis. Land use data from Hurtt et al ( 2006) and Soares-Filho et al (2006), climate data from UK Meteorological Office HadGem2-ES.

### 3.2.4. Bias correction of simulated streamflows

The streamflows resulting from the analysis were bias-corrected in order to minimize the inaccuracies arising from biases in the Earth System Model (ESM) simulations of Amazon climate (Randall et al. 2007; van Vliet et al. 2013). Several examples of bias-correction applied to hydrological simulations of future climate scenarios have been presented in the literature (e.g. Eisner et al. 2012; Hempel et al. 2013; Rojas et al. 2012; Muerth et al. 2013). The usual approach is to downscale and bias correct the meteorological inputs, typically precipitation and temperature (as for instance in van Vliet et al. 2013). As discussed in Hashino et al (2007), several techniques could be applied to bias correct meteorological forcing data: simple approaches as the 'delta factor' (Diaz-Nieto & Wilby 2005); other more sophisticated statistical approaches (Fang et al. 2015); otherwise original GCM data could be used to force a regional climate model specifically calibrated for the domain under consideration (Jacob et al. 2007). In other cases – especially in case of short

term forecasts – the bias correction was applied directly to the streamflow resulting from the hydrological analysis (e.g., Yuan & Wood 2012; Bogner & Pappenberger 2011).

In this study we chose this latter approach, applying a simple method to bias-correct the cumulative distributions resulting from our simulations of river flows from ED2+R. Two main reasons led to the choice of river flow rather than meteorological forcing bias correction: first, the bias-corrected meteorological data, in the case of the HadGem2-ES corrected data were produced within the ISI-MIP project (Warszawski et al. 2014; Hempel et al. 2013), were available at daily resolution, while the ED2.2 biosphere model requires a more detailed time resolution (we used the 3 hourly original data made available by the UK Meteorological Office); second, statistical bias-correction of meteorological data is typically applied to both temperature and precipitation. Modifying part of the variables through a statistical bias-correction could have created inconsistencies with the other variables needed for the land surface model forcing (long- and short-wave radiation – in all its components; humidity; pressure; u and v wind) causing the failure of the simulations or a cascade bias propagation.

The flow duration curves of the baseline scenario (Table 3-1) at seven different sub-basins were compared with the distribution of the historical observations from the Brazilian Water Agency (Agencia Nacional de Aguas - ANA) and the Observation Service for Geodynamical, hydrological and biogeochemical control of erosion/alteration and material transport in the Amazon, Orinoco and Congo basins (HYBAM). The ratio between the two distributions was used as multiplier to correct all the simulation datasets for the specific sub-basin (Figure 3-6). The approach was replicated for each of the seven sub-basins. As shown in Figure 3-6 (panel a), the simulation results overestimate the low values of flow, and underestimate the middle and high values. The bias-correction procedure aligns the flow

duration curves of the simulated values to the observed ones sensibly reducing the variation

of the simulated hydrograph from the observed one (Figure 3-6 panel b).
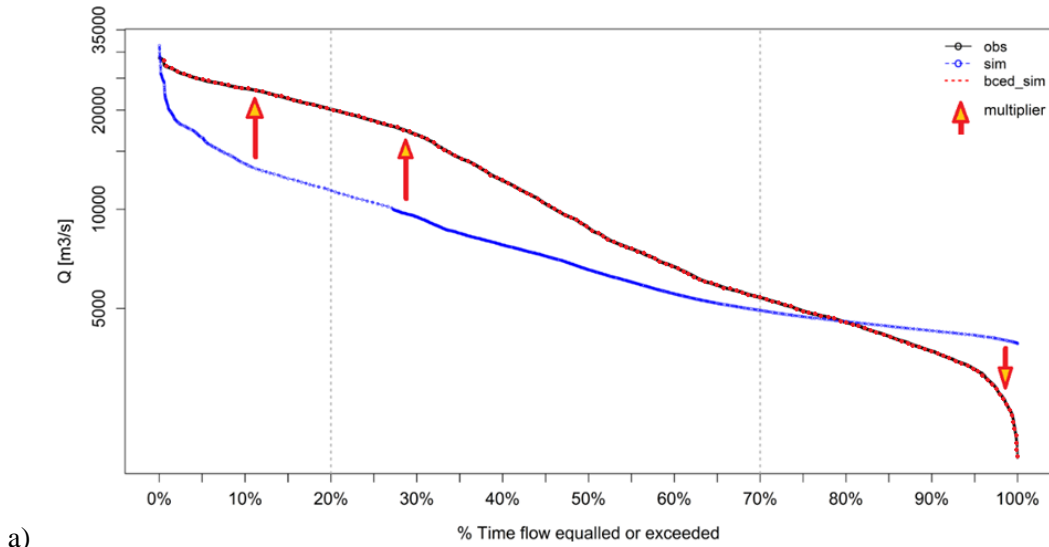


a)
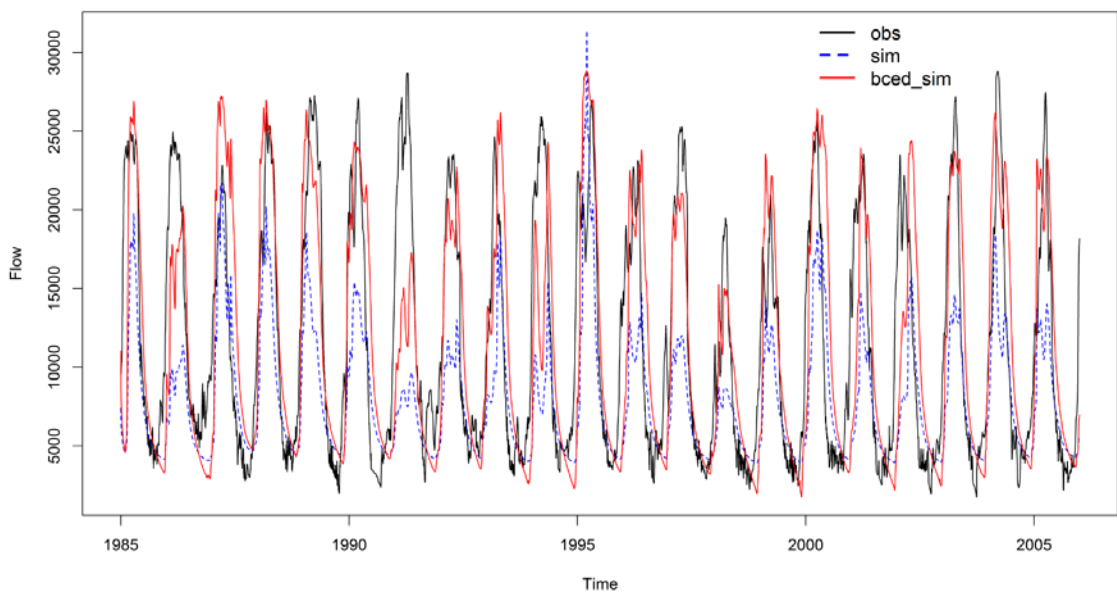


b)

**Figure 3-6 Bias correction of the streamflow at Itaituba. (a) Flow Duration Curve (FDC) of the baseline (1985-2005) scenario (sim - blue), observation (obs - black) and bias corrected (bced_sim - red). On the y axis flow (m³/s), on the x axis % of the time of exceedance of the specific threshold. (b) the three timeseries.**

### 3.2.5. Hydro-energy simulation

To assess the consequences of the hydrological alterations caused by environmental changes in the basins, the results of the routed biosphere simulation were used as input for a hydro-energy simulation, the U.S. Army Corps of Engineers' Hydrologic Engineering Center HEC-ResSim (Resevoir Simulation model) (USACE 2013).

HEC-ResSim is widely used to simulate the operations of single or cascade reservoirs in complex river systems. It consists of three main modules: watershed setup, reservoir network, and simulation (USACE 2013). River network and basin hydro-topographic characteristics were defined with the first module; the second module was used to define the hydropower reservoir characteristics and the main technical details of the power plants installed in the specific dams (dam characteristics, water levels, dead storage, head, spillways, etc.); the third module was used to simulate the reservoir operations under the 6 scenarios described above.

For the specific purpose of this paper we considered the largest dam proposed in the basin, planned to be built in Sao Luis do Tapajos, 50 km upstream of the Itaituba gauge, about 300 km from the confluence with the Amazon River. The design of the plant is a traditional run-of-the-river system (EPE, 2013); the dam is a 7.6 km long and 35.8 m high (top elevation is 54 meters above sea level), collecting the drainage from an area of 452,783 km$^2$, almost the entire basin. The total normal water storage volume is planned to be about $7,550 \cdot 10^8$ m$^3$ and a water surface of 722 km$^2$. The hydropower plant is divided in a main unit of 31 Kaplan turbines (7,827 MW), and a supplementary unit of 2 turbines (213 MW) with a total installed capacity of 8,040 MW. This particular type of turbines operate at a 92% efficiency at design flow (approximately 19,000 m$^3$/s for the entire project), but their shut down is required once inflows reach 30% of the flow.

To avoid the total shut down of the plant, turbines are typically installed at different elevations. To approximate this in our model, the installed capacity of the plant was assumed to be constant until flows dropped to 30% of design (5,800 $m^3$/s), below which the capacity was assumed to decrease linearly until it reached the equivalent production of 6 turbines in the project. The ability to modify the operational water level in this reservoir is extremely limited, considering that the operational guidelines restrict its level between 49.6 and 50 meters (asl). All technical data related to this dam were collected by the authors from the library of the Brazilian Electricity Regulatory Agency – (Agência Nacional de Energia Elétrica, ANEEL) in Brazilia. Sao Luiz do Tapajos is the largest dam planned for the basin: it was selected for this example because, given the scarce possibility to manage the water levels of the reservoirs, it is particularly sensitive to the inter- and intra-annual changes in streamflow.

## 3.3. Results

### 3.3.1. ED2+R Model calibration and validation

In Figure 3-7 we compare three different hydrographs: the outputs of the biosphere model ED2.2, the outputs of the land model integrated with the routing scheme (ED2+R), and the historical observations at the Itaituba gauge station (Lower Tapajos sub-basin). As can be seen in the figure, the integration of the routing scheme with the biosphere model substantially increases the ability of the model to reproduce the streamflows in the considered domain.

In Table 3-2 we present the results of the comparison between the native ED2.2 model, the ED2+R model and the observations at the outlet of the seven sub-basin of the domain under consideration. The table is divided in two main subsections representing the

values for two different periods: the first period was used to calibrate flow partitioning between the native ED2.2 and the ED2+R model, and the residence times characterizing overland, intermediate and groundwater flows from a cell to another (Figure 3-4); the second period was used for model validation.
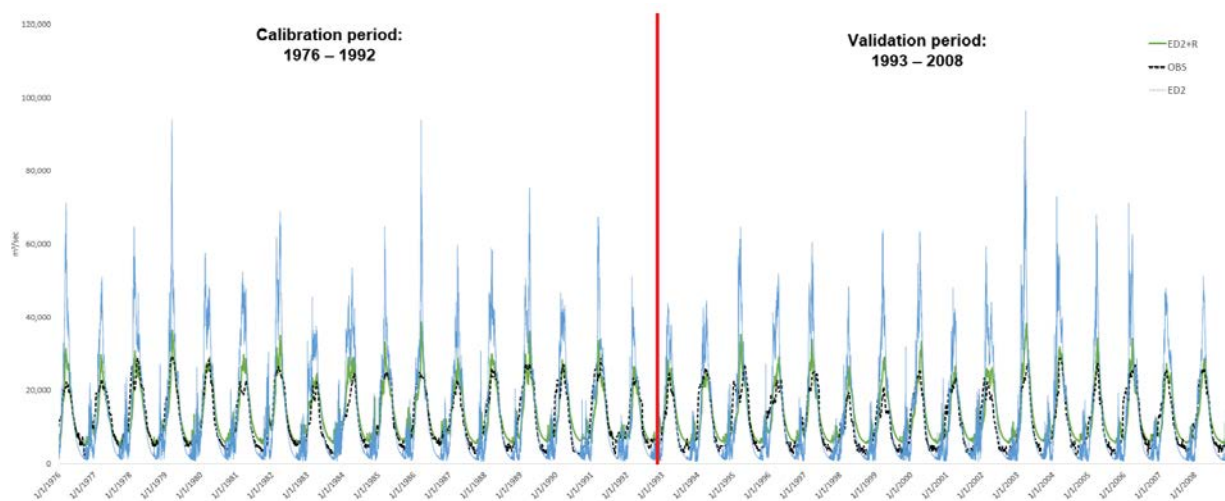


**Figure 3-7 Calibration and validation of the streamflow (m3/sec) at Itaituba (farthest downstream river gauge – Lower Tapajos sub-basin). ED2.2 output (blue line), ED2+R (green line), and Observations (black line). The red line splits the calibration and validation periods.**

The goodness-of-fit of the two simulated series with the observation is assessed using three measures: Nash-Sutcliffe (NSE), Pearson's R correlation coefficient, and volume ratio. In all the sub-basins, the application of the routing scheme allows a substantial increase of the goodness-of-fit between simulated and observed values (Table 3-2). Both routed (ED2+R) and non-routed (ED2.2) simulation results manage to reproduce reasonably well the observed water availability, in terms of volumes, in the basin; however, the application of the routing scheme improves the ability of the model to reproduce the spatio-temporal propagation of the water resources across the basin (Table 3-2 and Figure 3-8). The performance of the model in simulating the river flows in the basin is generally higher in the downstream sub-basins and poorer in the headwaters. This is due to two main causes: the spatial resolution of the land model, and the assumptions made for the bottom soil layer boundary that affects the base

68

flow. Both these characteristics are widely discussed in literature (Zulkafli et al. 2013; Smith et al. 2004; Lobligeois et al. 2014) and are mainly linked to the limitations in the spatial resolution of the input data for global or regional scale biosphere simulations as well as the computing capacity.

| Sub-basin | Calibration period (1976-1992) | | | | | | Validation period (1993-2008) | | | | | |
|---|---|---|---|---|---|---|---|---|---|---|---|---|
| | Nash-Sutcliffe | | Correlation | | Vol sim/Vol Obs | | Nash-Sutcliffe | | Correlation | | Vol sim/Vol Obs | |
| | ED vs OBS | ED2+R vs OBS | ED vs OBS | ED2+R vs OBS | ED vs OBS | ED2+R vs OBS | ED vs OBS | ED2+R vs OBS | ED vs OBS | ED2+R vs OBS | ED vs OBS | ED2+R vs OBS |
| Upper Juruena | -26.88 | **0.45** | 0.61 | **0.68** | 0.72 | **0.98** | -27.47 | **0.29** | 0.53 | **0.54** | 0.68 | **1.01** |
| Upper Teles Pires | -3.35 | **0.37** | 0.53 | **0.64** | 0.94 | **1.01** | -3.19 | **0.28** | 0.57 | **0.63** | 0.96 | **1.03** |
| Lower Juruena | -1.45 | **0.65** | 0.77 | **0.82** | 1.02 | 0.94 | -2.17 | **0.63** | 0.75 | **0.81** | 1.05 | 1.08 |
| Lower Teles Pires | -0.20 | **0.7** | 0.80 | **0.85** | 1.01 | 1.02 | -0.34 | **0.67** | 0.82 | **0.85** | 1.11 | 1.17 |
| Jamanxim | -0.74 | **0.67** | 0.82 | **0.85** | 1.55 | **1.13** | -0.1 | **0.55** | 0.83 | 0.77 | 1.43 | **1.09** |
| Upper Tapajos | -1.01 | **0.77** | 0.84 | **0.88** | 1.20 | **0.99** | -1.23 | **0.75** | 0.84 | **0.88** | 1.21 | **1.08** |
| Lower Tapajos | -0.40 | **0.76** | 0.84 | **0.88** | 1.11 | **1.06** | -0.5 | **0.68** | 0.82 | **0.86** | 1.13 | 1.13 |

Table 3-2 Calibration and validation results. Nash-Sutcliffe, Pearson's R and volume ratio optimal values = 1 ; in bold the values where the ED2+R results increase the performance of the non-routed results (ED2.2).

Upper Teles Pires and Upper Juruena have the lowest NSE: in these two sub-basins the model does reproduce reasonably well the water volumes, while the seasonal variability is less accurate. The NSE and correlation values substantially increased in the central and lower part of the basin determining the overall good result (Table 3-2 and Figure 3-8). The Jamanxim basin results, especially during the validation period, are affected by the very short and fragmented observation time series.

In Figure 3-8, we present the flow duration curves of the two simulations outputs and the observations for each of the sub-basin under consideration. The flow duration curve represents the probability of the flow values to exceed a specific value. Also in this plot, it is possible to see the substantial improvement of the model results applying the routing scheme. As seen in the figure, the simulated flow duration curves (red lines) match almost perfectly

the observations (blue lines) in the further upstream sub-basins, especially in the cases if the Upper Juruena and Upper Teles Pires. Downstream the model shows a general tendency of overestimating the lowest values of the distribution. This is evident also in the hydrograph in Figure 3-7, where the modeled values (green line) tend to overestimate the observations (black dotted line) in their lower peaks, during the dry seasons of the period under consideration.
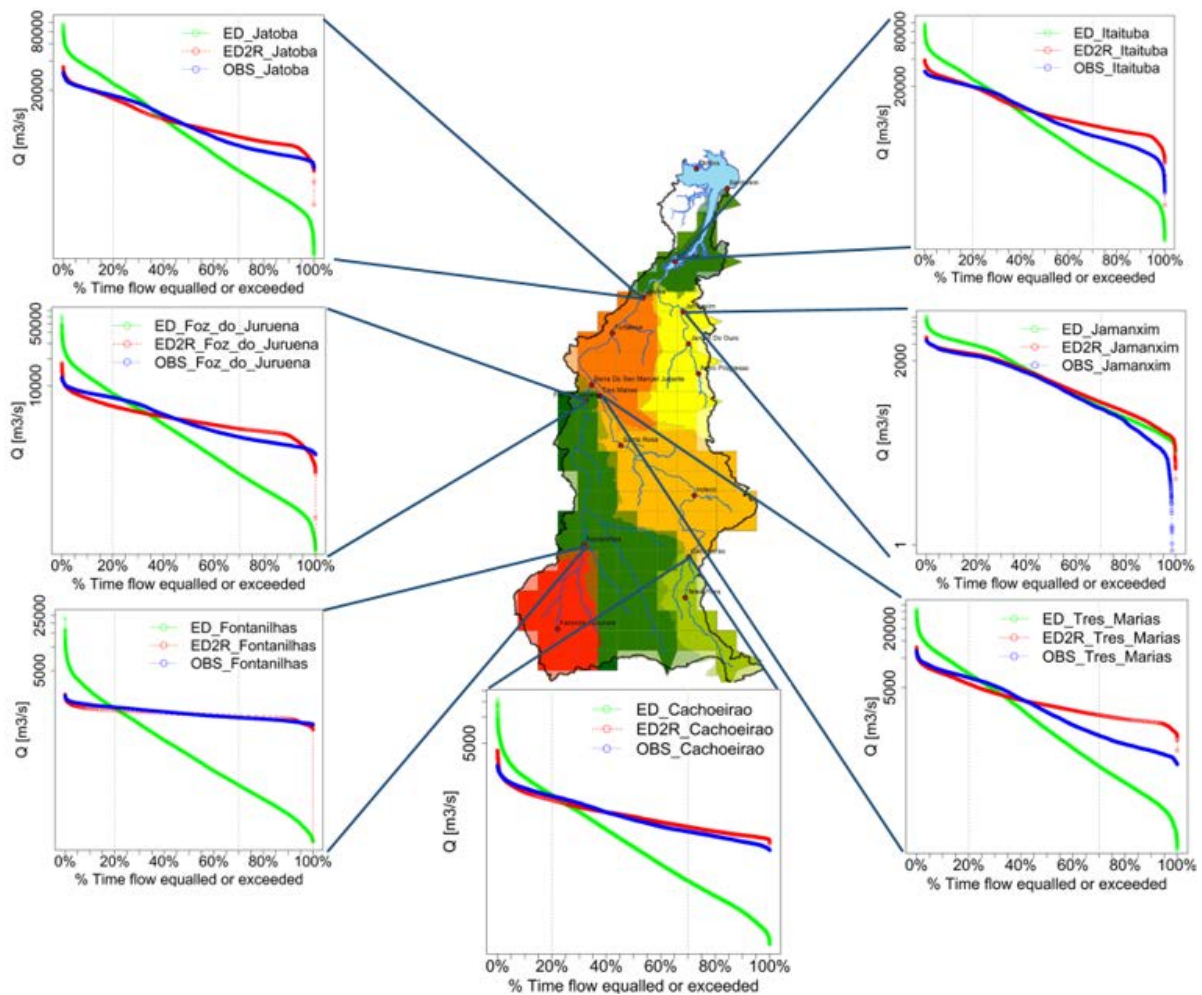


**Figure 3-8 Flow duration curves (percentage of time that flow – m3/s – is likely to equal or exceed determined thresholds) of observed values (blue), ED2.2 outputs (green), ED2+R (blue) at the outlet of the seven sub-basins.**

### 3.3.2. Future hydrological projections

Four main messages could be highlighted from the results we are presenting in this section:

1. Future climate scenarios, both moderate (RCP 4.5) and severe (RCP 8.5) are likely to cause a decline in the streamflow throughout the year;

2. Moreover, a substantial delay in the beginning of the wet season and a reduction in its duration is observed;

3. Land use change (deforestation and conversion to agriculture) is likely to increase the runoff and somehow compensate, at least in the short term, the impact of climate change in terms of flow reduction; in particular we observed that the reduction effect of climate change is expected to overrule the increasing effect of the Governance deforestation scenario and only compensated by the Extreme one;

4. The combination of climate land use change is expected to consistently increase the intra- and inter-annual variability in river flow.

71

### 3.3.2.1. Climate change effects

Figure 3-9 presents the flow duration curve of the six calculated scenarios (baseline, plus the five future projections) at the Itaituba station (Lower Tapajos sub-basin, in the state of Pará), the basin's furthest downstream flow gauge (full timeseries plots are available in Annex B , Figure B-1). Climate change is expected to consistently reduce daily flows throughout the year (panel b in Figure 3-9). This could be translated in a reduction of the volume of water available in the river system and a reduction of the highest and lowest peaks. The seasonal distribution of the climate change impact is shown in the panel b of Figure 3-10: future climate conditions are expected to cause a temporal shift of the seasonal flow pushing onward the beginning of the wet season of several weeks (panel b in Figure 3-10). Moreover the overall duration of the wet season is expected to be shortened. The seasonal peak month in streamflow is expected to shift from the period March-April, of the baseline scenario, to the month of May. Surprisingly, the severe climate change scenario (RCP 8.5) is not expected to exacerbate in magnitude the impacts on the river system: in some periods of the year its median values are higher than the ones associated with the moderate climate scenario (RCP 4.5) (panel b in Figure 3-9 and Figure 3-10). The main difference between the two scenarios is mainly represented by the variability of the flow throughout the year. Severe climate change (RCP 8.5) is expected to consistently increase the flow variability in both dry and wet seasons, more than the more optimistic scenario (RCP 4.5). Especially during the wet season,

there is a higher probability of a reduction in river flow. These results are confirmed also analyzing the maximum, minimum and average daily value of the different scenarios time series (Figure 3-10). Panels b and c of Figure 3-11 show the shift in seasonality, the contraction of the wet season (especially with the more severe climate scenario – RCP 8.5), and the substantial reduction of the maximum and minimum daily flows.



a)       All the scenarios



b)       Only climate change

**Figure 3-10 Monthly boxplot of the daily flow values for the baseline (1985-2005) and future (2025-2045) climate and land use change scenarios at Itaituba. On the y axis flow (m³/s), on the x axis months (from November to October). Baseline scenario in grey; no land use and moderate climate change (noLU_rcp45) in green; no land use and severe climate change (noLU_rcp85) in orange; moderate land use (Governance) and climate change (GOV_rcp45) in light-blue; moderate land use (Governance) and severe climate change (GOV_rcp85) in dark-blue; severe land use (Extreme) and severe climate change (EXT_rcp85) in red.**

### 3.3.2.2. Land use change effects

The general impact of the introduction of land use change, in the specific case deforestation, in our analysis has the expected trend of increasing runoff. The Extreme Deforestation scenario compensates the impacts of climate change (panel d in Figure 3-9 and Figure 3-10). The impact of climate change is expected to override the Governance scenario (panel d in Figure 3-9 and Figure 3-10). In probabilistic terms, as highlighted in Figure 3-9, the anthropogenic disturbance on land cover brings the flows of the future projections at the values of the baseline scenario. This is particularly evident analyzing the flow duration curve of the combination extreme deforestation and severe climate change (EXT_rcp85). Heavy deforestation compensates the impacts of climate change and overrules the baseline scenario for flow values below 95% exceedance (almost the entire distribution, except very low flow values). In the GOV_rcp85 scenario, instead, this happens only for values below 40% exceedance (medium, high, and very high values). Nonetheless, the interpretation of the flow duration curve alone could be partial and misleading. As highlighted in Figure 3-10 and Figure 3-11, in fact, the flows resulting from both the deforestation scenarios maintain the features of the two associated climate change scenarios adding a substantial increase in variability. In particular, the most extreme case (EXT_rcp85) is expected to increase the variability of both the higher and the lower flows with a general reduction of the median values respect to the baseline. The results associated with the mildest land use change scenario (Governance) are placed in the middle between the two extremes (no and extreme land use change) in combination with both the climate scenarios.

a)     Baseline
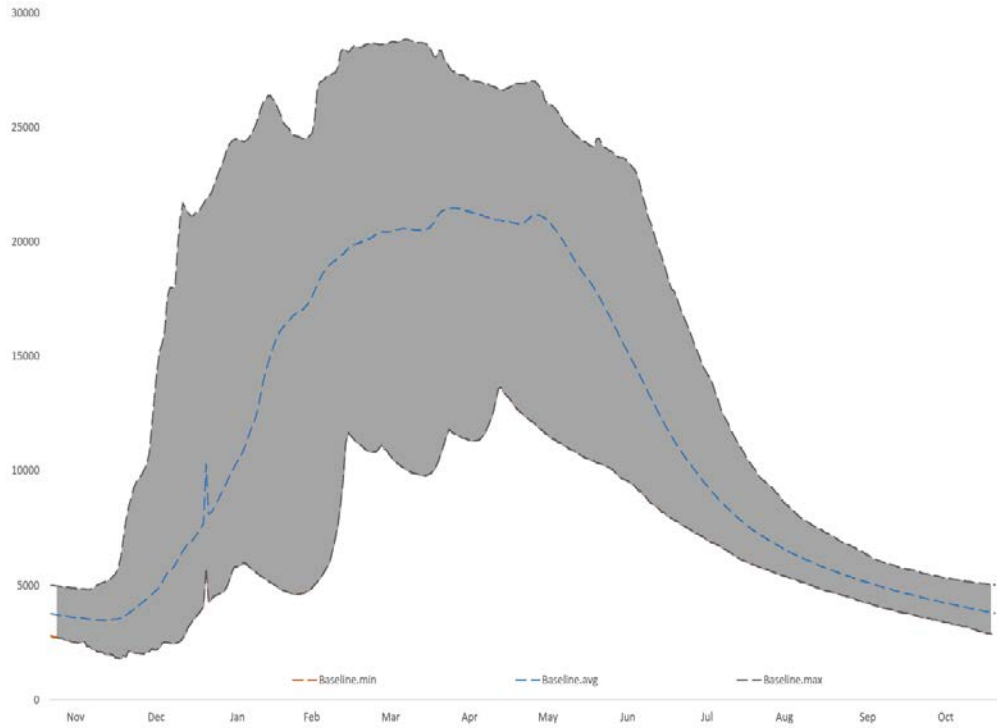


b)     No Land use – RCP 4.5
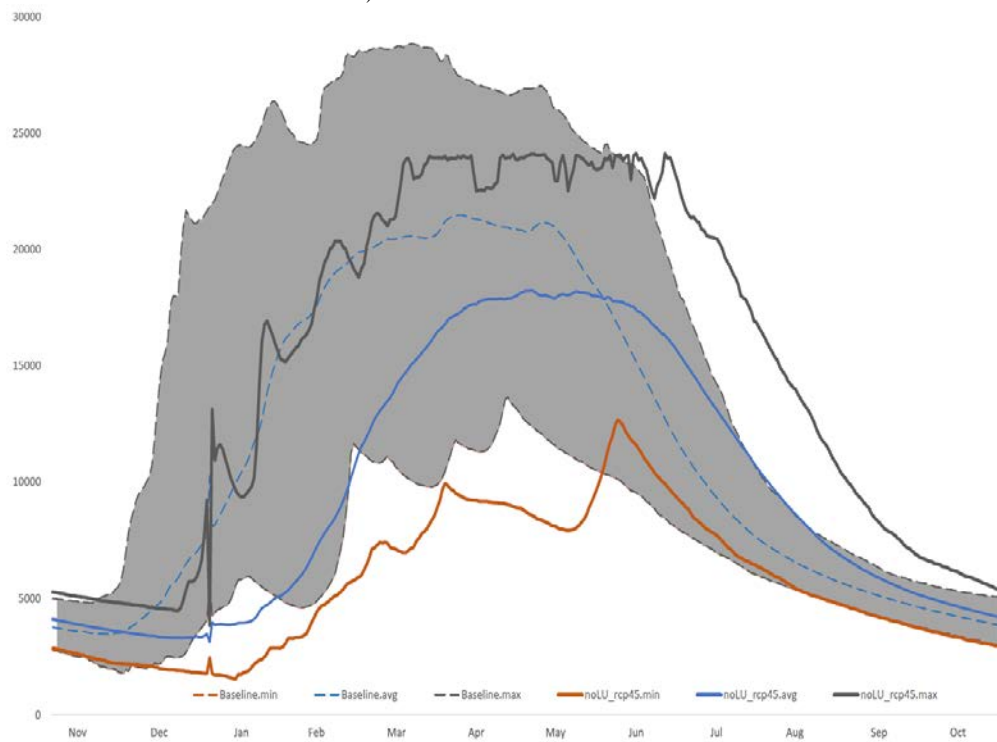
c) No Land use – RCP 8.5
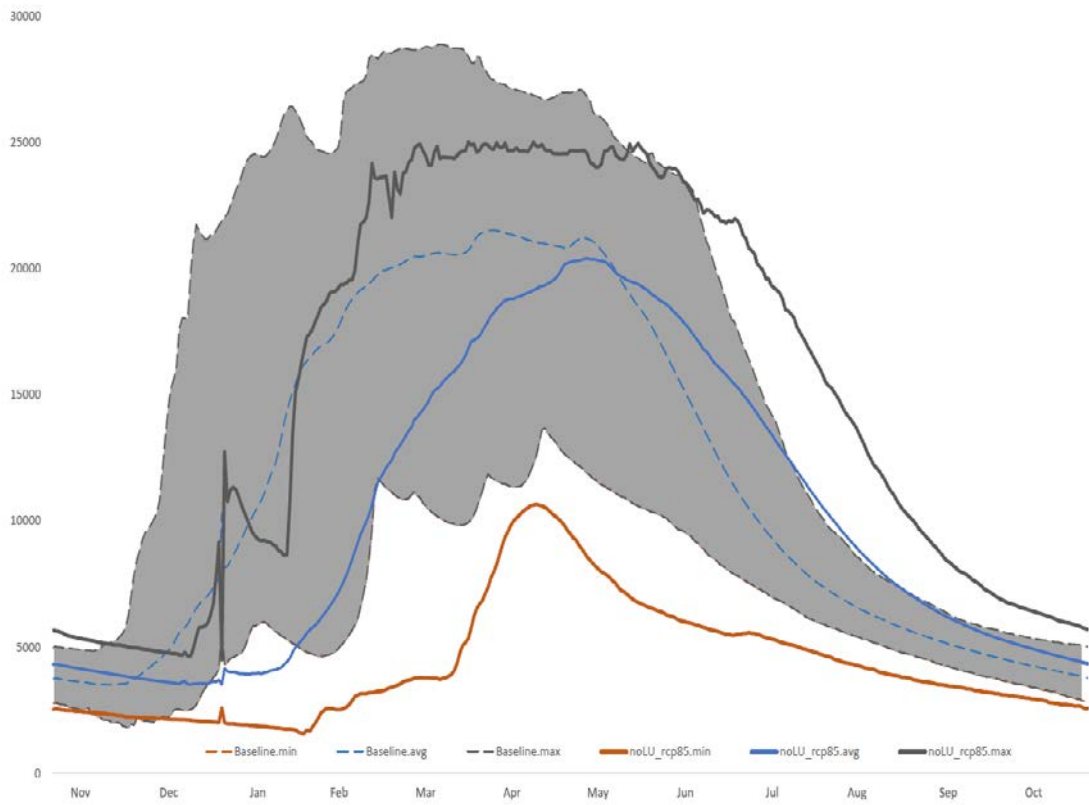


d) Governance Land use – RCP 4.5



77
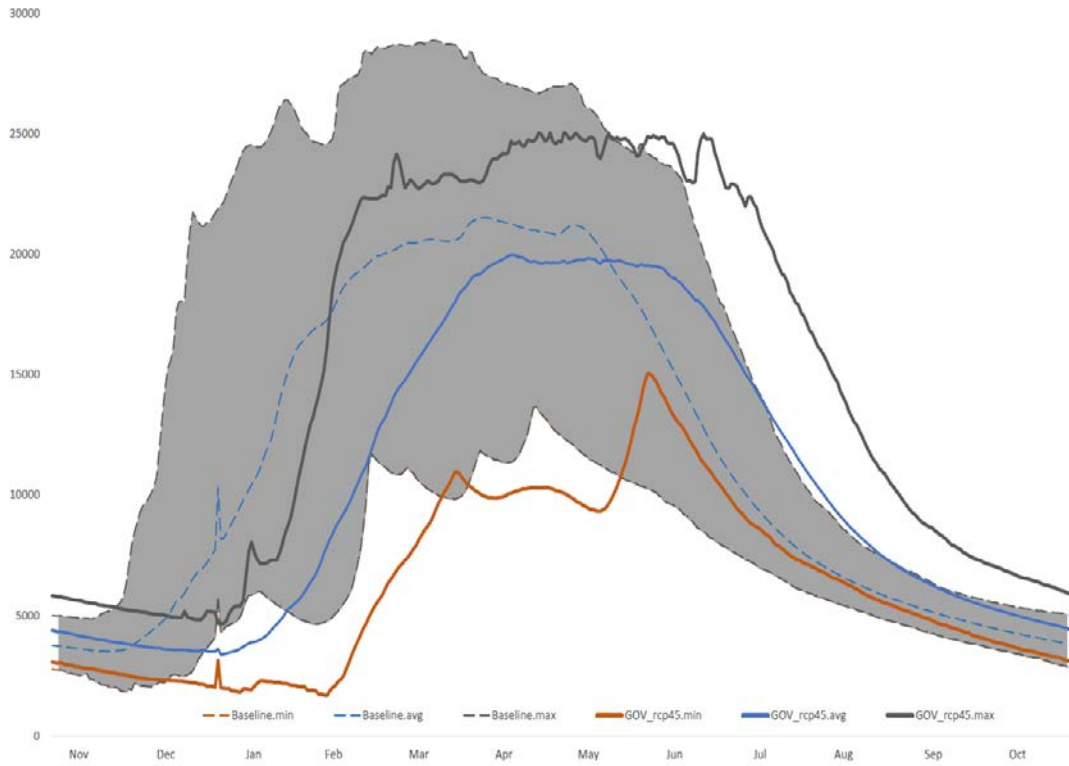
e) Governance Land use – RCP 8.5
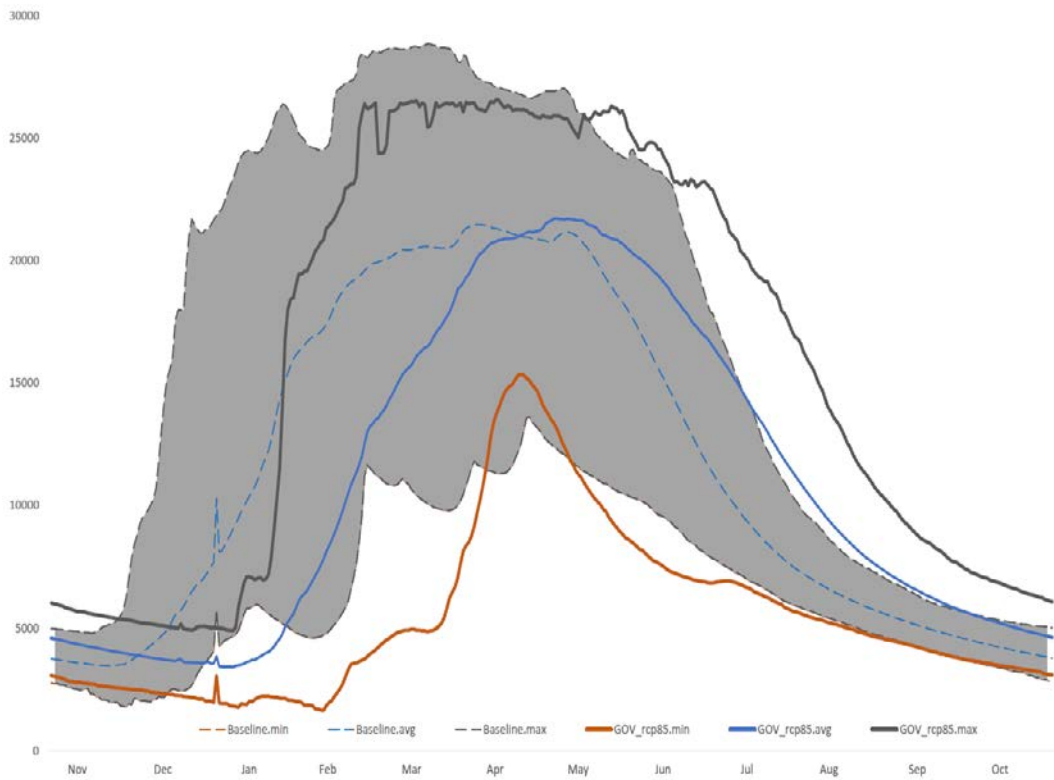


f) Extreme Land use – RCP 8.5
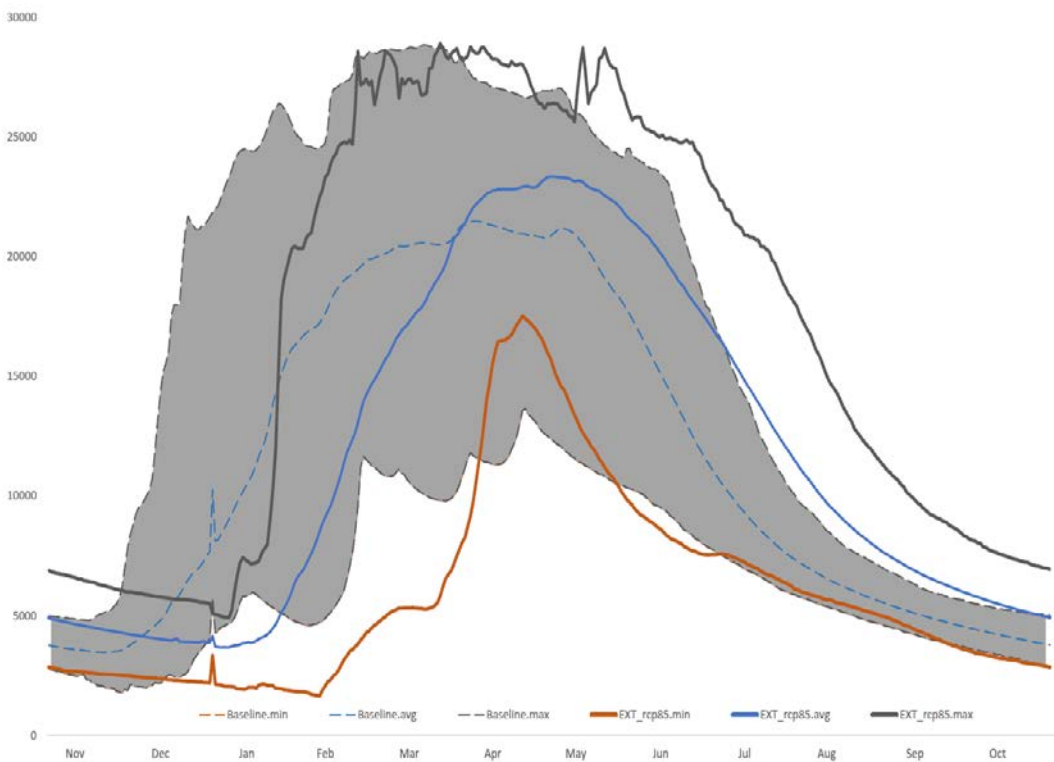


**Figure 3-11 Average, minimum and maximum daily flow values for the baseline (1985-2005) and future (2025-2045) climate and land use change scenarios at Itaituba. On the y axis flow (m³/s), on the x axis time (from November to October).**

78

### 3.3.2.3. Spatial variability

Figure 3-12 presents the spatial distribution of the impacts calculated using the different future scenarios throughout the basin. In particular, the histograms present the percentage variation from the baseline flow duration curve of the five future scenarios combining climate and land use change. The Upper Juruena sub-basin is the portion of the case study area where we estimated the lowest impact, while largest modifications to the streamflows were estimated in the Jamanxim river. Except for this subbasin, the highest variations are registered in the part of the distributions reserved to the highest flow values, thus associated with the wetter portion of the years. The general contrasting trends of climate and land use change are evident for all sub-basins. Moreover, the increasing variability associated with the introduction of deforestation in the simulations is particularly evident in the sub-basins where the flows are greatest: Lower Juruena, Upper and Lower Tapajos. One particular aspect to be highlighted is the completely different behavior of the two furthest upstream sub-basins: the Upper portions of Juruena and Teles Pires. In the Upper Juruena the model registered a limited difference between the scenarios under consideration; while in the Teles Pires the impacts are more substantial and various especially in the upper part of the distribution.
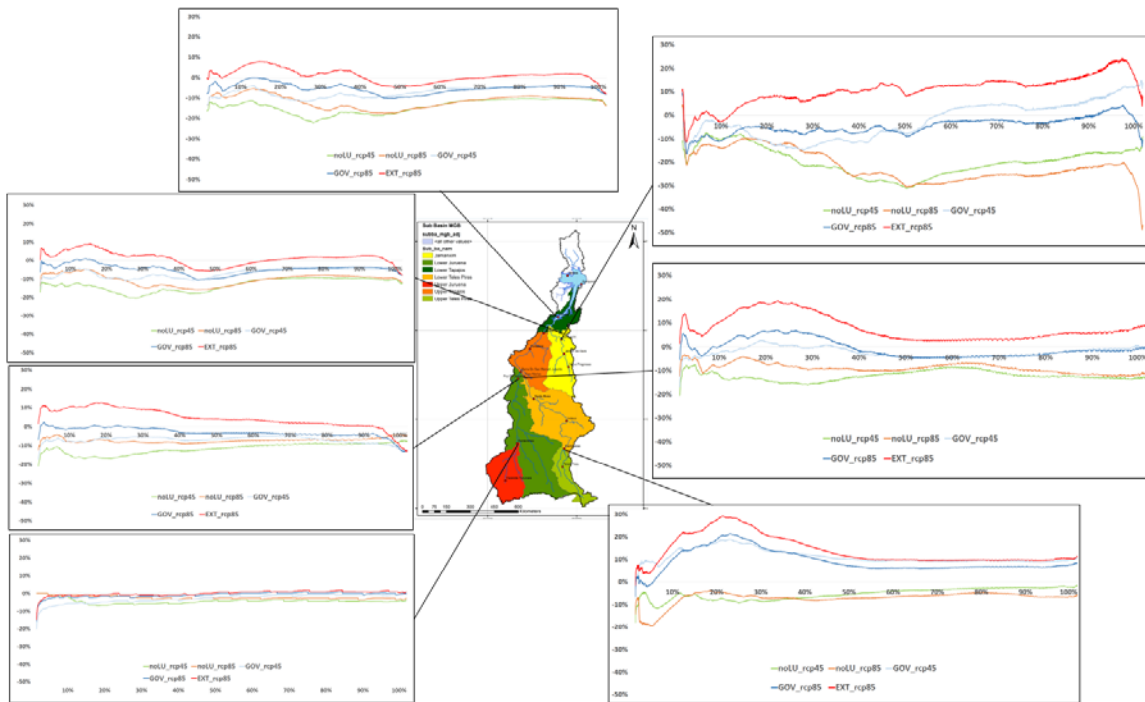
**Figure 3-12 Percentage variation respect to the baseline flow duration curve (FDC) (1985-2005) and future (2025-2045) climate and land use change scenarios for the 7 sub-basins. On the y axis percentage variation (-50% to +30%), on the x axis percentage time of exceedance of a specific flow. No land use and moderate climate change (noLU_rcp45) in green; no land use and severe climate change (noLU_rcp85) in orange; moderate land use (Governance) and climate change (GOV_rcp45) in light-blue; moderate land use (Governance) and severe climate change (GOV_rcp85) in dark-blue; severe land use (Extreme) and severe climate change (EXT_rcp85) in red.**

### 3.3.3. Implications for hydropower production

The streamflows resulting from the six scenarios were used to run a reservoir routing and hydropower simulation model. Given the nature of the experiment and the technical characteristics of the Sao Luiz do Tapajos dam – a run-of-the-river dam with minimal possibility to vary the water levels – the simulated electricity production follows similar patterns as streamflows. However, this example should be considered emblematic for the possible behavior of the hydropower system planned for the Tapajos. Most of the plants designed for the basin are run-of-the-river, and only few relatively small dams have the

80

possibility to operate the water levels of few meters (ANEEL). This means that the entire

planned hydropower system is vulnerable to inter- and intra-annual flow variability.

a)



b)
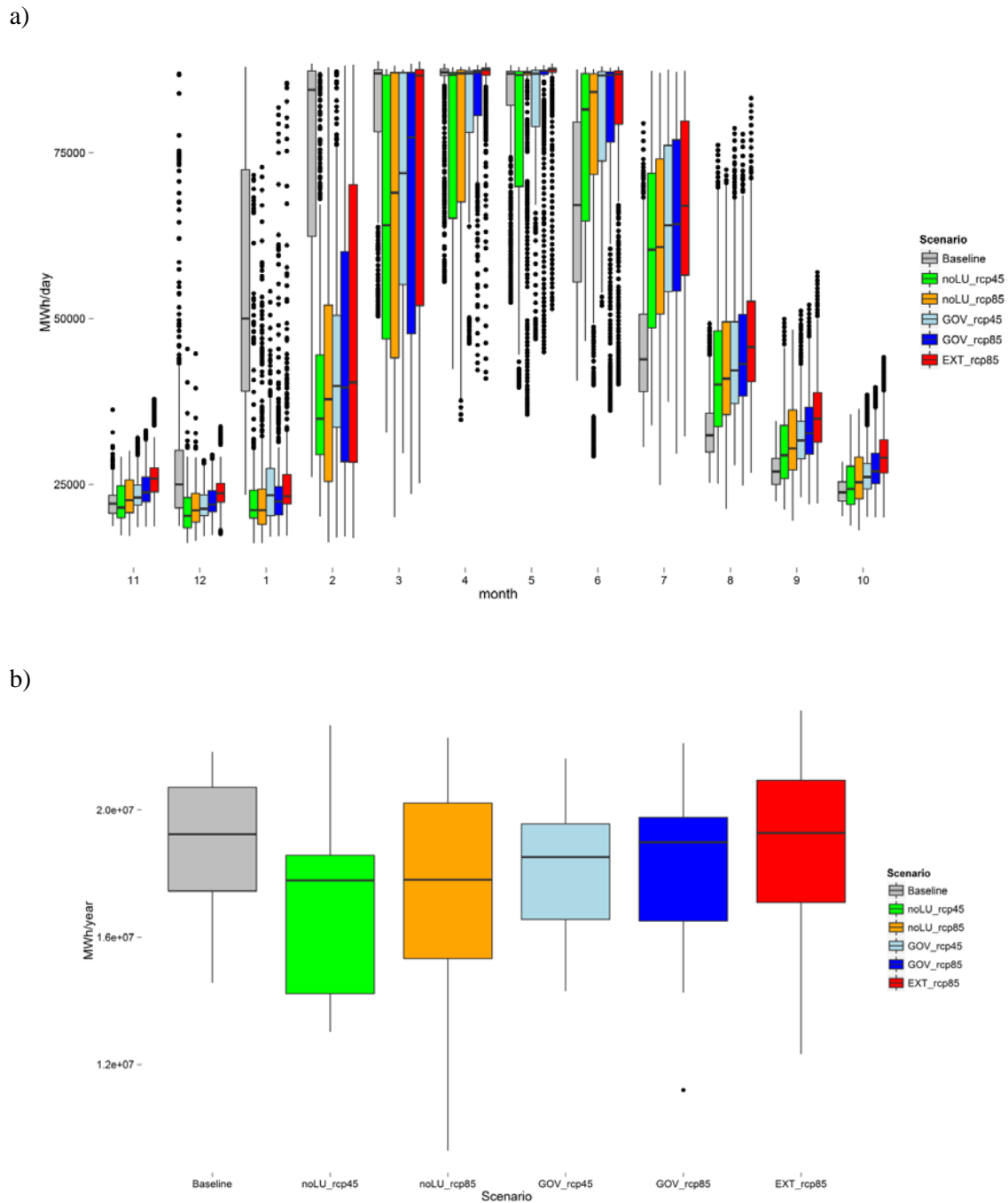


**Figure 3-13 Hydropower production at Sao Luiz do Tapajos. a) daily production (MWh/day) by month; b) annual production (MWh/year) for the periods 1985-2005 for baseline and 2025-2045 for the future scenarios. No land use and moderate climate change (noLU_rcp45) in green; no land use and severe climate change (noLU_rcp85) in orange; moderate land use (Governance) and climate change**

Overall, the simulations of hydropower generation for the Sao Luiz do Tapajos shows a net reduction in seasonal and annual production for most scenarios with the exception of the extreme case (Figure 3-13). Regarding the yearly cumulative values (panel b), we can immediately identify the distinct effects of climate and land use. The electricity generation at Sao Luiz do Tapajos is expected to be substantially affected by change in climate, with higher impacts in terms of magnitude with the moderate climate change scenario (RCP 4.5) and in variability with the severe scenario (RCP 8.5). Deforestation is expected to increase the runoff, at least in the short term, and consequently mitigating the impact of climate change on hydro-electricity generation. The most extreme scenario (EXT_rcp85), in terms of yearly cumulative production, is expected to be of similar magnitude as the baseline scenario, but a significant increase in monthly and inter-annual variability is expected.

Similar results could be highlighted for the seasonal distribution of the production. Future climate is expected to bring a consistent delay in the seasonal distribution of the flow, which is reflected in the electricity production (panel a in Figure 3-13). The losses in production are consistent throughout the year considering only climate change, the introduction of land use reverts the trends increasing inter- and intra-annual variability. Another detail to consider is the decrease in all the scenarios of the very low flows (above 95% exceedance in Figure 3-9). The general decrease of flows in the very dry periods could increase the probability and duration of shutdown of the plants due to low flows.

## 3.4. Discussion

The results presented in this paper are based on the analysis of the combined possible impacts of climate and land use change on the river flows in a specific portion of the Brazilian Amazon. We explored the complex dynamic through a series of simulations in a

terrestrial biophysical model integrated with a routing scheme (ED2+R) forced with two scenarios calculated by an IPCC-AR5 climate model, and two different land cover scenarios. Our scope was twofold: one the one hand, we aim at understanding and quantifying the individual and combined impacts caused by the two main environmental changes analyzed; on the other hand we aim at producing reliable streamflow scenarios able to constitute the base for additional water related studies in the area, in particular for agricultural productivity and hydropower future development.

The climate model results used for this analysis (HadGem2-ES) has been widely analyzed in literature (Good et al. 2013; Joetzjer et al. 2013; Sillmann et al. 2013) and found effective in reproducing the climate in the area under consideration (Good et al. 2013; Sillmann et al. 2013). As shown by previous studies, in fact, changes in sea surface temperature in the tropical portions of the oceans, cloud dynamics, and vegetation response are the main causes of uncertainty in the simulation of tropical climate (Li et al. 2006). Cox et al (2000 and 2004) highlighted, on the one hand how General Circulation Models (GCM) and Earth System Models (ESM) tend to underestimate the precipitation in the Amazon; on the other hand, how the projected decreasing trends, in combination with the feedbacks from the tropical biome, is likely to cause a catastrophic future scenario. The HadCM3-LC IPCC-AR4 model, in a business as usual scenario, projected the almost complete dieback of the Amazon forest (Cox et al. 2004). The introduction of the new generation of ESMs, in particular here we refer to the new generation of the Hadley Center models (HadGem2-ES), produced slightly more optimistic projections, but confirmed in part the possibility of Amazon forest dieback. These results were recently confirmed by two studies based on the feedback between decreasing precipitation and forest productivity in the Amazon (Hilker et al. 2014; Zhang et al. 2015). Our results confirmed the dominant trends of climate change in the hydrological cycle of the case study area. Climate change, in both moderate and severe scenarios, is

expected to substantially reduce the annual streamflow in the Tapajos river basin delaying the beginning of the rainy season and reducing its duration. Moreover the peak flows in both rainy and dry season are expected to generally decrease.

Deforestation is expected to have, in general, a less dominant trend in terms of impacts on the hydrology in the area under consideration. It is important to highlight that the simulations conducted for this study do not incorporate vegetation-climate feedbacks, which would have probably dampened the direct effects of deforestation (Swann et al. 2015; Zhang et al. 2015). Deforestation, in fact, impacts on evapotranspiration, one important component of the precipitation in the area (van der Ent et al. 2010; van der Ent et al. 2011).

In line with the existing literature on this topic (Bosch & Hewlett 1982; Andréassian 2004; Brown et al. 2005; Bruijnzeel 1990; Sahin & Hall 1996), we found that land use change is likely to invert the streamflow decreasing trends caused by climate change and to increase overall variability. These results are consistent with the data collected during the experiments conducted in the neighboring Xingu basin (Dias et al. 2015; Hayhoe et al. 2011). In particular, Pinto Dias et al (2015) found that in the small catchments they analyzed, the conversion of forested land to soybean production brought an average increase in discharge of almost 100%.

A significant contribution of this paper to the study of future hydrological changes in large basins is the use of the biosphere model (ED2.2) that simulated vegetation and hydrological dynamics at the plant patch level, and dynamically simulate the human and natural disturbances over time.

As mentioned above, climate change is expected to impact the basin rather homogeneously, with some different degrees of sensitivity between the larger and the smaller sub-basins. The impact of deforestation, on the other hand, is more evident in the Eastern part of the basin, especially in the headwaters. The relatively higher sensitivity of the Upper,

84

Lower Teles Pires, and Jamanxim, respect to the other sub-basins, is likely to be linked with the topographic characteristics of the specific areas. Moreover, as discussed in Arias et al (forthcoming), the relatively lower water accumulation of these hydrological units means that impacts of environmental changes on flows are more evident. Sub-basins characterized by higher flows and larger areas (like Lower Juruena, Upper and Lower Tapajos), in fact, are more likely to be more resilient to climate and land use changes, at least until the tipping point in deforestation (when rainfall begins to be affected) is reached.

The results of this analysis are particularly important to provide policy makers with relevant information about the future development of the area. Brazil is planning to extensively exploit this basin for hydropower production, with the construction of up to 44 dams (EPE 2013), some of which are particularly significant in terms of size, such as the Sao Luiz do Tapajos considered in this chapter. Due to the specific topography of the basin, almost all the plants planned for the Tapajos, Jamanxim, Juruena, and Teles Pires sub-basins are designed as run-of-the-river (with limited or no storage capacity). As noted earlier, the lack of storage would make the hydropower production completely dependent on daily to weekly streamflows, with very little or no possibility to buffer the seasonal and sub-seasonal variability. Overall reduction of the streamflows, jointly with the shift and the shortening of the wet season, could seriously impact the productivity of the planned hydropower system. Moreover, the climate patterns in the southern part of the basin are expected to impact the agricultural sector, main economic resource of this area. The possible decline in the rainfed agricultural productivity driven by climate change could push the farmers to invest in adaptation strategies that could include irrigation. This would further increase the anthropogenic pressure on the river flows and represent a competitive water demand for the energy sector.

## 3.5. Conclusions

In this study we used the biosphere model ED2.2 integrated with a routing scheme (ED2+R) to analyze the hydrological alterations caused by the two main environmental changes, climate and land use, in a large basin of the Brazilian Amazon, the Tapajos. Land surface models are extremely efficient tools to study the hydrological dynamics under climate and land use changing conditions. These models are usually set to simulate long periods in large domains, usually at global or continental scale. Their ability in reconstructing the water balance at relatively fine geographical and temporal resolution taking into consideration global dynamics, makes them powerful instruments for hydrological simulations. In order to translate the results of the land surface simulation in terms of river flows, the simulated results need to be processed using a hydrological routing scheme. The results showed that the integration of a land surface model with a routing scheme substantially improves the ability of the land surface simulation to reproduce the hydrological and streamflows dynamics at basin scale.

We used the integrated model to simulate different combinations of climate and land use change disturbances for the period 2025-2045, comparing the results with respect to a baseline scenario shaped on the climate and land use of the period 1985-2005. We analyzed the hydrological alterations caused by climate change simulating the land surface dynamics forcing our biosphere model with two climate scenarios estimated by the Earth System Model HadGem2-ES. Human disturbances on land use were simulated using two scenarios with two different degree of deforestation, one more limited, and the other more extreme. Our model results confirmed that the two environmental drivers will affect the area in similar ways as what experimental evidence has revealed so far in the area. Climate change is expected to consistently reduce the streamflows in the river system throughout the year, bringing a considerable delay in the flow seasonality and increasing the overall variability. Land use

change is expected to partially reduce the diminishing trend in flow, with increasing impact on the inter- and intra-annual variability. The cumulative effect of both drivers, however, appears to be dominated by global climate change effects, except for when the extreme deforestation case is considered. Although not directly considered in this study, the inclusion of biosphere-atmosphere feedbacks in the extreme deforestation scenario is expected to reduce precipitation in the region, and therefore we expect the drying effect of climate change to actually drive future patterns in the foreseeable future. The streamflows resulting from our analysis were used to run a hydro-energy model (HEC-ResSim) simulating the operation of one of the big dams planned for the basin, Sao Luiz do Tapajos. The theoretical productivity of the plant follows the hydrological trends, stressing how the designed hydropower system, due to the general lack of storage capacity, is incapable to buffer the flow variability. This element makes the hydropower system, planned to be a substantial part of the national electric supply, extremely vulnerable to hydrological alterations caused by the combined effect of climate and land use change.

# 4. Agricultural adaptation to climate change: evidence from the Upper Tapajos River Basin[6]

## Abstract

Brazil is amongst the main agricultural producers and exporters in the world. Agriculture is one of the main causes of deforestation especially in the region of Cerrado and the southern part of the Amazon forest. One of the most productive parts of the country, in this context, is the state of Mato Grosso, where the extremely favorable climatic conditions allow rainfed production of mainly soybean, maize, rice and cotton with two production cycles per year. This study examines the sustainability of rainfed agriculture in 49 counties in the upper Tapajos river basin, in the state of Mato Grosso. It analyzes agricultural development, main cause of deforestation in the Upper part of the Tapajos river basin and assesses the sensitivity to climate variables of the main crops produced - corn, soybean, rice and cotton – to climate variability. The paper also estimates the potential yield losses under future climate scenarios and discusses a possible adaptation strategy, namely irrigation, quantifying the potential water demand.

The historical yields in the period 1991 – 2010 (Brazilian Agricultural Census - IBGE) and the climatic conditions reported by the Global Land Data Assimilation System (GLDAS) global dataset (Rodell et al., 2004) for the 49 counties were used to calibrate a crop model (FAO - AquaCrop). Future climate change impacts (ISIMIP bias corrected UK

---

[6] *This Chapter is based on*:

Farinosi, F., Arias, M. E., Giupponi, C., Sue Wing, I., Garrett, R., Lee, E., Moorcroft, P.R. (*in preparation*). "Agricultural adaptation to climate change: evidence from the Upper Tapajos River Basin"

Meteorological Office Hadley Center HadGem2-ES RCP 4.5 and 8.5) were used to evaluate the impacts of climate change on yields. A possible irrigation scenario, and its consequences for the hydrology of the river system, was investigated. We found that climate change could substantially delay the first cycle of production. Delaying the planting dates of the first cycle reduces the period with favorable conditions for the second cycle of production. The introduction of irrigation as adaptation strategy represents a viable solution that could maintain the production levels at today's values. An adaptation strategy based on irrigation, however, would result in an increase in water demand causing potential conflicts with alternative uses, especially hydropower.

## 4.1. Introduction

Brazil is amongst the main agricultural producers and exporters in the world. The country is the second largest world producer of soybeans (27.3% of world production in 2012) and the third of corn (8.1%, FAOSTAT). Jointly with cattle production, agriculture is the main economic activity in the most remote areas of the country, especially in the state of Mato Grosso where these two sectors represent more than 25% of the GDP (Governo do Mato Grosso 2013; IPEA 2015). Moreover, agricultural and cattle products represent a large portion of the country's exports (Assad et al. 2010), accounting for a major share of the national trade balance (IPEA 2015).

Agriculture is largely developed in the Southern part of Brazil, with significant production of high economic value crops. Grain production and pasture, especially in the recent past, have been mainly concentrated in the central part of the country, an area that was primarily covered by the Cerrado biome. This area is characterized by a relatively low productivity and is logistically disconnected from the main access points to the global market. Only in the recent decades, thanks to technological development – mechanization,

introduction of different cultivars and fertilization techniques – this area became economically favorable for grain production. Agricultural expansion in the Cerrado area is the main cause of deforestation of the central part of Brazil, with increasing pressure on the Brazilian Amazon (Soares-Filho et al. 2006). Between 1990 and 2004, demand for land increased substantially, with serious consequences for the rich natural ecosystems of the area (Figure 4-1) (Assad et al. 2010; Nepstad et al. 2014). Recent studies about land use change in the Amazon and surrounding regions rose the political pressure on the national institutions that adopted several actions for limiting the deforestation in the southern Amazon (Nepstad et al. 2014; Macedo et al. 2012).
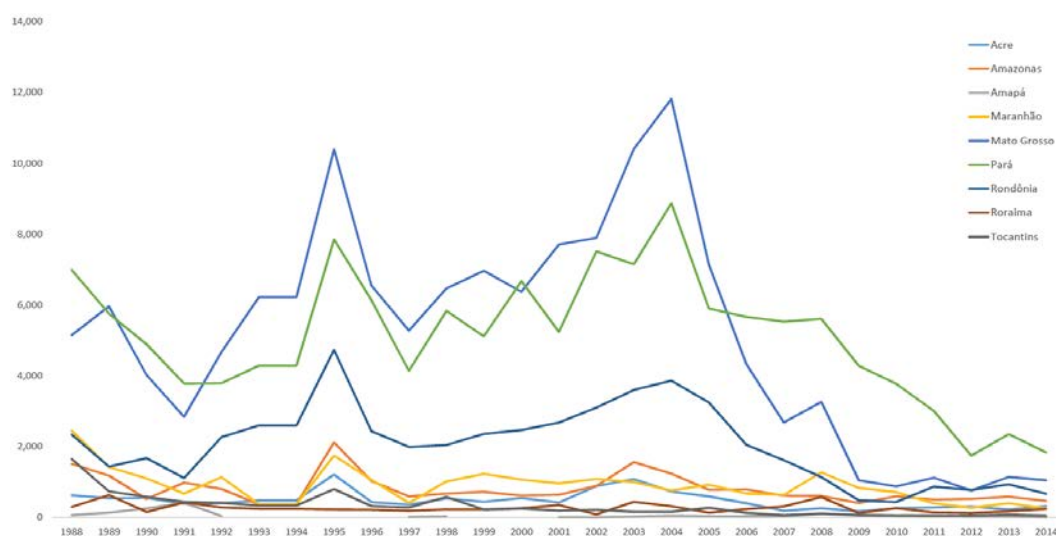


**Figure 4-1 Deforestation rates by state in Brazil (km²/year), 1998-2014. Authors' elaboration based on INPE – PROBIO data (http://www.obt.inpe.br/prodes/prodes_1988_2014.htm).**

Great concerns are animating the debate about future sustainability of the agricultural sector under changing short and long terms climate conditions (Assad et al. 2010; Assad & Pinto 2008; Margulis & Dubeux 2011). In the next decades, Brazilian agriculture is called to face the difficult challenge of increasing the productivity per unit of land ensuring the economic and environmental sustainability of both grain and cattle productions under changing conditions (Cohn et al. 2014).

The main objective of this study is to understand how the intensive rainfed monoculture in the Cerrado area could be impacted by changes in the climate conditions and what strategy the farmers could adopt to minimize the impacts. We used a crop model – FAO AquaCrop (Vanuytrecht, Raes, Steduto, et al. 2014; Raes et al. 2009; Steduto et al. 2009) - to simulate future crop yields under two different Representative Concentration Pathways (RCP 4.5 – moderate, and 8.5 – extreme climate change; Vuuren et al. 2011) of a bias corrected Earth System Model output (ISI-MIP (Warszawski et al. 2014; Hempel et al. 2013) – HadGem2-ES (Bellouin et al. 2007; Johns et al. 2006; Martin et al. 2006; Ringer et al. 2006)) participating to the Coupled Model Intercomparison Project Phase 5 (CMIP5) (Taylor et al. 2012). The analysis focuses on the region of Mato Grosso within the Tapajos river basin, one of the main tributaries of the Amazon river.

The remainder of the chapter is organized as follow. Next two subsections (4.1.1 and 4.1.2) describe the case study area, the historical agricultural production and the analysis of other similar studies. Section 4.2 describes methodology and data. Section 4.3 describes the analysis. Section 4.4 reports the main findings and discusses the possible implications.

### 4.1.1. The Tapajos River Basin

The Tapajos river basin is a large basin draining an area of 476,674 square kilometers in center-north Brazil (Figure 4-1). The river system is the fifth largest tributary of the Amazon flowing northward on the territories of the States of Mato Grosso, Para' and Amazonas. Main rivers in the basin are Rio Tapajós, Rio Jamanxim, Rio Teles Pires, and Rio Juruena.
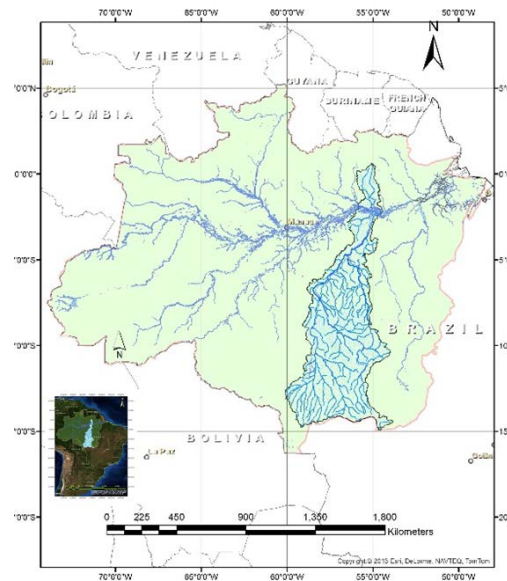
**Figure 4-2 Tapajos River basin (light blue) and Amazon River basin (light green) geographical location. Author's elaboration.**

The basin's elevation goes from about 800 meters asl in the southern part, to about 7 at the confluence with the Amazon river. The geological conformation of the soil goes from the Brazilian shield in the south to the soft sediments typical of the alluvial plains in the northern part. The region has a typical tropical climate with a long rainy season in the period September – May and a dry season in June-August. The precipitation is very abundant ranging from about 1,500 mm/year in the south up to 2,900 in the northern part of the basin (ANA 2011; Hales & Petry 2013). The biomes vary from the Cerrado in the south to tropical rainforest in the north: the portion of the basin laying in Mato Grosso state have been heavily deforested in the past to open space for agriculture (Figure 4-3), with different consequences for the local hydrological and atmospheric circulation (Hayhoe et al. 2011; van der Ent et al. 2010; Vergara & Scholz 2011). The northern part of the basin in the states of Para and Amazonas are largely protected for social (indigenous lands) or environmental reasons (state and national parks; ANA 2011). The Tapajos river basin economy is mainly based on agribusiness and related services. An ambitious hydropower development plan has been designed by Brazilian institutions (EPE 2013). A system of more than forty relatively large

dams has been designed for this basin, representing one of the largest portions of the planned

Brazilian future investments in electricity production.
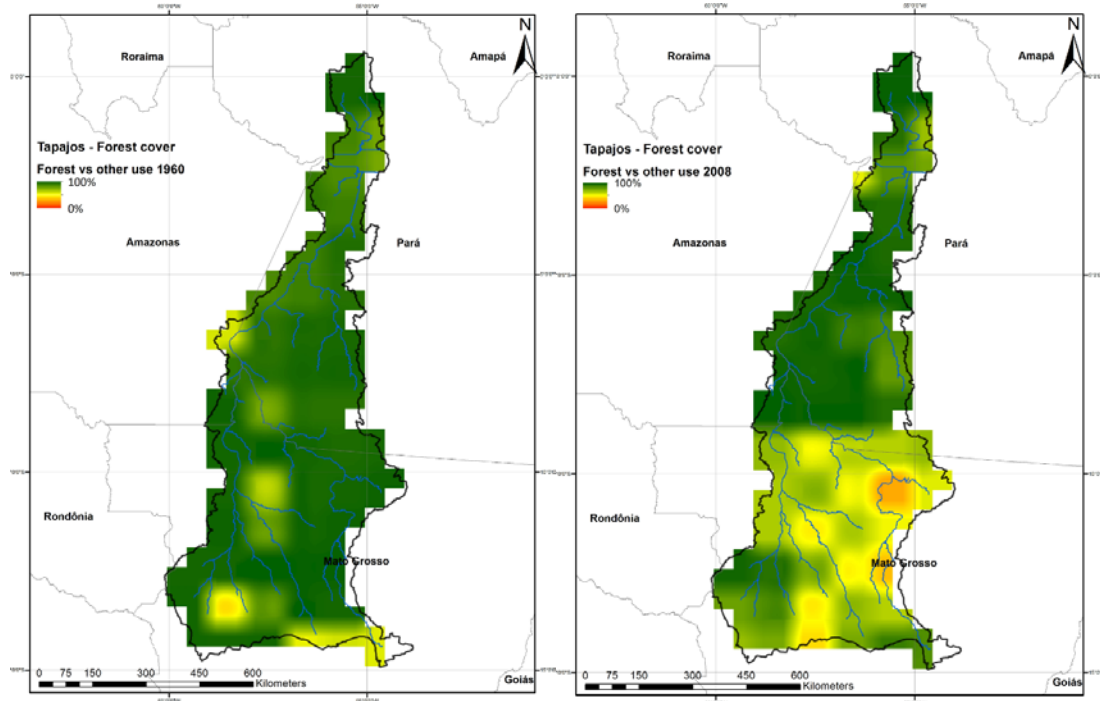


**Figure 4-3 Tapajos River basin land cover 1960 (left) vs 2008 (right). Green indicates full forest cover, red full deforestation. Author's elaboration based on (Hurtt et al. 2011; Hurtt et al. 2006; Soares-Filho et al. 2006) data**

### 4.1.2. Agriculture in the Upper Tapajos River Basin

This study focuses on the portion of the basin laying in the territory of the state of Mato Grosso, the Upper Tapajos river basin. The main rivers in this portion are Rio Juruena in the west and Rio Teles Pires in the eastern part. The area under consideration, covering over 413,000 square kilometers, is organized in 49 counties (Figure 4-4).
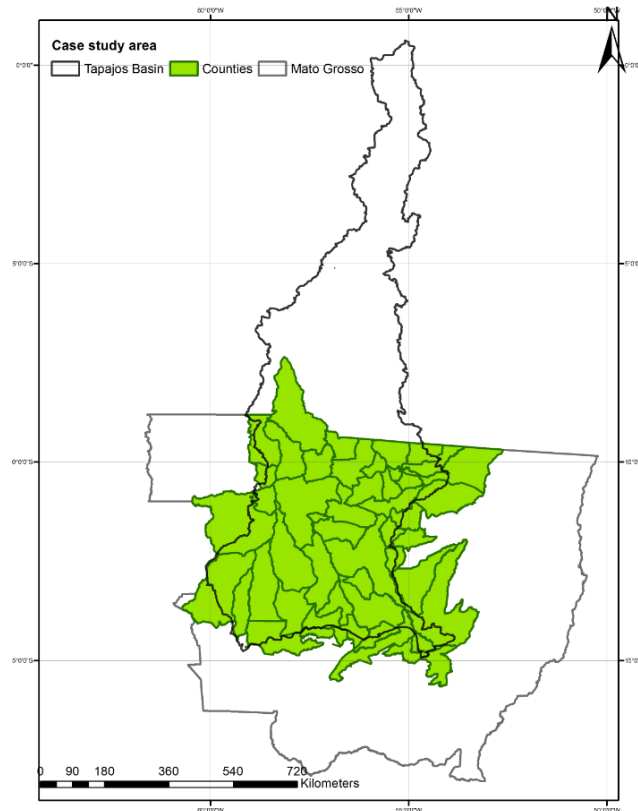
**Figure 4-4 Upper Tapajos River basin, case study area organized in 49 municipalities in the Mato Grosso State.**

Historically, this area was not considered particularly favorable for agriculture: despite the abundant rainfall and the good physical characteristics of the soil, crop productions suffered the extremely low pH, lack of phosphorous and aluminum saturation (Malavolta et al. 1965; Fageria et al. 1997). Agricultural productivity was considered too low and this discouraged major investments in the area (EMBRAPA 2004). In the 1970s, only 2% of the Brazilian soybean production came from the state of Mato Grosso, but this share has increased exponentially in the last decade and reached 60% thanks to the introduction of new techniques. Soybean is the largest production in the area, with about 65% of the cultivated area, followed by corn (18%), cotton (4%) and rice (3%) (Figure 4-5) (IBGE 2015; IBGE 2006). The production in the area is almost totally rainfed, only in some exceptional cases it is possible to find pivot irrigation for nursery or very limited cultivation of particular products. The production is mainly concentrated in the rainy season, from September to May.

In this period, farmers manage to produce two yields of crops, with the practice of sowing corn or cotton after harvesting soybean being common (EMBRAPA & AGROCONSULT 2010; EMBRAPA 2004).
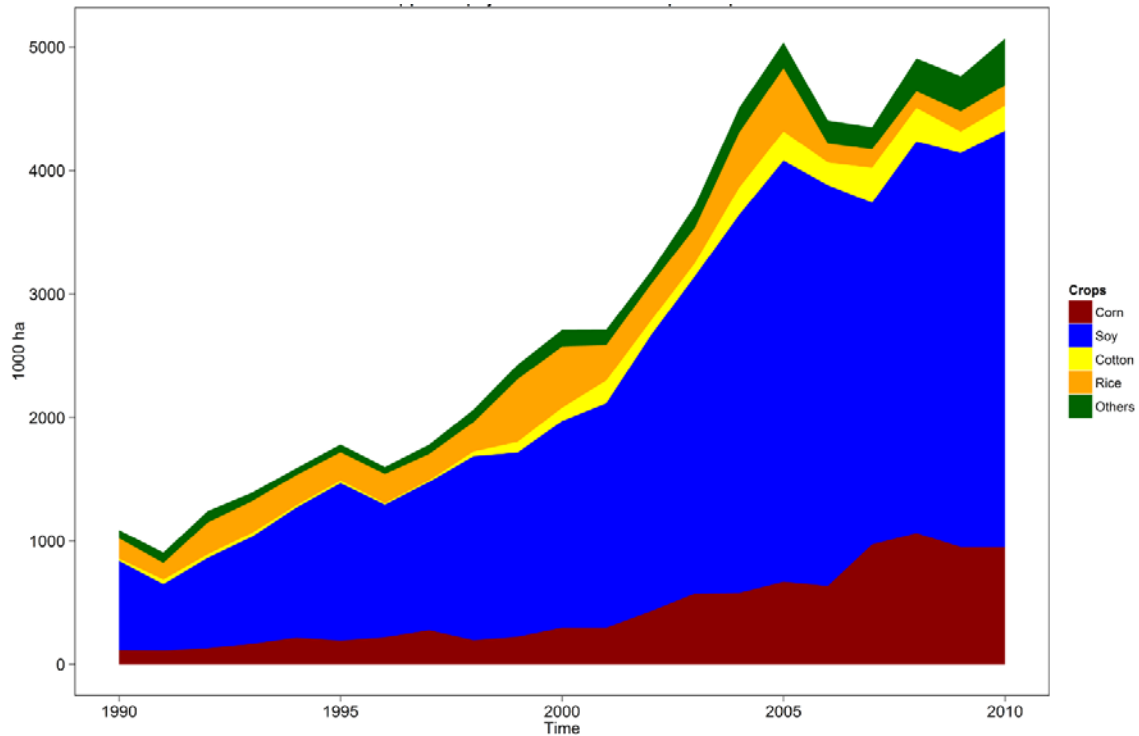
**Figure 4-5 Cultivated areas per crop in the case study area in the period 1990-2010 (values in thousand ha).**

This analysis considered the four main crops cultivated in the case study area: soybean, corn, cotton and rice (Figure 4-5). The production yield per unit of area of the selected crops in the region is below the national average (except for soybean) and considerably lower than in other countries (Table 4-1). Despite the low yield per unit of area, the availability of large cultivated areas, abundant rainfall, the possibility of having two cycle of production, and the high level of mechanization in largest farms (controlling the largest part of the cultivated areas) allow the economic profitability of the sector.

| Crop | Upper Tapajos average (ton/ha) | Brazil average (ton/ha) | Upper Tapajos Total production (in million tons) |
|---|---|---|---|
| Soybean | 3.0 | 2.94 | 10,078.44 |
| Corn | 3.3 | 4.36 | 3,773.30 |
| Rice (rainfed) | 3.0 | 4.13 | 497.82 |
| Cotton | 2.9 | 3.55 | 526.42 |

**Table 4-1 Crop productivity in 2010 (IBGE 2015).**

The other agricultural sector extremely important for this area, livestock farming, is not part of this analysis.

### 4.1.3. Notes on climate change impacts on Brazilian agricultural production

Agriculture and water management are arguably some of the sectors most affected by climate change (USCCSP 2008). The analysis of climate change impacts in agriculture has been deeply explored in literature, with several different approaches finalized at achieving the best possible future scenarios given the information available. Different approaches could be identified for different geographical and temporal scales. Two main families of studies can be identified (Assad et al. 2010): the first approach is based on the physical modeling of crop evolution in given environmental and technological conditions – model based approaches (Decker 1986; Rosenzweig et al. 2014; Steduto et al. 2012; Brisson et al. 1998; Jones & et al 2011; Keating et al. 2003; van Ittersum & Donatelli 2003; Brisson et al. 2003; Assad & Pinto 2008); the second approach is the one based on the statistical or econometric analysis. Statistical models are used to understand the correlation between agricultural productivity and the production/environmental factors (Schlenker & Roberts 2009; Wing & Fisher-Vanden 2013; Lobell & Burke 2010; Assad et al. 2013); in the Ricardian/hedonic models (or other econometric approaches like fixed effect) the impact of climate variations on the agricultural sector is expressed in terms of changes in farmland value (Mendelsohn &

Nordhaus 1996; Deschênes & Greenstone 2007; Margulis & Dubeux 2011; Evenson & Alves 1998; Sanghi & Mendelsohn 2008; Sanghi et al. 1997; Feres et al. 2008) or in terms of changes in the general economic flows as computed by general equilibrium models (Ferreira Filho & Moraes 2015).

A large number of the model-based analyses in the literature are scaled for large domains, regional as in Assad and Pinto (2008) or global as in the models analyzed in Rosenzweig et al (2014). In some other cases bio-physical models are used to analyse the crop dynamics in a specific site, using very detailed and site specific observations for model input and calibration (Araya et al. 2010; Abedinpour et al. 2012; Mainuddin et al. 2013). The strenght of the biophysical modeling approach is to isolate the impacts of the main environmental and meterological/climatic variables on the specific crop in the specific site, avoiding the risk of having the model outcome biased by confounding factors attaining more to the economic characteristics of the agricultural sector in the area. On the other hand, this approach could result extremely difficult to be efficiently applied to large areas or global analysis. Statistical and econometric approaches are more flexible and could be more easily adapted to regional and global analysis, with an unavoidable loss of details.

Regarding the geographycal area this study focuses on, the general outcome of existing literature is that the impacts of climate change on the agricultural production are expected to be mild in the first part of the 21st century, and more substantial in the second part. Brazil is likely to be negatively affected especially in the most drought vulnerable areas, like the north-east, with some gains in the southern part of the country (Feres et al. 2008). As pointed out by Assad & Pinto (2008) and Margulis & Dubeux (2011), the areal extent of the country considered at "low risk" of being affected by climate change are likely to decline in the coming decades, due mainly to changes in temperature and precipitation patterns. One of the conclusions of Assad & Pinto (2008), referring to the area under consideration for our

analysis, stressed that climate change could prevent the farmers to produce two yields per year, substantially undermining the economic profitability of the area.

## 4.2. Methodology and Data

The study we are presenting aims at analyzing a relatively large area organized in relatively small number of homogeneous units (the 49 *municipios* [counties] selected) with good availability of detailed agricultural production data. In order to obtain a detailed analysis, we combined site specific information with global gridded data and run a series of crop biophysical modeling exercises aimed at understanding the sensitivity of the main crops cultivated in the area to changes in climate. This section is divided in two subsections: the first will present the FAO AquaCrop model, the second the data used for the analysis.

### 4.2.1. FAO AquaCrop model

FAO AquaCrop is a water driven dynamic crop model designed to simulate the growth of herbaceous crops under different management and environmental conditions (P. Steduto et al. 2009; Raes et al. 2009; Hsiao et al. 2009; Pasquale Steduto et al. 2009; Vanuytrecht, Raes, Steduto, et al. 2014). The model is based on the widely used production function (4-1) introduced for the first time in the *FAO Irrigation & Drainage Paper 33* (Doorenbos & Kassam 1979):

$$\left(1 - \frac{Y_a}{Y_x}\right) = K_y \left(1 - \frac{ET_a}{ET_x}\right) \tag{4-1}$$

Where $Y_x$ and $Y_a$ represent the maximum and actual yields; $ET_x$ and $ET_a$ maximum and actual evapotranspiration; $K_y$ is a yield response factor representing the effect of a

reduction in evapotranspiration on yield losses (Doorenbos & Kassam 1979; Doorenbos & Pruitt 1977). The evapotranspiration component is crop specific (4-2):

$$ET_x = K_c ET_o \qquad \text{(4-2)}$$

with $K_C$ is the specific crop coefficient and $ET_o$ is the potential evapotranspiration calculated following the FAO Penman-Monteith function (4-3) (Allen et al. 1998; Doorenbos & Kassam 1979):

$$ET_o = \frac{0.408 \, \Delta \, (R_n - G) \, + \, \gamma \, \dfrac{900}{T + 273} \, u_2 \, (e_s - e_a)}{\Delta + \gamma \, (1 \, + \, 0.34 \, u_2)} \qquad \text{(4-3)}$$

The specific formulation of the model is slightly different from the equation (4-1). The main difference is the decomposition of the evapotranspiration $ET$ in two distinct factors (Figure 4-6): soil evaporation $E$ and crop transpiration $Tr$, this in order to isolate the non-productive consumption of water (P. Steduto et al. 2009; Steduto et al. 2012).
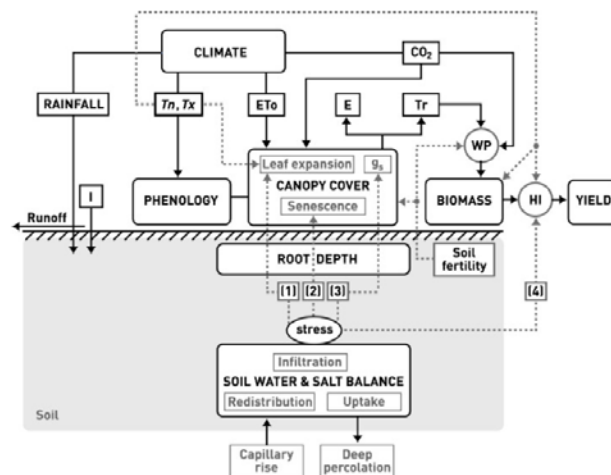


**Figure 4-6 Chart of AquaCrop (retrieved from Steduto et al. 1999) "(I - Irrigation; Tn - Min air temperature; Tx - Max air temperature; ETo - Reference evapotranspiration; E – Soil evaporation; Tr -**

The model computes biomass $B$ production as function of the productivity of the specific crop per units of water, given environmental and management conditions, and the water transpired during the growing cycle (Figure 4-6). The yield $Y$ is calculated as function of the biomass produced during the growing cycle and the harvest index $HI$. This model has been extensively used for different crops at various geographical scales in different part of the globe (Araya et al. 2010; Abedinpour et al. 2012; Mainuddin et al. 2013; Stricevic et al. 2011; Mhizha et al. 2014; Heng et al. 2009). AquaCrop has been already successfully used in combination with both CMIP3 (Vanuytrecht, Raes, Willems, et al. 2014) and CMIP5 climate projections (Karunaratne et al. 2015). Further information about the AquaCrop model are available in Steduto el al. (2009), Vanuytrecht et al. (2014), and other studies (Raes et al. 2009; Hsiao et al. 2009; Pasquale Steduto et al. 2009; Raes et al. 2011).

### 4.2.2. Data

AquaCrop was parameterized using specific information about local environment and management made available by the Brazilian Enterprise for Agriculture and Animal Research (EMBRAPA). For each of the crops selected (soybean, corn, cotton and rice), specific information were chosen for the parameterization of: crop life cycle; time to crop emergence, flowering, start of canopy senescence and to maturity (length of crop cycle), planting dates, crop coefficient $K_c$, and root depth (EMBRAPA & AGROCONSULT 2010; EMBRAPA 2004; EMBRAPA 2010; EMBRAPA 2003a; EMBRAPA 2003b). Soil characteristics were also made available by EMBRAPA (1981) and the Brazilian Institute of Geography and

Statistics (IBGE 2009). In this area the soil composition is a clay-loam mixture very well drained (EMBRAPA 1981).

The crop model was calibrated and validated using the historical yield data for the 49 counties selected in the period 1991-2010 (IBGE 2015). Historical agricultural production was simulated using high-resolution (0.25 x 0.25 degrees) daily meteorological data from the Global Land Data Assimilation System (GLDAS) dataset (Rodell et al. 2004). AquaCrop was calibrated for the production of the 4 selected crops in the 49 counties in the domain for the period 1991-2010. The calibration process allowed to identify the specific soil fertility values for each of the combination county-crop. Agricultural production time series were statistically de-trended in order to remove the confounding factors of the increasing technological productivity.

Future yield projections were obtained simulating the agricultural production in the 49 sites selected in combination with two distinct climate change Representative Concentration Pathways (RCP 4.5 – moderate, and RCP 8.5 – extreme climate change) (Vuuren et al. 2011) computed using the coupled Earth System Model (ESM) HadGem2-ES of the UK Met Office Hadley Centre for the CMIP5 (Taylor et al. 2012) simulations (Bellouin et al. 2007; Johns et al. 2006; Martin et al. 2006; Ringer et al. 2006). Three sets of simulations were run:

1. Rainfed first yield (soybean, corn, rice, cotton);

2. Rainfed first and second yield (1st: soybean, corn, rice, cotton; 2nd: corn, cotton);

3. Irrigated first and second yield (1st: soybean, corn, rice, cotton; 2nd: corn, cotton).

In order to account for the climate model uncertainty, the future crop yield projections were computed using the HadGem2-ES outputs bias-corrected by the Inter-Sectoral Impact Model Intercomparison Project (ISI-MIP) (Hempel et al. 2013; Warszawski et al. 2014).
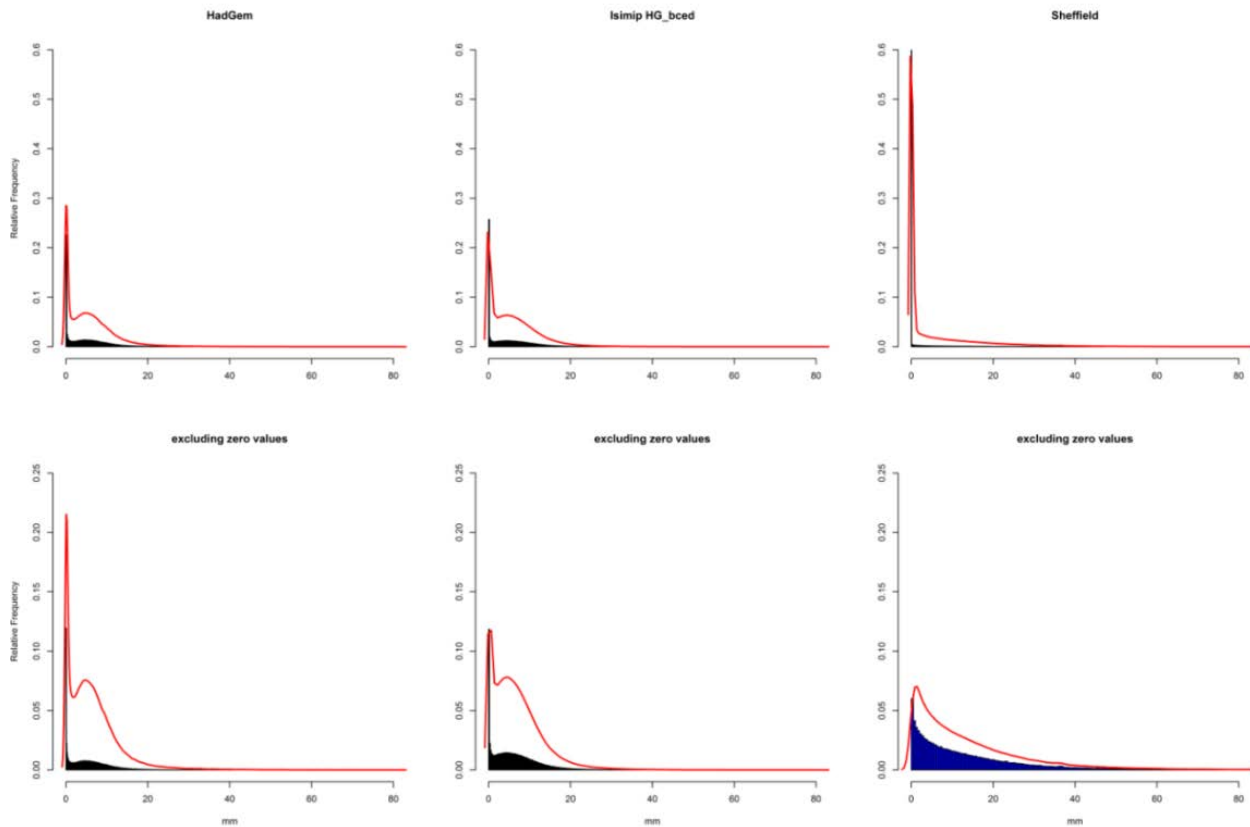
**Figure 4-7 Relative frequency of the precipitation daily values (in mm) of the HadGem2-ES (left), ISI-MIP bias corrected (centre), and observed (right) (Sheffield et al. 2006) for the period 1985-2005 in the case study domain. Top row includes the zero values, the bottom row excludes the zero values.**

Climate models tend to underestimate the days with no precipitation and the extreme precipitation events. Moreover, they tend to misrepresent the probability distribution of the precipitation events. As it is possible to highlight from Figure 4-7, HadGem2-ES is no exception. The bias correction process improves the distribution of the precipitation events in the domain under consideration.

## 4.3. Results

### 4.3.1. Calibration

The scope of this analysis is to study the impacts of climate change to crop productivity in the area under consideration. In order to do that, we needed to parameterize the bio-physical model to reproduce the historical observation in terms of agricultural

103

productivity for the selected pool of crops for each of the 49 counties of the domain. The second phase of the analysis consisted in running the model with the projected climate scenarios keeping all the other variables fixed over time. In general, the model satisfactorily manages to re-produce the historical agricultural production with some limitations in reproducing the variations over time (Figure 4-8).
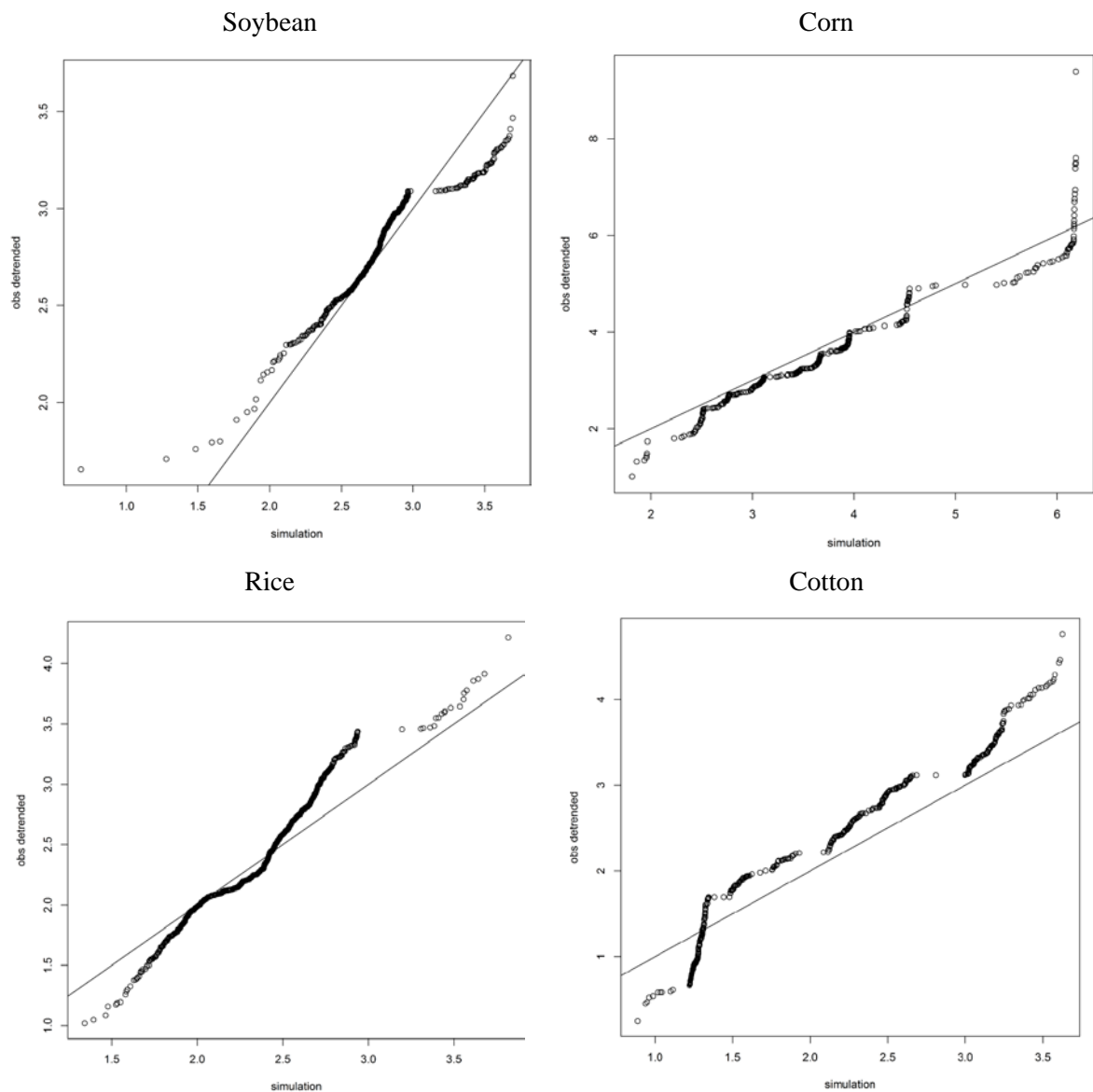


**Figure 4-8 QQ-plot simulated agricultural production vs de-trended observations in the 49 counties of the domain for the period 1991-2010.**

The model reproduces mean inter-annual variability of the observations, while variance of the simulated values is consistently lower than the observed ones (see Figure 4-8 for aggregated results. Detailed results at county level are available in the Annex C ). The main reason of this difference is due to the impossibility of the model to reproduce the variability of the management decision at farm level (planting dates and management parameters are the same for the specific county in the specific year, there is no sub-county variation). The model is set to select an optimal planting date in the time period suggested by the Brazilian Enterprise for Agriculture and Animal Research (EMBRAPA) for the counties part of the analysis:

- Soybean (sowing): October 1$^{st}$ – December 31$^{st}$;

- Corn (sowing): September 15$^{th}$ – December 31$^{st}$;

- Rice (transplanting): October 1$^{st}$ – January 31$^{st}$;

- Cotton (sowing): December 15$^{th}$ – January 31$^{st}$ (see Annex C for further information).

Since the model is set to reproduce the farm management decisions in rainfed agricultural conditions, the choice of the optimal planting date is linked to the amount of precipitation in the selected period. The model identifies the wet spells (at least 40 mm rain in a 5 days period) and chooses the event allowing to the crop to grow (usually the second or third event).

### 4.3.2. Climate change scenario analysis

The problem addressed in this analysis was structured around the response of the simulated system to changes in climate. In this section, we present an analysis of the scenarios chosen for the study.
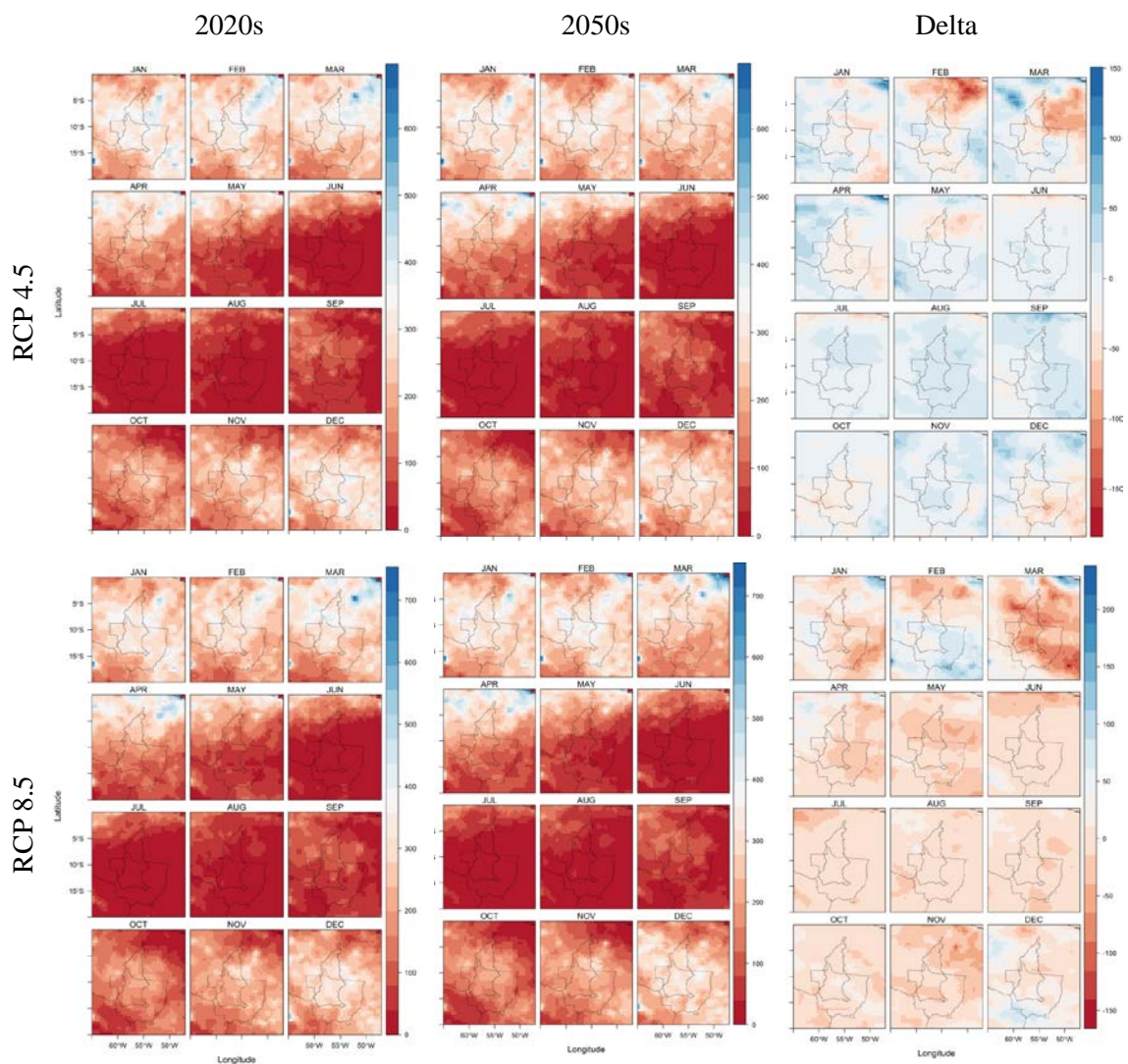
**Figure 4-9 Spatial distribution of the cumulative monthly precipitation from the two ISI-MIP bias corrected HadGem2-ES scenarios (RCP 4.5 top row, RCP 8.5 bottom row). Average for the decades 2011-2020 (left) and 2041-2050 (center). On the right panel the difference between the decade 2041-2050 and the 2011-2020**.

Figure 4-9 shows the trends in precipitation of the two climate scenarios chosen for the analysis developed in this study. Comparing the average monthly cumulative precipitation of the fifth and second decades of the 21$^{st}$ century, it is possible to conclude that the climate model estimates a wetter dry season (Jun to Aug) and a drier rainy season for the moderate (RCP 4.5) scenario. The extreme climate scenario (RCP 8.5) is generally drier all over the

year. For both scenarios is possible to highlight a shift onward of the beginning of the rainy season with a consequent reduction of the wet period (Figure 4-10).
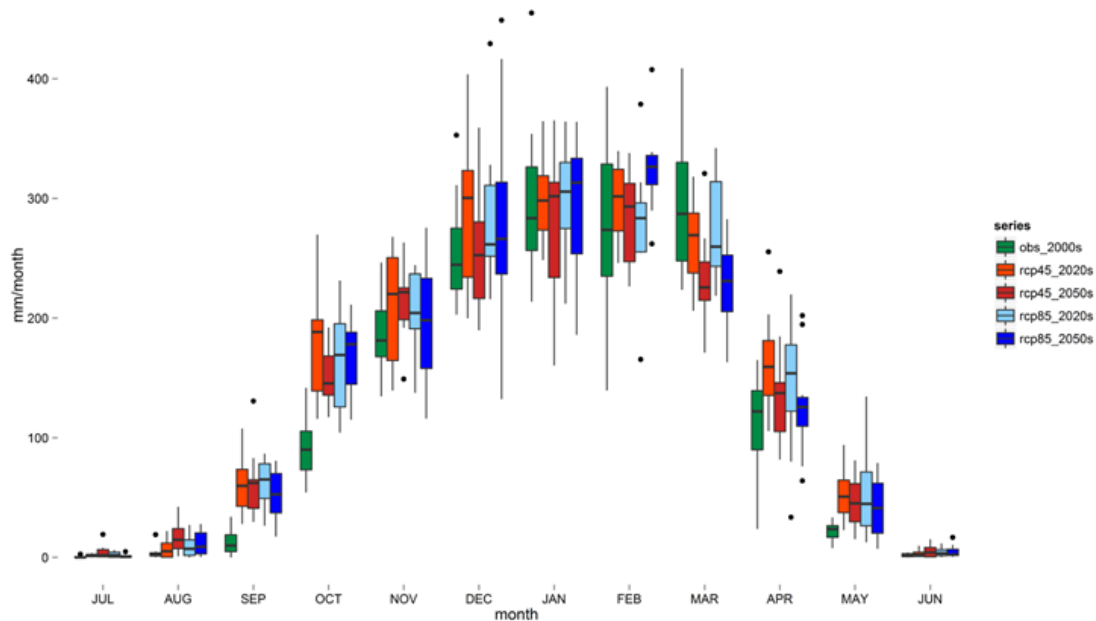


**Figure 4-10 Seasonal distribution of the cumulative monthly precipitation from the two ISI-MIP bias corrected HadGem2-ES scenarios (RCP 4.5 and RCP 8.5: 2011-2020 light red and light blue; 2041-2050 red and blue respectively) and observations (2001-2010 green).**

The differences between seasonal distributions of observed data versus the modeled projections suggest that the climate model, in general, overestimates the rainy season duration for the domain of this study (Figure 4-10). For both the scenarios climate change is expected to delay the beginning (especially in the case of the moderate one) and the peak (especially for the extreme one) of the rainy season reducing the overall length of the season itself. This aspect is extremely important for the result of this analysis.

### 4.3.3. Future projection results

The calibrated model was used to estimate the projected production for each of the combinations crop-county under the two climate scenarios. As described above (see section

4.2.2), three sets of simulations were run. The first one considered only the first yield for the four crops maintaining the agricultural management in use for the historical runs: same parameters for fertility and crop characteristics, with no irrigation. From the results of this set of simulations, we found that projected climate change is not expected to sensibly affect crop yields (Figure 4-11). The average production is expected to remain stable under the two scenarios considered, with some problems in a limited number of locations, mainly due to the increasing temperature under the most extreme scenario. It has to be noted that in this simulation the model is free to select the optimal sowing date basing on meteorological conditions.
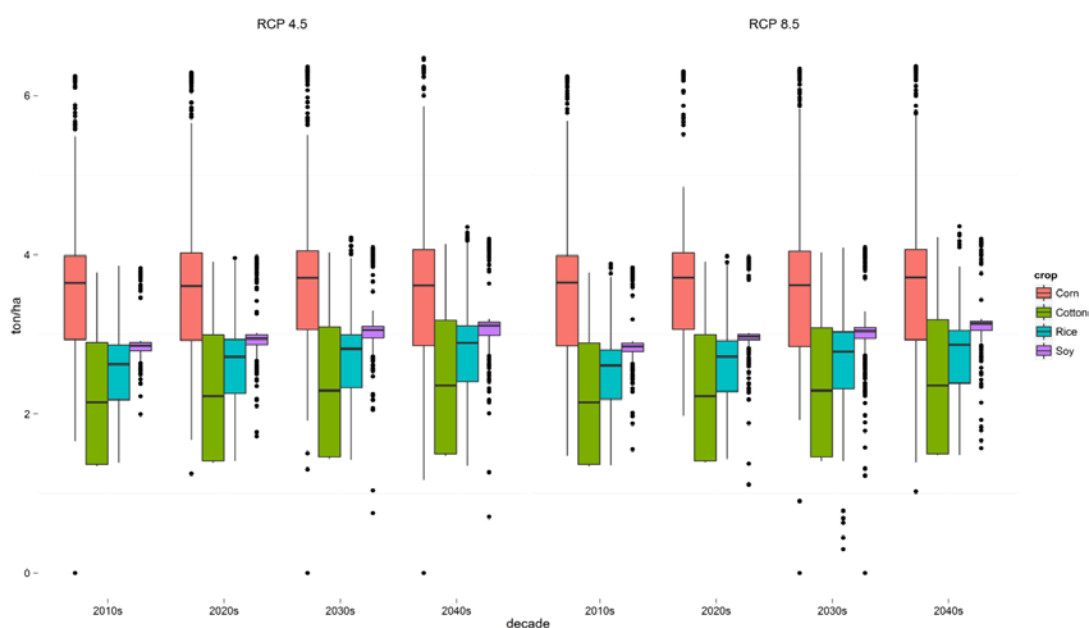


**Figure 4-11 Crop first yield rainfed simulation 2011-2050 in the 49 counties of the domain (ton/ha). The values in the boxplot represent the results for each of the county per year. The results were divided in periods of 10 years.**

The main impact highlighted by the results of the first set of simulations is not identifiable in the productivity, but in the planting dates shift. For both climate scenarios and all the four crops considered, in fact, the planting dates were consistently shifted forward by the model Figure 4-12. This aspect of the simulations represents the adaptation strategies that

farmers would normally put in place to adapt to the changes in the seasonality of water availability.
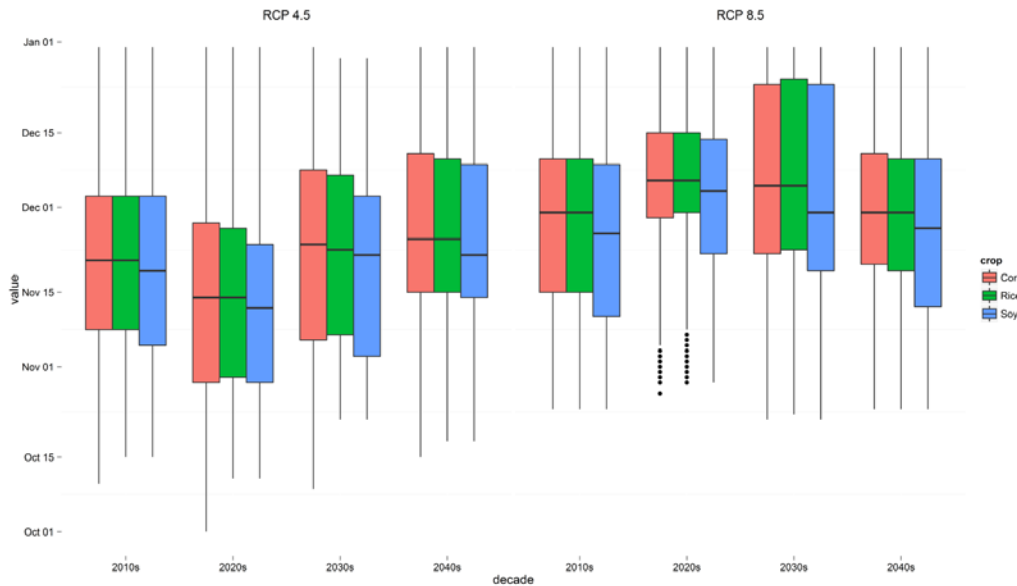


**Figure 4-12 Evolution of the planting dates of the first yield with rainfed agriculture. The values in the boxplot represent the results for each of the county per year. The results were divided in periods of 10 years.**

The second set of simulations replicates the first one adding to the production the second crop rotation. The model was set in order to consider corn and cotton sowing in concurrence with soybean harvesting. The second rotation starts in the middle of the rainy season, when abundant rainfall and soil moisture ensure (or at least have ensured in the past) the successful growth of the new cultivation. Nonetheless, the reduction of the rainy season duration and the onward shift of its peak projected by both the climate scenarios are expected to cause serious consequences to the sustainability of this agricultural practice in the area under consideration. On the one hand, the delayed planting of the first yield causes a shift in the beginning of the second production; on the other hand, the reduction of the rainy season length causes a higher probability of water stress during the flowering stage, one of the most vulnerable part of the crop life cycle. This dynamics is expected to seriously affect the

possibility of harvesting two yields in the study region under both climate scenarios (Figure 4-13).
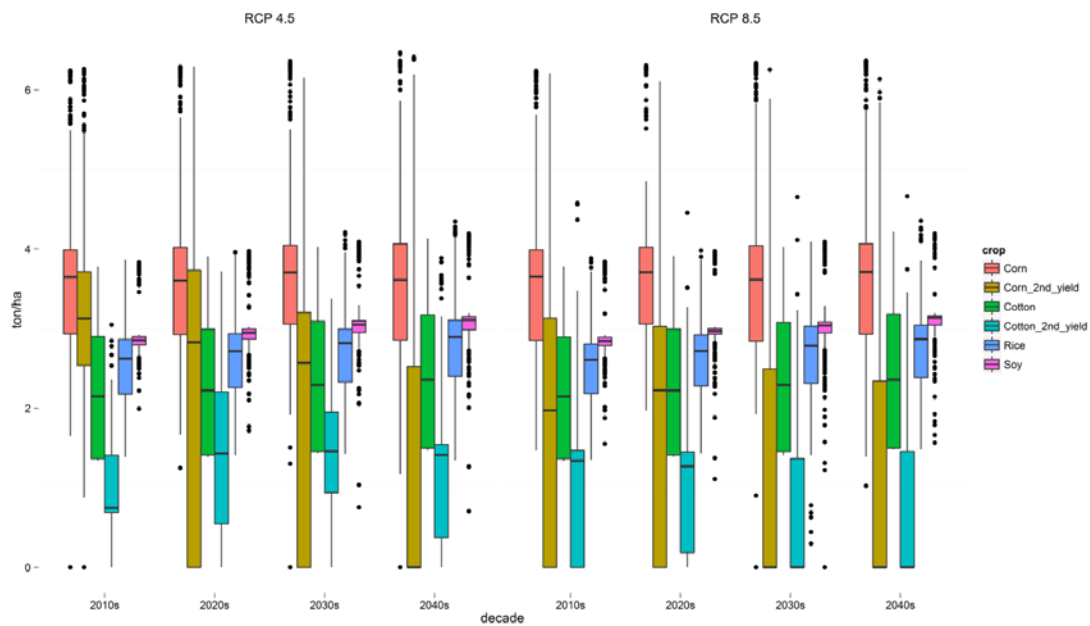


**Figure 4-13 Crop first and second yields rainfed simulation 2011-2050 in the 49 counties of the domain (ton/ha). The values in the boxplot represent the results for each of the county per year. The results were divided in periods of 10 years.**

In the third set of simulations we added a climate change adaptation scenario introducing irrigation to the agricultural system object of this analysis. In this stage we fixed the planting dates of the two production cycles described above and computed the potential irrigation requirements. Under this adaptation scenario, the productivity of the two yields is expected to maintain today's levels, with the exception of some of the crops (mainly rice), in some specific locations towards the end of the simulation period under the most extreme scenario (RCP 8.5) due to temperature stress (Figure 4-14).
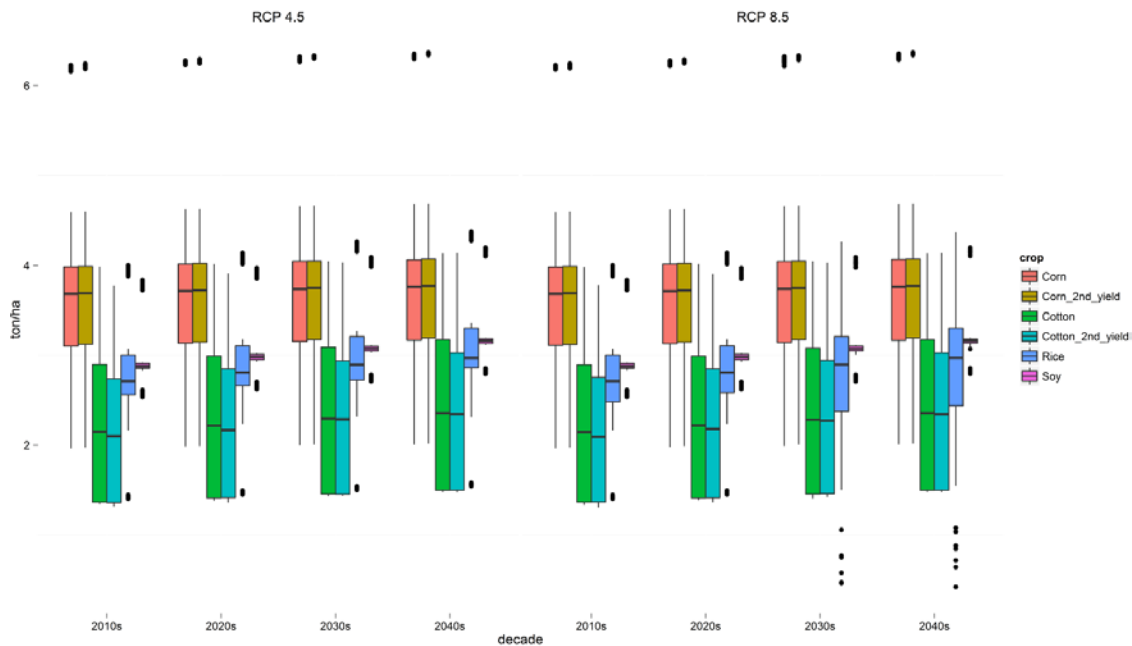
**Figure 4-14 Crop first and second yields irrigated simulation 2011-2050 in the 49 counties of the domain (ton/ha). The values in the boxplot represent the results for each of the county per year. The results were divided in periods of 10 years.**

Under this scenario, the irrigation requirements are expected to be particularly concentrated at the beginning of the rainy season. This would maintain the productivity of the first rotation without compromising the second cycle of production. As expected, the simulated water requirement of the second yield is almost negligible at the beginning of the simulation period, especially under the milder climate change scenario (RCP 4.5). Nonetheless, water demand is projected to increase over time, in line with the drier climate conditions towards the end of the simulation period (Figure 4-15).
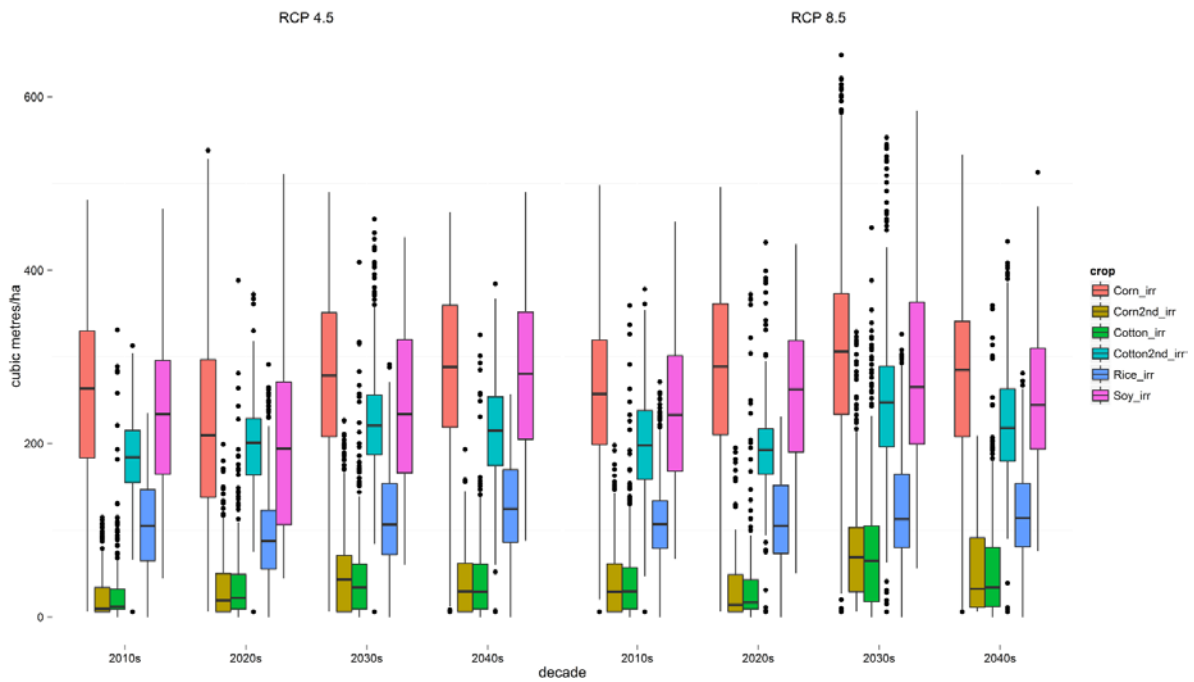
**Figure 4-15 Crop first and second yields irrigated simulation 2011-2050 in the 49 counties of the domain (m³/ha). The values in the boxplot represent the results for each of the county per year. The results were divided in periods of 10 years.**

## 4.4. Discussion and conclusions

In a recent study, two of the main experts of the Brazilian agriculture, discussing the possible impacts of climate change in the domain of this analysis, concluded:

*"The strength of the Brazilian agriculture, the aspect that ensures its competitiveness for export, has been the production with zero tillage technique of two yields, mainly soybean and corn, with the alternative option of introducing cotton when the micro-climate is suitable. This intensive way of exploiting the Cerrado area allows the economic sustainability of the production infrastructure and the needed logistics for its commercialization. If the reduction of the favorable agricultural season was going to reduce the possibility of harvesting a second yield, the profitability of intensive annual agricultural productions in the*

*Cerrado would be reduced"*[7] (Assad & Pinto 2008). The results of this study confirm this hypothesis and quantifies the possible losses in terms of productivity. Climate change, in fact, is expected to delay the beginning of the rainy season and shorten its duration. An autonomous adaptation strategy by the delay of the planting date of the first cycle of production accordingly with the variation in the rainy season. This would save the first cycle of production, but compromising the second one. Delaying the planting dates of the first yield, would in fact result in a delay of the second cycle of production. This delay, jointly with the projected reduction of the rainy season duration, is expected to cause a significant stress to the crops of the second rotation. This stress is expected to significantly reduce the second yield.

As discussed in the chapter, irrigation techniques could represent an effective strategy to mitigate the impacts of climate change on this area, which historically found one of its strengths in a double yield rainfed production. In the Upper Tapajos river basin, a potential increase in water demand for irrigation would compete with other alternative usages. This could represent a potential problem for the extensive hydropower system planned for this basin. The hydropower production system planned for the area is mainly based on large run-of-the-river technology, with limited water storage capacity. This type of hydropower infrastructure is particularly vulnerable to the seasonality of streamflows, which is typical of

---

[7] Authors' translation of the original paragraph: "*O ponto forte da agricultura brasileira, que a torna particularmente competitiva para exportação, foi o cultivo de duas safras anuais (soja e milho principalmente) em regime de plantio direto, com a introdução alternativa do algodão quando o microclima é adequado. É essa forma intensiva de explorar o Cerrado que remunera a infra-estrutura de produção e a logística necessária para a sua comercialização. Se a redução do período favorável ao plantio impeder a freqüência da segunda safra, a rentabilidade da agricultura intensiva de lavouras anuais no Cerrado vai ser reduzida*" (Assad & Pinto 2008).

tropical rivers. In this study, we maintained the agricultural system based on the historical characteristics in terms of agricultural areas, number of cycles and crop types. Assuming this agricultural system is maintained, the eventual introduction of irrigation in the area, would create a relatively limited water demand respect to the abundant flows of the river system in this basin. The additional water demand would be mainly concentrated at the beginning and the end of the rainy season. This could increase the vulnerability of the river system, especially at the beginning of the rainy season. In fact, seasonal peak precipitation and flows in this system have been historically separated by a time interval of about two months. The irrigation of the first cycle of production could increase the water demand in a period of low flow. The irrigation of the second cycle of production, instead, would increase the water demand in the period where the river flows are more abundant, thus the system is less vulnerable. The combination of autonomous adaptation, i.e. delaying the planting dates, in the first cycle of production and irrigation in the second, could represent the most effective adaptation strategy. However, this is a conservative scenario. Changing the rainfed agricultural system into an irrigated one could create the option for introducing a third cycle of production during the dry season.

It is interesting to note that the introduction of irrigation could mistakenly represent an option of virtually unconstrained supply of water for the agricultural system in the area. This could induce the farmers to introduce higher value crops with higher water requirements.

In the long term, the change in crop mix induced by the specific form of adaptation adopted and the resulting greater water demand, especially during the dry season, could enter in conflict with the possibility to sustain the hydroelectricity production over the dry season.

# 5. Conclusion

This thesis analyzes the impacts of global environmental changes on water and water-related activities. It examines the connections between the complex dynamics of hydropower, agricultural production, and river basin hydrology, in different socioeconomic and environmental contexts at different geographical scales, using specific tools developed by different disciplines. The goal of this work is threefold. First, it analyzes how global climate and land use change are expected to impact the spatial and temporal distribution of the water resources. Second, it examines how human activities, such as hydropower and agricultural production, are likely to be influenced by global environmental changes in land use and climate. Third, it explores how different socioeconomic and environmental systems could adapt to the changing conditions in climate and land use.

Different problems and different geographical scales require different analysis tools. Two types of instruments, that are available for assessing the impact of global changes, are represented by statistical analysis and physical modeling. The first one can effectively identify robust patterns/relations between the variable under consideration and the changing environmental and socioeconomic dynamics basing on historical observations. The second approach describes in more details the mechanisms of the socioeconomic and environmental dynamics and reproduces the system under consideration. It requires very detailed data and that for is more suitable for regional or local scale analyses.

In this work, the vulnerability of global hydropower production to climate change was analyzed using a statistical model. Although storage hydropower could help to mitigate climate change and cope with water scarcity and flood events, climate change is expected to modify the future conditions in which the hydropower operators are called to manage the storage capacity. Moreover, attempts to minimize environmental and social impacts of hydropower facilities has led to an increased development of relatively smaller sized

reservoirs, mainly run-of-the-river, which are actually the most sensitive to changes in average seasonal runoffs as well as in extreme dry and wet conditions. Results of the analysis reported in this thesis suggest that regional pattern of future climate as well as the sensitivity of facilities with reservoirs of different size should be considered when planning these long-lived, less adaptable hydraulic infrastructure. This also points at the potential bias that might exist in the state-of-the art literature on mitigation scenarios reviewed in the IPCC Working Group III (Clarke & Jiang 2014), which so far has not considered the linkages between impacts, adaptation, and mitigation. Current mitigation scenarios, which do not account for the climate change feedback on the potential of renewable energy sources, such as hydropower, could underestimate or overestimate mitigation costs, and provide a biased picture of future possible energy mix through possible interactions with competing mitigation options.

Impacts of land use and climate change on the ecosystem water cycle and river basin hydrology was studied using a biosphere model coupled with a routing scheme. Physical models were used to analyze the impacts of changing conditions to hydropower and agricultural production in a basin in the Amazon. Land surface models are extremely efficient tools to study the hydrological dynamics under climate and land use changing conditions. These models are usually set to simulate long periods in large domains, usually at global or continental scale. Their ability in reconstructing the water balance at relatively fine geographical and temporal resolution taking into consideration global dynamics, makes them powerful instruments for hydrological simulations. In order to translate the results of the land surface simulation in terms of river flows, the simulated results need to be processed using a hydrological routing scheme. In this thesis we used the biosphere model ED2.2 integrated with a routing scheme (ED2+R) to analyze the hydrological alterations caused by the two main environmental changes, climate and land use, in a large basin of the Brazilian Amazon,

the Tapajos. This thesis simulates different combinations of climate and land use change disturbances for the future, comparing the results with respect to a baseline scenario shaped on the historical climate and land use. Hydrological alterations caused by climate change were analyzed simulating the land surface dynamics forcing the biosphere model with two distinct climate scenarios. Human disturbances on land use were simulated using degrees of deforestation, one more limited, and the other more extreme. Model results confirmed that the two environmental drivers will affect the area in similar ways as what experimental evidence has revealed so far in the area. Climate change is expected to consistently reduce the streamflows in the river system throughout the year, bringing a considerable delay in the flow seasonality and increasing the overall variability. Land use change is expected to revert the diminishing trend in flow, with increasing impact on the inter- and intra-annual variability. The cumulative effect of both of these two drivers, however, appears to be overrun by global climate change effects.

The streamflows resulting from the presented analysis were used to run a hydro-energy model (HEC-ResSim) simulating the operation of one of the big dams planned for the basin, Sao Luiz do Tapajos. The theoretical productivity of the plant follows the hydrological trends, stressing how the designed hydropower system, due to the general lack of storage capacity, is incapable to buffer the flow variability. This element makes the hydropower system, planned to be a substantial part of the national electric supply, extremely vulnerable to hydrological alterations caused by the combined effect of climate and land use change.

Moreover, the water resources in this basin are expected to experience an additional source of stress in the future, represented by agricultural demand. In this thesis, a crop model (FAO-Aquacrop) was used to simulate the effect of the changing environmental conditions on the future productivity of the rainfed agriculture in the Upper Tapajos river basin. The results of this thesis confirm this hypothesis and quantifies the possible losses in terms of

117

productivity. Climate change, in fact, is expected to delay the beginning of the rainy season and shorten its duration. An autonomous adaptation strategy by the delay of the planting date of the first cycle of production accordingly with the variation in the rainy season. This would save the first cycle of production, but compromising the second one. Delaying the planting dates of the first yield, would in fact result in a delay of the second cycle of production. This delay, jointly with the projected reduction of the rainy season duration, is expected to cause a significant stress to the crops of the second rotation. This stress is expected to significantly reduce the second yield. As discussed in the chapter, irrigation techniques could represent an effective strategy to mitigate the impacts of climate change on this area, which historically found one of its strengths in a double yield rainfed production.

In the Upper Tapajos river basin, a potential increase in water demand for irrigation would compete with other alternative usages. This could represent a potential problem for the extensive hydropower system planned for this basin. The hydropower production system planned for the area is mainly based on large run-of-the-river technology, with limited water storage capacity. This type of hydropower infrastructure is particularly vulnerable to the seasonality of streamflows, which is typical of tropical rivers. In this thesis, we maintained the agricultural system based on the historical characteristics in terms of agricultural areas, number of cycles and crop types. Assuming this agricultural system is maintained, the eventual introduction of irrigation in the area, would create a relatively limited water demand respect to the abundant flows of the river system in this basin. The additional water demand would be mainly concentrated at the beginning and the end of the rainy season. This could increase the vulnerability of the river system, especially at the beginning of the rainy season. In fact, seasonal peak precipitation and flows in this system have been historically separated by a time interval of about two months. The irrigation of the first cycle of production could increase the water demand in a period of low flow. The irrigation of the second cycle of

production, instead, would increase the water demand in the period where the river flows are more abundant, thus the system is less vulnerable. The combination of autonomous adaptation, i.e. delaying the planting dates, in the first cycle of production and irrigation in the second, could represent the most effective adaptation strategy. However, this is a conservative scenario. Changing the rainfed agricultural system into an irrigated one could create the option for introducing a third cycle of production during the dry season.

It is interesting noting that the introduction of irrigation in that specific place could be mistakenly perceived as a virtually unconstrained supply of water for the agricultural system in the area. This could have a perverse effect and induce farmers to introduce higher value crops with higher water requirements. In the long-term, the change in crop mix induced by this specific form of adaptation, resulting in greater water demand especially during the dry season, could generate conflicts between alternative competing uses for water, and limit the possibility to sustain hydroelectricity production during the dry season.

This thesis provides a significant contribution to the debate about uncertainty and stationarity in water management. It proves with practical examples how different socio-economic and ecological systems at different geographical scale are interconnected. This means that the dynamics influencing one system affect, directly or indirectly, the interconnected systems, causing a cascade effect.

In this thesis are developed the stepping stones for a more comprehensive study that is left for future research. Future research should contribute to the findings exposed above with two main additions. The first regards the inclusion of the biosphere-atmosphere feedbacks in climate and land use impact assessment. Second contribution is represented by the quantification of the tradeoffs between competitive human activities, as for instance hydropower and agriculture, in the same socio-economic and ecological system for a more integrated impact assessment. The integrated analysis of complex systems is here proven to

have a key role in the interconnections between water, food and energy production. This covers an important role for achieving sustainable development.

# References

Abedinpour, M. et al., 2012. Performance evaluation of AquaCrop model for maize crop in a semi-arid environment. Agricultural Water Management, 110, pp.55–66. Available at: http://linkinghub.elsevier.com/retrieve/pii/S037837741200100X.

Albani, M. et al., 2006. The contributions of land-use change, CO 2 fertilization, and climate variability to the Eastern US carbon sink. Global Change Biology, 12(12), pp.2370–2390. Available at: http://doi.wiley.com/10.1111/j.1365-2486.2006.01254.x.

Allen, R.G. et al., 1998. Crop evapotranspiration - Guidelines for computing crop water requirements. Irrigation and Drainage Paper No. 56 Food and Agriculture Organization of the United Nations (FAO). Available at: http://www.fao.org/docrep/x0490e/x0490e00.htm.

ANA, 2011. Plano Estratégico de Recursos Hídricos da Bacia Amazônica – Afluentes da Margem Direita (in Portuguese), Brasilia, Brazil, Brazil. Available at: http://margemdireita.ana.gov.br/.

Andréassian, V., 2004. Waters and forests: from historical controversy to scientific debate. Journal of Hydrology, 291(1-2), pp.1–27. Available at: http://linkinghub.elsevier.com/retrieve/pii/S0022169403005171.

Araya, A. et al., 2010. Test of AquaCrop model in simulating biomass and yield of water deficient and irrigated barley (Hordeum vulgare). Agricultural Water Management, 97(11), pp.1838–1846. Available at: http://linkinghub.elsevier.com/retrieve/pii/S037837741000226X.

Arora, V.K., Chiew, F.H.S. & Grayson, R.B., 1999. A river flow routing scheme for general circulation models. Journal of Geophysical Research, 104(D12), p.14347. Available at: http://doi.wiley.com/10.1029/1999JD900200.

Assad, E.D. et al., 2010. Impacts of Climate Change on Brazilian Agriculture – Refocusing Impact Assessments to 2050,

Assad, E.D. et al., 2013. Impacts of climate change on the agricultural zoning of climate risk for cotton cultivation in Brazil. Pesquisa Agropecuária Brasileira, 48(1), pp.1–8. Available at: http://www.scielo.br/scielo.php?script=sci_arttext&pid=S0100-204X2013000100001&lng=en&nrm=iso&tlng=en.

Assad, E.D. & Pinto, H.S., 2008. Global warming and future scenarios for Brazilian Agriculture (in Portuguese),

Bellouin, N. et al., 2007. Improved representation of aerosols for HadGEM2. Hadley Centre Technical Note, (73). Available at: http://www.metoffice.gov.uk/media/pdf/8/f/HCTN_73.pdf.

Bellucci, A. et al., 2008. NAO–ocean circulation interactions in a coupled general circulation model. Climate Dynamics, 31(7-8), pp.759–777. Available at: http://link.springer.com/10.1007/s00382-008-0408-4.

Bierkens, M.F.P., 2015. Global hydrology 2015: State, trends, and directions. Water Resources Research, 51(7), pp.4923–4947. Available at: http://doi.wiley.com/10.1002/2015WR017173.

Blasing, T.J., Sullivan, A. & Madani, K., 2013. Response of California Summer Hydroelectricity Generation to Spring Temperature. British Journal of Environment and Climate Change, 3(3), pp.316–332. Available at: http://www.sciencedomain.org/abstract.php?iid=267&id=10&aid=2032.

Bogner, K. & Pappenberger, F., 2011. Multiscale error analysis, correction, and predictive uncertainty estimation in a flood forecasting system. Water Resources Research, 47(7), p.n/a–n/a. Available at: http://doi.wiley.com/10.1029/2010WR009137.

Bosch, J.M. & Hewlett, J.D., 1982. A review of catchment experiments to determine the effect of vegetation changes on water yield and evapotranspiration. Journal of Hydrology, 55(1-4), pp.3–23. Available at: http://linkinghub.elsevier.com/retrieve/pii/0022169482901172.

Briscoe, J., 2012. Fluid prejudice. , pp.1–10.

Briscoe, J., 2015. Water Security in a Changing World. Daedalus, 144(3), pp.27–34. Available at: http://www.mitpressjournals.org/doi/10.1162/DAED_a_00339.

Brisson, N. et al., 2003. An overview of the crop model stics. European Journal of Agronomy, 18(3-4), pp.309–332. Available at: http://linkinghub.elsevier.com/retrieve/pii/S1161030102001107.

Brisson, N. et al., 1998. STICS: a generic model for the simulation of crops and their water and nitrogen balances. I. Theory and parameterization applied to wheat and corn. Agronomie, 18(5-6), pp.311–346. Available at: http://www.agronomy-journal.org/10.1051/agro:19980501.

Brown, A.E. et al., 2005. A review of paired catchment studies for determining changes in water yield resulting from alterations in vegetation. Journal of Hydrology, 310(1-4), pp.28–61. Available at: http://linkinghub.elsevier.com/retrieve/pii/S0022169404005906.

Bruckner, T., Bashmakov, I.A. & Mulugetta, Y., 2014. Energy Systems. In Climate Change 2014: Mitigation of Climate Change. Contribution of Working Group III to the Fifth Assessment Report of the Intergovernmental Panel on Climate Change. Cambridge, United Kingdom and New York, NY, USA, United Kingdom and New York, NY, USA: Cambridge University Press, Cambridge, United Kingdom.

Bruijnzeel, L.A., 1990. Hydrology of Moist Forest and the Effects of Conversion: A State of Knowledge Review, Paris, France, France.

Buckley, B.M. et al., 2010. Climate as a contributing factor in the demise of Angkor, Cambodia. Proceedings of the National Academy of Sciences, 107(15), pp.6748–6752. Available at: http://www.pnas.org/cgi/doi/10.1073/pnas.0910827107.

Chambwera, M. & Heal, G., 2014. Economics of Adaptation. In Climate Change 2014: Impacts, Adaptation, and Vulnerability. Part A: Global and Sectoral Aspects. Contribution of Working Group II to the Fifth Assessment Report of the Intergovernmental Panel on Climate Change. Cambridge, United Kingdom and New York, NY, USA, United Kingdom and New York, NY, USA: Cambridge University Press, Cambridge, United Kingdom. Available at: https://ipcc-wg2.gov/AR5/images/uploads/WGIIAR5-Chap17_FINAL.pdf.

De Cian, E., Lanzi, E. & Roson, R., 2013. Seasonal temperature variations and energy demand. Climatic Change, 116(3-4), pp.805–825. Available at: http://link.springer.com/10.1007/s10584-012-0514-5.

Clarke, L. & Jiang, K., 2014. Assessing Transformation Pathways. In Climate Change 2014: Mitigation of Climate Change. Contribution of Working Group III to the Fifth Assessment Report of the Intergovernmental Panel on Climate Change. Cambridge, United Kingdom and New York, NY, USA, United Kingdom and New York, NY, USA: Cambridge University Press, Cambridge, United Kingdom.

Coe, M.T. et al., 2013. Deforestation and climate feedbacks threaten the ecological integrity of south-southeastern Amazonia. Philosophical transactions of the Royal Society of London. Series B, Biological sciences, 368(1619), p.20120155. Available at: http://rstb.royalsocietypublishing.org/content/368/1619/20120155.short.

Cohn, A.S. et al., 2014. Cattle ranching intensification in Brazil can reduce global greenhouse gas emissions by sparing land from deforestation. Proceedings of the National Academy of Sciences, 111(20), pp.7236–7241. Available at: http://www.pnas.org/cgi/doi/10.1073/pnas.1307163111.

Collins, W.. et al., 2008. Evaluation of the HadGEM2 model. Met Office Hadley Centre Technical Note, HCTN 74. Available at: http://www.metoffice.gov.uk/media/pdf/8/7/HCTN_74.pdf.

Collins, W.J. et al., 2011. Development and evaluation of an Earth-System model – HadGEM2. Geoscientific Model Development, 4(4), pp.1051–1075. Available at: http://www.geosci-model-dev.net/4/1051/2011/.

Collischonn, W. et al., 2007. The MGB-IPH model for large-scale rainfall—runoff modelling. Hydrological Sciences Journal, 52(5), pp.878–895. Available at: http://www.tandfonline.com/doi/abs/10.1623/hysj.52.5.878.

Cosgrove, W.J. & Loucks, D.P., 2015. Water management: Current and future challenges and research directions. Water Resources Research, 51(6), pp.4823–4839. Available at: http://doi.wiley.com/10.1002/2014WR016869.

Cox, P.M. et al., 2000. Acceleration of global warming due to carbon-cycle feedbacks in a coupled climate model. Nature, 408(6809), pp.184–187. Available at: http://www.nature.com/doifinder/10.1038/35041539.

Cox, P.M. et al., 2004. Amazonian forest dieback under climate-carbon cycle projections for the 21st century. Theoretical and Applied Climatology, 78(1-3). Available at: http://link.springer.com/10.1007/s00704-004-0049-4.

Davidson, E.A. et al., 2012. The Amazon basin in transition. Nature, 481(7381), pp.321–328.

Decker, W.L., 1986. The impact of climate change from increased atmospheric carbon dioxide on American agriculture University.,

Deschênes, O. & Greenstone, M., 2007. The Economic Impacts of Climate Change: Evidence from Agricultural Output and Random Fluctuations in Weather. American Economic Review, 97(1), pp.354–385. Available at: http://pubs.aeaweb.org/doi/abs/10.1257/aer.97.1.354.

Dias, L.C.P. et al., 2015. Effects of land cover change on evapotranspiration and streamflow of small catchments in the Upper Xingu River Basin, Central Brazil. Journal of Hydrology: Regional Studies, 4, pp.108–122. Available at: http://linkinghub.elsevier.com/retrieve/pii/S2214581815000543.

Diaz-Nieto, J. & Wilby, R.L., 2005. A comparison of statistical downscaling and climate change factor methods: impacts on low flows in the River Thames, United Kingdom. Climatic Change, 69(2-3), pp.245–268. Available at: http://link.springer.com/10.1007/s10584-005-1157-6.

Doorenbos, J. & Kassam, A.H., 1979. Yield response to water. Irrigation and Drainage Paper No. 33 Food and Agriculture Organization of the United Nations (FAO), p.193.

Doorenbos, J. & Pruitt, W.O., 1977. Crop Water Requirements. Irrigation and Drainage Paper No. 24 Food and Agriculture Organization of the United Nations (FAO), Rome.

Durack, P.J., Wijffels, S.E. & Matear, R.J., 2012. Ocean Salinities Reveal Strong Global Water Cycle Intensification During 1950 to 2000. Science, 336(6080), pp.455–458. Available at: http://www.sciencemag.org/cgi/doi/10.1126/science.1212222.

Eisner, S., Voss, F. & Kynast, E., 2012. Statistical bias correction of global climate projections &amp;ndash; consequences for large scale modeling of flood flows. Advances in Geosciences, 31, pp.75–82. Available at: http://www.adv-geosci.net/31/75/2012/.

EMBRAPA, 2003a. Cultivo do Arroz de Terras Altas (in Portuguese). Available at: http://sistemasdeproducao.cnptia.embrapa.br/FontesHTML/Arroz/ArrozTerrasAltas/index.htm.

EMBRAPA, 2010. Cultivo do Milho (in Portuguese). Available at: http://www.cnpms.embrapa.br/publicacoes/milho_6_ed/index.htm.

EMBRAPA, 2003b. Cultura do Algodão no Cerrado (in Portuguese). Available at: http://sistemasdeproducao.cnptia.embrapa.br/FontesHTML/Algodao/AlgodaoCerrado/.

EMBRAPA, 1981. Mapa de solos do Brasil, escala 1:5 000 000.

EMBRAPA, 2004. Tecnologias de Produção de Soja Região Central do Brasil (in Portuguese). Available at: http://www.cnpso.embrapa.br/producaosoja/SojanoBrasil.htm.

EMBRAPA & AGROCONSULT, 2010. Parâmetros das culturas do zoneamento agrícola de riscos climáticos,

van der Ent, R.J. et al., 2010. Origin and fate of atmospheric moisture over continents. Water Resources Research, 46(9), p.n/a–n/a. Available at: http://doi.wiley.com/10.1029/2010WR009127.

van der Ent, R.J. & Savenije, H.H.G., 2011. Length and time scales of atmospheric moisture recycling. Atmospheric Chemistry and Physics, 11(5), pp.1853–1863. Available at: http://www.atmos-chem-phys.net/11/1853/2011/.

EPE, 2013. Plano Decenal de Expansao da Energia (2022), Available at: http://www.epe.gov.br/PDEE/20140124_1.pdf.

Evenson, R.E. & Alves, D.C.O., 1998. Technology, climate change, productivity and land use in Brazilian agriculture. Planejamento e Politicas Publicas, 18.

Fageria, N.K. et al., 1997. Characterization of fertility and particle size of várzea soils of Mato Grosso and Mato Grosso do sul states of Brazil. Communications in Soil Science

and Plant Analysis, 28(1-2), pp.37–47. Available at: http://www.tandfonline.com/doi/abs/10.1080/00103629709369770.

Fang, G.H. et al., 2015. Comparing bias correction methods in downscaling meteorological variables for a hydrologic impact study in an arid area in China. Hydrology and Earth System Sciences, 19(6), pp.2547–2559. Available at: http://www.hydrol-earth-syst-sci.net/19/2547/2015/.

FAO, FAOSTAT. Available at: http://faostat.fao.org/site/339/default.aspx.

FAO, IFAD & WFP, 2014. The State of Food Insecurity in the World 2014, Rome, Italy, Italy.

Feres, J., Reis, E. & Speranza, J., 2008. Assessing the Impact of Climate Change on the Brazilian Agricultural Sector,

Ferreira Filho, J.B. de S. & Moraes, G.I. de, 2015. Climate change, agriculture and economic effects on different regions of Brazil. Environment and Development Economics, 20(01), pp.37–56. Available at: http://www.journals.cambridge.org/abstract_S1355770X14000126.

Fleury, L.C. & Almeida, J., 2013. A construção da Usina Hidrelétrica de Belo Monte: conflito ambiental e o dilema do desenvolvimento. Ambiente & Sociedade, 16(4), pp.141–156. Available at: http://www.scielo.br/scielo.php?script=sci_arttext&pid=S1414-753X2013000400009&lng=pt&nrm=iso&tlng=en.

Fogli, P. et al., 2009. INGV–CMCC Carbon: a carbon cycle earth system model, Available at: http://www.cmcc.it/publications/rp0061-ingv-cmcc-carbon-icc-a-carbon-cycle-earth-system-model.

Franz, K.J. & Hogue, T.S., 2011. Evaluating uncertainty estimates in hydrologic models: borrowing measures from the forecast verification community. Hydrology and Earth System Sciences, 15(11), pp.3367–3382. Available at: http://www.hydrol-earth-syst-sci.net/15/3367/2011/.

Galloway, G.E., 2011. If Stationarity is Dead, What Do We Do Now?1. JAWRA Journal of the American Water Resources Association, 47(3), pp.563–570. Available at: http://doi.wiley.com/10.1111/j.1752-1688.2011.00550.x.

Gent, P.R. et al., 2011. The Community Climate System Model Version 4. Journal of Climate, 24(19), pp.4973–4991. Available at: http://journals.ametsoc.org/doi/abs/10.1175/2011JCLI4083.1.

Gleick, P.H., 1998. Water and conflict. In The World's Water 1998-1999. pp. 105–135.

Gleick, P.H., 2014. Water, Drought, Climate Change, and Conflict in Syria. Weather, Climate, and Society, 6(3), pp.331–340. Available at: http://journals.ametsoc.org/doi/abs/10.1175/WCAS-D-13-00059.1.

Gleick, P.H., Yolles, P. & Hatami, H., 1994. Water, war & peace in the Middle East. Environment, 36(3), p.6–. Available at: http://www.atmos.washington.edu/~davidc/ATMS211/articles_optional/Water_War_Middle_East.pdf.

Good, P. et al., 2013. Comparing Tropical Forest Projections from Two Generations of Hadley Centre Earth System Models, HadGEM2-ES and HadCM3LC. Journal of Climate, 26(2), pp.495–511. Available at: http://journals.ametsoc.org/doi/abs/10.1175/JCLI-D-11-00366.1.

Governo do Mato Grosso, ., 2013. Situação econômica internacional, nacional e regional - subsídio a elaboração da lei orçamentária para 2014 (in Portuguese), Available at: http://www.seplan.mt.gov.br/arquivos/MATERIAS SEPLAN/PLOA 2014_SITUACAO ECONOMICA DO ESTADO LOA 2014.pdf.

Grey, D. & Sadoff, C.W., 2006. Water for Growth and Development,

Gualdi, S., Scoccimarro, E. & Navarra, A., 2008. Changes in Tropical Cyclone Activity due to Global Warming: Results from a High-Resolution Coupled General Circulation Model. Journal of Climate, 21(20), pp.5204–5228. Available at: http://journals.ametsoc.org/doi/abs/10.1175/2008JCLI1921.1.

Hales, J. & Petry, P., 2013. Freshwater Ecoregions of the world - 302: Taajos-Juruena. Available at: http://www.feow.org/ecoregions/details/320.

Hamududu, B. & Killingtveit, A., 2012. Assessing Climate Change Impacts on Global Hydropower. Energies, 5(12), pp.305–322. Available at: http://www.mdpi.com/1996-1073/5/2/305/.

Hashino, T., Bradley, A.A. & Schwartz, S.S., 2007. Evaluation of bias-correction methods for ensemble streamflow volume forecasts. Hydrology and Earth System Sciences, 11(2), pp.939–950. Available at: http://www.hydrol-earth-syst-sci.net/11/939/2007/.

Hayhoe, S.J. et al., 2011. Conversion to soy on the Amazonian agricultural frontier increases streamflow without affecting stormflow dynamics. Global Change Biology, 17(5), pp.1821–1833. Available at: http://doi.wiley.com/10.1111/j.1365-2486.2011.02392.x.

Hempel, S. et al., 2013. A trend-preserving bias correction &ndash; The ISI-MIP approach. Earth System Dynamics, 4(2), pp.219–236.

Heng, L.K. et al., 2009. Validating the FAO AquaCrop Model for Irrigated and Water Deficient Field Maize. Agronomy Journal, 101(3), p.488. Available at: https://www.agronomy.org/publications/aj/abstracts/101/3/488.

Hilker, T. et al., 2014. Vegetation dynamics and rainfall sensitivity of the Amazon. Proceedings of the National Academy of Sciences, under revi(45), pp.16041–16046. Available at: http://www.pnas.org/lookup/doi/10.1073/pnas.1404870111.

Hsiao, T.C. et al., 2009. Aquacrop-The FAO crop model to simulate yield response to water: III. Parameterization and testing for maize. Agronomy Journal, 101(3), pp.448–459.

Hurtt, G.C. et al., 2011. Harmonization of land-use scenarios for the period 1500-2100: 600 years of global gridded annual land-use transitions, wood harvest, and resulting secondary lands. Climatic Change, 109(1), pp.117–161.

Hurtt, G.C. et al., 2006. The underpinnings of land-use history: three centuries of global gridded land-use transitions, wood-harvest activity, and resulting secondary lands. Global Change Biology, 12(7), pp.1208–1229. Available at: http://doi.wiley.com/10.1111/j.1365-2486.2006.01150.x.

Hurtt, G.C., Moorcroft, P.R. & Pacala, S.W., 2013. Ecosystem Demography Model: Scaling Vegetation Dynamics Across South America. Ecosystem Demography Model: Scaling Vegetation Dynamics Across South America. Model product. Available at: http://daac.ornl.gov/MODELS/guides/EDM_SA_Vegetation.html.

IBGE, 2006. Censo Agropecuário.

IBGE, 2009. Mapa Pedologica de solos - Estado de Mato Grosso.

IBGE, 2015. Sistema IBGE de Recupearacao Automatica. Available at: http://www.sidra.ibge.gov.br/bda/acervo/acervo9.asp?e=c&p=PA&z=t&o=11.

IEA, 2013. World Energy Outlook 2013,

IPCC, 2008. Climate Change and Water B. C. Bates et al., eds.,

IPCC, 2014. Fifth Assessment Report - Intergovernmental Panel on Climate Change, Geneva, Switzerland.

IPCC, 2012. Summary for policymakers - Special report on managing the risk of extreme events and disasters to advance climate change adaptation (SREX), Intergovernmental Panel on Climate Change.

IPEA, 2015. Carta de Conjuntura (in Portuguese), Available at: http://www.ipea.gov.br/portal/index.php?option=com_alphacontent&view=alphacontent &Itemid=59.

van Ittersum, M.K. & Donatelli, M., 2003. Modelling cropping systems—highlights of the symposium and preface to the special issues. European Journal of Agronomy, 18(3-4), pp.187–197. Available at: http://linkinghub.elsevier.com/retrieve/pii/S1161030102000953.

Jacob, D. et al., 2007. An inter-comparison of regional climate models for Europe: model performance in present-day climate. Climatic Change, 81(S1), pp.31–52. Available at: http://link.springer.com/10.1007/s10584-006-9213-4.

Joetzjer, E. et al., 2013. Present-day and future Amazonian precipitation in global climate models: CMIP5 versus CMIP3. Climate Dynamics, 41(11-12), pp.2921–2936. Available at: http://link.springer.com/10.1007/s00382-012-1644-1.

Johns, T.C. et al., 2006. The New Hadley Centre Climate Model (HadGEM1): Evaluation of Coupled Simulations. Journal of Climate, 19(7), pp.1327–1353. Available at: http://journals.ametsoc.org/doi/abs/10.1175/JCLI3712.1.

Jones, J. & et al, 2011. Use of crop models for climate-agricultural decisions. In D. Hillel & C. Rosenzweig, eds. Handbook of Climate Change and Agroecosystems. Imperial College Press - London, pp. 131–157.

Kaniewski, D., Guiot, J. & Van Campo, E., 2015. Drought and societal collapse 3200 years ago in the Eastern Mediterranean: a review. Wiley Interdisciplinary Reviews: Climate Change, 6(4), pp.369–382. Available at: http://doi.wiley.com/10.1002/wcc.345.

Karunaratne, A., Walker, S. & Ruane, A., 2015. Modelling bambara groundnut in Southern Africa: towards a climate resilient future. Climate Research. Available at: http://www.int-res.com/prepress/c01300.html.

Keating, B.. et al., 2003. An overview of APSIM, a model designed for farming systems simulation. European Journal of Agronomy, 18(3-4), pp.267–288. Available at: http://linkinghub.elsevier.com/retrieve/pii/S1161030102001089.

Knox, R.G. et al., 2015. Hydrometeorological effects of historical land-conversion in an ecosystem-atmosphere model of Northern South America. Hydrology and Earth System Sciences, 19(1), pp.241–273. Available at: http://www.hydrol-earth-syst-sci.net/19/241/2015/hess-19-241-2015.pdf.

Kruijt, B. et al., 2014. AMAZALERT Final project summary for policy makers (D6.7), Available at: http://www.eu-amazalert.org/publications/deliveryreports.

Kumar, N.M. et al., 2009. On the use of Standardized Precipitation Index (SPI) for drought intensity assessment. Meteorological Applications, 16(3), pp.381–389. Available at: http://doi.wiley.com/10.1002/met.136.

Langutt, D., Finkelstein, I. & Litt, T., 2013. Climate and the Late Bronze Collapse: New Evidence from the Southern Levant. Tel Aviv, 40(2), pp.149–175. Available at: http://www.maneyonline.com/doi/abs/10.1179/033443513X13753505864205.

Lee, Y.H., Pierce, J.R. & Adams, P.J., 2013. Representation of nucleation mode microphysics in a global aerosol model with sectional microphysics. Geoscientific Model Development, 6(4), pp.1221–1232. Available at: http://www.geosci-model-dev.net/6/1221/2013/.

Lehner, B. et al., 2011. High-resolution mapping of the world's reservoirs and dams for sustainable river-flow management (GranD database). Frontiers in Ecology and the Environment, 9(9), pp.494–502. Available at: http://www.esajournals.org/doi/abs/10.1890/100125.

Lemos, A.L.F. & Silva, J. de A., 2011. Desmatamento na Amazônia Legal: Evolução, Causas, Monitoramento e Possibilidades de Mitigação Através do Fundo Amazônia. Floresta e Ambiente, 18(1), pp.98–108. Available at: http://www.floram.org/articles/view/id/4ff1c2231ef1faee0f00000f.

Lewis, S.L., Edwards, D.P. & Galbraith, D., 2015. Increasing human dominance of tropical forests. Science, 349(6250), pp.827–832. Available at: http://www.sciencemag.org/cgi/doi/10.1126/science.aaa9932.

Li, W., Fu, R. & Dickinson, R.E., 2006. Rainfall and its seasonality over the Amazon in the 21st century as assessed by the coupled models for the IPCC AR4. Journal of Geophysical Research, 111(D2), p.D02111. Available at: http://doi.wiley.com/10.1029/2005JD006355.

Liermann, C.R. et al., 2012. Implications of Dam Obstruction for Global Freshwater Fish Diversity. BioScience, 62(6), pp.539–548. Available at: http://bioscience.oxfordjournals.org/cgi/doi/10.1525/bio.2012.62.6.5.

Lobell, D.B. & Burke, M.B., 2010. On the use of statistical models to predict crop yield responses to climate change. Agricultural and Forest Meteorology, 150(11), pp.1443–1452. Available at: http://linkinghub.elsevier.com/retrieve/pii/S0168192310001978.

Lobligeois, F. et al., 2014. When does higher spatial resolution rainfall information improve streamflow simulation? An evaluation using 3620 flood events. Hydrology and Earth System Sciences, 18(2), pp.575–594. Available at: http://www.hydrol-earth-syst-sci.net/18/575/2014/.

Longo, M., 2014. Amazon Forest Response to Changes in Rainfall Regime: Results from an Individual-Based Dynamic Vegetation Model. Harvard University. Available at: http://dash.harvard.edu/handle/1/11744438.

Macedo, M.N. et al., 2012. Decoupling of deforestation and soy production in the southern Amazon during the late 2000s. Proceedings of the National Academy of Sciences, 109(4), pp.1341–1346. Available at: http://www.pnas.org/cgi/doi/10.1073/pnas.1111374109.

Mainuddin, M., Kirby, M. & Hoanh, C.T., 2013. Impact of climate change on rainfed rice and options for adaptation in the lower Mekong Basin. Natural Hazards, 66(2), pp.905–938. Available at: http://link.springer.com/10.1007/s11069-012-0526-5.

Malavolta, E. et al., 1965. Estudos sôbre a fertilidade dos solos do cerrado. I. Efeito da calagem na disponibilidade do fósforo. Annais da Escola Superior de Agricultura "Luiz de Queiroz", 22. Available at: http://www.revistas.usp.br/aesalq/article/viewFile/38779/41663.

Malhi, Y. et al., 2008. Climate change, deforestation, and the fate of the Amazon. Science (New York, N.Y.), 319(5860), pp.169–172.

Margulis, S. & Dubeux, S.B.C., 2011. The Economy of Climate Change in Brazil: Costs and Opportunites, Sao Paulo, Brazil.

Marsland, S.J. et al., 2003. The Max-Planck-Institute global ocean/sea ice model with orthogonal curvilinear coordinates. Ocean Modelling, 5(2), pp.91–127. Available at: http://linkinghub.elsevier.com/retrieve/pii/S146350030200015X.

Martin, G.M. et al., 2006. The Physical Properties of the Atmosphere in the New Hadley Centre Global Environmental Model (HadGEM1). Part I: Model Description and Global Climatology. Journal of Climate, 19(7), pp.1274–1301. Available at: http://journals.ametsoc.org/doi/abs/10.1175/JCLI3636.1.

McKee, T.B., Doesken, N.J. & Kleist, J., 1993. The relationship of drought frequency and duration to time scales. Preprints, 8th Conference on Applied Climatology,, pp.pp. 179–184.

McLaughlin, D. & Kinzelbach, W., 2015. Food security and sustainable resource management. Water Resources Research, 51(7), pp.4966–4985. Available at: http://doi.wiley.com/10.1002/2015WR017053.

Medvigy, D. et al., 2009. Mechanistic scaling of ecosystem function and dynamics in space and time: Ecosystem Demography model version 2. Journal of Geophysical Research: Biogeosciences, 114(G1), p.G01002. Available at: http://doi.wiley.com/10.1029/2008JG000812.

Mendelsohn, R. & Nordhaus, W., 1996. The Impact of Global Warming on Agriculture: Reply. American Economic Review, 86(5), pp.1312–1315. Available at: http://search.ebscohost.com/login.aspx?direct=true&db=bth&AN=9701203795&site=eh ost-live&scope=site.

Mhizha, T. et al., 2014. Use of the FAO AquaCrop model in developing sowing guidelines for rainfed maize in Zimbabwe. Water SA, 40(2), p.233. Available at: http://www.ajol.info/index.php/wsa/article/view/102216.

Millar, C.I. & Stephenson, N.L., 2015. Temperate forest health in an era of emerging megadisturbance. Science, 349(6250), pp.823–826. Available at: http://www.sciencemag.org/cgi/doi/10.1126/science.aaa9933.

Miller, R.L. et al., 2014. CMIP5 historical simulations (1850-2012) with GISS ModelE2. Journal of Advances in Modeling Earth Systems, 6(2), pp.441–477. Available at: http://doi.wiley.com/10.1002/2013MS000266.

Milly, P.C.D. et al., 2015. Commentary on critiques of "Stationarity is dead: Whither water management?" Water Resources Research, p.n/a–n/a. Available at: http://doi.wiley.com/10.1002/2015WR017408.

Milly, P.C.D. et al., 2008. Stationarity Is Dead: Whither Water Management? Science, 319(5863), pp.573–574. Available at: http://www.sciencemag.org/cgi/doi/10.1126/science.1151915.

Montanari, A. & Koutsoyiannis, D., 2014. Modeling and mitigating natural hazards: Stationarity is immortal! Water Resources Research, 50(12), pp.9748–9756. Available at: http://doi.wiley.com/10.1002/2014WR016092.

Moorcroft, P.R., Hurtt, G.C. & Pacala, S.W., 2001. A method for scaling vegetation dynamics: The ecosystem demography model (ED). Ecological Monographs, 71(4), pp.557–586.

Muerth, M.J. et al., 2013. On the need for bias correction in regional climate scenarios to assess climate change impacts on river runoff. Hydrology and Earth System Sciences, 17(3), pp.1189–1204. Available at: http://www.hydrol-earth-syst-sci.net/17/1189/2013/.

Mukheibir, P., 2013. Potential consequences of projected climate change impacts on hydroelectricity generation. Climatic Change, 121(1), pp.67–78. Available at: http://link.springer.com/10.1007/s10584-013-0890-5.

Muller, M. et al., 2015. Built infrastructure is essential. Science, 349(6248), pp.585–586. Available at: http://www.sciencemag.org/cgi/doi/10.1126/science.aac7606.

Nash, E. & Sutcliffe, V., 1970. River flow forecasting Through conceptual models PART I-A Discussion of principles. Journal of Hydrology, 10, pp.282–290.

Nazarenko, L. et al., 2015. Future climate change under RCP emission scenarios with GISS ModelE2. Journal of Advances in Modeling Earth Systems, 7(1), pp.244–267. Available at: http://doi.wiley.com/10.1002/2014MS000403.

Nepstad, D. et al., 2014. Slowing Amazon deforestation through public policy and interventions in beef and soy supply chains. Science, 344(6188), pp.1118–1123. Available at: http://www.sciencemag.org/cgi/doi/10.1126/science.1248525.

Oppenheimer, M., Campos, M. & Warren, R., 2014. Emergent Risks and Key Vulnerabilities. In Climate Change 2014: Impacts, daptation, and Vulnerability. Part A: Global and Sectoral Aspects. Contribution of Working Group II to the Fifth Assessment Report of the Intergovernmental Panel on Climate Change. Cambridge, United Kingdom and New York, NY, USA, United Kingdom and New York, NY, USA: Cambridge University Press, Cambridge, United Kingdom, pp. 1039–1099. Available at: https://ipcc-wg2.gov/AR5/images/uploads/WGIIAR5-Chap19_FINAL.pdf.

Orlowsky, B. & Seneviratne, S.I., 2013. Elusive drought: uncertainty in observed trends and short- and long-term CMIP5 projections. Hydrology and Earth System Sciences, 17(5), pp.1765–1781. Available at: http://www.hydrol-earth-syst-sci.net/17/1765/2013/.

Paiva, R.C.D. et al., 2012. On the sources of hydrological prediction uncertainty in the Amazon. Hydrology and Earth System Sciences, 16(9), pp.3127–3137. Available at: http://www.hydrol-earth-syst-sci.net/16/3127/2012/.

Paz, A.R., Collischonn, W. & Lopes da Silveira, A.L., 2006. Improvements in large-scale drainage networks derived from digital elevation models. Water Resources Research, 42(8), p.n/a–n/a. Available at: http://doi.wiley.com/10.1029/2005WR004544.

Pearson, K., 1895. Note on regression and inheritance in the case of two parents. Proceedings of the Royal Society of London, 58.

Prudhomme, C. et al., 2013. Hydrological droughts in the 21st century, hotspots and uncertainties from a global multimodel ensemble experiment. Proceedings of the National Academy of Sciences of the United States of America. Available at: http://www.ncbi.nlm.nih.gov/pubmed/24344266.

Raddatz, T.J. et al., 2007. Will the tropical land biosphere dominate the climate–carbon cycle feedback during the twenty-first century? Climate Dynamics, 29(6), pp.565–574. Available at: http://link.springer.com/10.1007/s00382-007-0247-8.

Raes, D. et al., 2011. Aquacrop – Reference Manual, Rome, Italy. Available at: http://www.fao.org/nr/water/aquacrop.html.

Raes, D. et al., 2009. Aquacrop-The FAO crop model to simulate yield response to water: II. main algorithms and software description. Agronomy Journal, 101(3), pp.438–447.

Randall, D.A. et al., 2007. Cilmate Models and Their Evaluation. In S. Solomon et al., eds. Climate Change 2007: The Physical Science Basis. Contribution of Working Group I to the Fourth Assessment Report of the Intergovernmental Panel on Climate Change. New York, NY, USA: Cambridge University Press, Cambridge, United Kingdom. Available at: http://www.iges.org/people/Shukla's Articles/2007/Climate Models.pdf.

Reed, S.M., 2003. Deriving flow directions for coarse-resolution (1-4 km) gridded hydrologic modeling. Water Resources Research, 39(9), p.n/a–n/a. Available at: http://doi.wiley.com/10.1029/2003WR001989.

REN21, 2013. Renewables 2013 Global Status Report, Paris. Available at: http://www.ren21.net/Portals/0/documents/Resources/GSR/2013/GSR2013_lowres.pdf.

Ringer, M.A. et al., 2006. The Physical Properties of the Atmosphere in the New Hadley Centre Global Environmental Model (HadGEM1). Part II: Aspects of Variability and Regional Climate. Journal of Climate, 19(7), pp.1302–1326. Available at: http://journals.ametsoc.org/doi/abs/10.1175/JCLI3713.1.

Ripl, W., 2003. Water: the bloodstream of the biosphere. Philosophical Transactions of the Royal Society B: Biological Sciences, 358(1440), pp.1921–1934. Available at: http://rstb.royalsocietypublishing.org/cgi/doi/10.1098/rstb.2003.1378.

Rodell, M. et al., 2004. The Global Land Data Assimilation System (GLDAS). Bulletin of the American Meteorological Society, 85(3), pp.381–394. Available at: http://journals.ametsoc.org/doi/abs/10.1175/BAMS-85-3-381.

Rojas, R. et al., 2012. Assessment of future flood hazard in Europe using a large ensemble of bias-corrected regional climate simulations. Journal Of Geophysical Research-Atmospheres, 117. Available at: <Go to ISI>://000310685900002.

Rosenzweig, C. et al., 2014. Assessing agricultural risks of climate change in the 21st century in a global gridded crop model intercomparison. Proceedings of the National Academy of Sciences, 111(9), pp.3268–3273. Available at: http://www.pnas.org/lookup/doi/10.1073/pnas.1222463110.

Ruddiman, W., 2005. Plows, Plagues and Petroleum: How Humans Took Control of Climate, Princeton University Press.

Sahin, V. & Hall, M.J., 1996. The effects of afforestation and deforestation on water yields. Journal Of Hydrology, 178, pp.293–309.

Salas, J.D. & Obeysekera, J., 2014. Revisiting the Concepts of Return Period and Risk for Nonstationary Hydrologic Extreme Events. Journal of Hydrologic Engineering, 19(3), pp.554–568. Available at: http://ascelibrary.org/doi/10.1061/%28ASCE%29HE.1943-5584.0000820.

Sanghi, A. et al., 1997. Global Warming Impacts on Brazilian Agriculture: Estimates of the Ricardian Model. Economia Aplicada, 1(1).

Sanghi, A. & Mendelsohn, R., 2008. The impacts of global warming on farmers in Brazil and India. Global Environmental Change, 18(4), pp.655–665. Available at: http://linkinghub.elsevier.com/retrieve/pii/S0959378008000496.

Schaeffer, R. et al., 2012. Energy sector vulnerability to climate change: A review. Energy, 38(1), pp.1–12. Available at: http://linkinghub.elsevier.com/retrieve/pii/S0360544211007870.

Schlenker, W. & Roberts, M.J., 2009. Nonlinear temperature effects indicate severe damages to U.S. crop yields under climate change. Proceedings of the National Academy of Sciences, 106(37), pp.15594–15598. Available at: http://www.pnas.org/cgi/doi/10.1073/pnas.0906865106.

Schmidt, G.A. et al., 2011. Climate forcing reconstructions for use in PMIP simulations of the last millennium (v1.0). Geoscientific Model Development, 4(1), pp.33–45. Available at: http://www.geosci-model-dev.net/4/33/2011/.

Schmidt, G.A. et al., 2014. Configuration and assessment of the GISS ModelE2 contributions to the CMIP5 archive. Journal of Advances in Modeling Earth Systems, 6(1), pp.141–184. Available at: http://doi.wiley.com/10.1002/2013MS000265.

Scoccimarro, E. et al., 2011. Effects of Tropical Cyclones on Ocean Heat Transport in a High-Resolution Coupled General Circulation Model. Journal of Climate, 24(16), pp.4368–4384. Available at: http://journals.ametsoc.org/doi/abs/10.1175/2011JCLI4104.1.

SEI, 2011. Understanding the Nexus,

Sheffield, J., Goteti, G. & Wood, E.F., 2006. Development of a 50-Year High-Resolution Global Dataset of Meteorological Forcings for Land Surface Modeling. Journal of Climate, 19(13), pp.3088–3111. Available at: http://journals.ametsoc.org/doi/abs/10.1175/JCLI3790.1.

Sillmann, J. et al., 2013. Climate extremes indices in the CMIP5 multimodel ensemble: Part 1. Model evaluation in the present climate. Journal of Geophysical Research: Atmospheres, 118(4), pp.1716–1733. Available at: http://doi.wiley.com/10.1002/jgrd.50203.

Sivapalan, M., Savenije, H.H.G. & Blöschl, G., 2012. Socio-hydrology: A new science of people and water. Hydrological Processes, 26(8), pp.1270–1276. Available at: http://doi.wiley.com/10.1002/hyp.8426.

Smith, M.B. et al., 2004. Runoff response to spatial variability in precipitation: an analysis of observed data. Journal of Hydrology, 298(1-4), pp.267–286. Available at: http://linkinghub.elsevier.com/retrieve/pii/S0022169404002483.

Soares-Filho, B.S. et al., 2006. Modelling conservation in the Amazon basin. Nature, 440(7083), pp.520–3. Available at: http://www.ncbi.nlm.nih.gov/pubmed/16554817.

Stakhiv, E.Z., 2011. Pragmatic Approaches for Water Management Under Climate Change Uncertainty1. JAWRA Journal of the American Water Resources Association, 47(6), pp.1183–1196. Available at: http://doi.wiley.com/10.1111/j.1752-1688.2011.00589.x.

Steduto, P. et al., 2009. Aquacrop-the FAO crop model to simulate yield response to water: I. concepts and underlying principles. Agronomy Journal, 101(3), pp.426–437.

Steduto, P. et al., 2009. Concepts and Applications of AquaCrop: The FAO Crop Water Productivity Model. In Crop Modeling and Decision Support. Berlin, Heidelberg: Springer Berlin Heidelberg, pp. 175–191. Available at: http://link.springer.com/10.1007/978-3-642-01132-0_19.

Steduto, P. et al., 2012. Crop yield response to water - FAO 66. FAO Irrigation and Drainage Paper, (66), p.505.

Stricevic, R. et al., 2011. Assessment of the FAO AquaCrop model in the simulation of rainfed and supplementally irrigated maize, sugar beet and sunflower. Agricultural Water Management, 98(10), pp.1615–1621. Available at: http://linkinghub.elsevier.com/retrieve/pii/S0378377411001193.

Strobl, E. & Strobl, R.O., 2011. The distributional impact of large dams : Evidence from cropland productivity in Africa. Journal of Development Economics, 96(2), pp.432–450. Available at: http://dx.doi.org/10.1016/j.jdeveco.2010.08.005.

Swann, A.L.S. et al., 2015. Future deforestation in the Amazon and consequences for South American climate. Agricultural and Forest Meteorology, 214-215, pp.12–24. Available at: http://linkinghub.elsevier.com/retrieve/pii/S0168192315002130.

Syvitski, J.P.M., 2005. Impact of Humans on the Flux of Terrestrial Sediment to the Global Coastal Ocean. Science, 308(5720), pp.376–380. Available at: http://www.sciencemag.org/cgi/doi/10.1126/science.1109454.

Syvitski, J.P.M. et al., 2009. Sinking deltas due to human activities. Nature Geoscience, 2(10), pp.681–686. Available at: http://www.nature.com/doifinder/10.1038/ngeo629.

Taylor, K.E., Stouffer, R.J. & Meehl, G.A., 2012. An Overview of CMIP5 and the Experiment Design. Bulletin of the American Meteorological Society, 93(4), pp.485–498. Available at: http://journals.ametsoc.org/doi/abs/10.1175/BAMS-D-11-00094.1.

Trumbore, S., Brando, P. & Hartmann, H., 2015. Forest health and global change. Science, 349(6250), pp.814–818. Available at: http://www.sciencemag.org/cgi/doi/10.1126/science.aac6759.

UN/DESA, 2015. World Population Prospects: The 2015 Revision, Key Findings and Advance Tables, Available at: http://esa.un.org/unpd/wpp/Publications/Files/Key_Findings_WPP_2015.pdf.

US EIA, 2013. International Energy Outlook 2013, Available at: http://www.eia.gov/forecasts/ieo/.

USACE, 2013. HEC-ResSim: Reservoir System Simulation. , p.556. Available at: http://www.hec.usace.army.mil/software/hec-ressim/documentation/HEC-ResSim_31_UsersManual.pdf.

USCCSP, 2008. The Effects of Climate Change on Agriculture, Land Resources, Water Resources, and Biodiversity in the United States, Available at: http://www.usda.gov/oce/climate_change/SAP4_3/CCSPFinalReport.pdf.

Vanuytrecht, E., Raes, D., Steduto, P., et al., 2014. AquaCrop: FAO's crop water productivity and yield response model. Environmental Modelling & Software, 62, pp.351–360. Available at: http://linkinghub.elsevier.com/retrieve/pii/S136481521400228X.

Vanuytrecht, E., Raes, D., Willems, P., et al., 2014. Comparing climate change impacts on cereals based on CMIP3 and EU-ENSEMBLES climate scenarios. Agricultural and Forest Meteorology, 195-196, pp.12–23. Available at: http://linkinghub.elsevier.com/retrieve/pii/S0168192314001178.

Vergara, W. & Scholz, S.M., 2011. Assessment of the Risk of Amazon Dieback, Washington DC, USA, USA.

Vichi, M. et al., 2011. Global and regional ocean carbon uptake and climate change: sensitivity to a substantial mitigation scenario. Climate Dynamics, 37(9-10), pp.1929–1947. Available at: http://link.springer.com/10.1007/s00382-011-1079-0.

Vitousek, P.M., 1997. Human Domination of Earth's Ecosystems. Science, 277(5325), pp.494–499. Available at: http://www.sciencemag.org/cgi/doi/10.1126/science.277.5325.494.

van Vliet, M.T.H. et al., 2013. Global river discharge and water temperature under climate change. Global Environmental Change, 23(2), pp.450–464. Available at: http://linkinghub.elsevier.com/retrieve/pii/S0959378012001331.

van Vliet, M.T.H. et al., 2012. Vulnerability of US and European electricity supply to climate change. Nature Climate Change, 2(9), pp.676–681. Available at: http://www.nature.com/doifinder/10.1038/nclimate1546.

Vogel, R.M. et al., 2015. Hydrology: The interdisciplinary science of water. Water Resources Research, 51(6), pp.4409–4430. Available at: http://doi.wiley.com/10.1002/2015WR017049.

Volodin, E.M., Dianskii, N.A. & Gusev, A. V., 2010. Simulating present-day climate with the INMCM4.0 coupled model of the atmospheric and oceanic general circulations. Izvestiya, Atmospheric and Oceanic Physics, 46(4), pp.414–431. Available at: http://link.springer.com/10.1134/S000143381004002X.

Vuuren, D.P. et al., 2011. The representative concentration pathways: an overview. Climatic Change, 109(1-2), pp.5–31. Available at: http://link.springer.com/10.1007/s10584-011-0148-z.

Warszawski, L. et al., 2014. The Inter-Sectoral Impact Model Intercomparison Project (ISI–MIP): Project framework. Proceedings of the National Academy of Sciences, 111(9), pp.3228–3232. Available at: http://www.pnas.org/lookup/doi/10.1073/pnas.1312330110.

WCD, 2000. Dams and Development: A New Framework for Decision-making,

Werrell, C.E., Femia, F. & (eds.), 2013. The Arab Spring and Climate Change. A Climate and Security Correlations Series,

Wing, I.S. & Fisher-Vanden, K., 2013. Confronting the challenge of integrated assessment of climate adaptation: a conceptual framework. Climatic Change, 117(3), pp.497–514. Available at: http://link.springer.com/10.1007/s10584-012-0651-x.

Yuan, X. & Wood, E.F., 2012. Downscaling precipitation or bias-correcting streamflow? Some implications for coupled general circulation model (CGCM)-based ensemble seasonal hydrologic forecast. Water Resources Research, 48(12), p.n/a–n/a. Available at: http://doi.wiley.com/10.1029/2012WR012256.

Zarfl, C., Lumsdon, A.E. & Tockner, K., 2015. A global boom in hydropower dam construction.

Zhang, K. et al., 2015. The fate of Amazonian ecosystems over the coming century arising from changes in climate, atmospheric CO2, and land use. Global Change Biology, 21(7), pp.2569–2587. Available at: http://doi.wiley.com/10.1111/gcb.12903.

Zulkafli, Z. et al., 2013. A critical assessment of the JULES land surface model hydrology for humid tropical environments. Hydrology and Earth System Sciences, 17(3), pp.1113–1132. Available at: http://www.hydrol-earth-syst-sci.net/17/1113/2013/.

# Annex A   Supplementary material for Chapter 2

|  | (1) | (2) |
|---|---|---|
| 6SPI < -1.5 |  | -0.012** |
|  |  | (5.649e-03) |
| 6SPI > 1.5 |  | -0.005 |
|  |  | (6.414e-03) |
| 24SPI < -1.5 |  | -0.010*** |
|  |  | (3.112e-03) |
| 24SPI > 1.5 |  | -0.001 |
|  |  | (4.785e-03) |
| T<5°C | 0.003** | 0.003** |
|  | (1.037e-03) | (1.042e-03) |
| T>27.5°C | 0.001 | 0.001 |
|  | (9.817e-04) | (1.006e-03) |
| lro_sum | 0.018 | -0.001 |
|  | (2.086e-02) | (2.575e-02) |
| lro_spr | 0.048*** | 0.038** |
|  | (1.454e-02) | (1.487e-02) |
| lro_wint | 0.050** | 0.041* |
|  | (2.308e-02) | (2.278e-02) |
| lro_fall | 0.013 | 0.004 |
|  | (1.862e-02) | (1.760e-02) |
| nuke_sh | -3.074*** | -3.039*** |
|  | (6.895e-01) | (6.847e-01) |
| coal_sh | -1.653** | -1.643** |
|  | (6.407e-01) | (6.427e-01) |
| gasoil_sh | -1.780*** | -1.773*** |
|  | (4.057e-01) | (4.072e-01) |
| Constant | 21.668*** | 22.024*** |
|  | (4.420e-01) | (4.546e-01) |
| Fixed effect | Y | Y |
| Year dummies | Y | Y |
| Observations | 2,465 | 2,465 |
| R-squared | 0.412 | 0.417 |
| Number of id2 | 85 | 85 |

Robust standard errors in parentheses
*** p<0.01, ** p<0.05, * p<0.1, + p<0.15

**Table A-1 Estimation results using unscaled seasonal runoff**

|  | (1) | (2) |
|---|---|---|
| 6SPI < -1.5 |  | -0.010** |
|  |  | (4.959e-03) |
| 6SPI > 1.5 |  | -0.004 |
|  |  | (5.367e-03) |
| 24SPI < -1.5 |  | -0.011*** |
|  |  | (3.502e-03) |
| 24SPI > 1.5 |  | -0.000 |
|  |  | (5.005e-03) |
| T<5°C | 0.002 | 0.002 |
|  | (1.343e-03) | (1.309e-03) |
| T>27.5°C | 0.001 | 0.001 |
|  | (1.024e-03) | (1.041e-03) |
| lprecip_sum | 0.008 | -0.008 |
|  | (3.579e-02) | (3.719e-02) |
| lprecip_spr | 0.103*** | 0.083** |
|  | (3.502e-02) | (3.687e-02) |
| lprecip_wint | 0.038 | 0.025 |
|  | (2.778e-02) | (2.500e-02) |
| lprecip_fall | 0.082*** | 0.055* |
|  | (2.919e-02) | (2.987e-02) |
| nuke_sh | -3.062*** | -3.036*** |
|  | (6.921e-01) | (6.904e-01) |
| coal_sh | -1.664** | -1.655** |
|  | (6.477e-01) | (6.499e-01) |
| gasoil_sh | -1.798*** | -1.787*** |
|  | (4.042e-01) | (4.083e-01) |
| Constant | 20.881*** | 21.509*** |
|  | (6.790e-01) | (7.346e-01) |
| Fixed effect | Y | Y |
| Year dummies | Y | Y |
| Observations | 2,465 | 2,465 |
| R-squared | 0.412 | 0.417 |
| Number of id2 | 85 | 85 |

Robust standard errors in parentheses
*** p<0.01, ** p<0.05, * p<0.1, + p<0.15

**Table A-2 Estimation results using unscaled total precipitation**

**Model 3**                                      **Model 5**
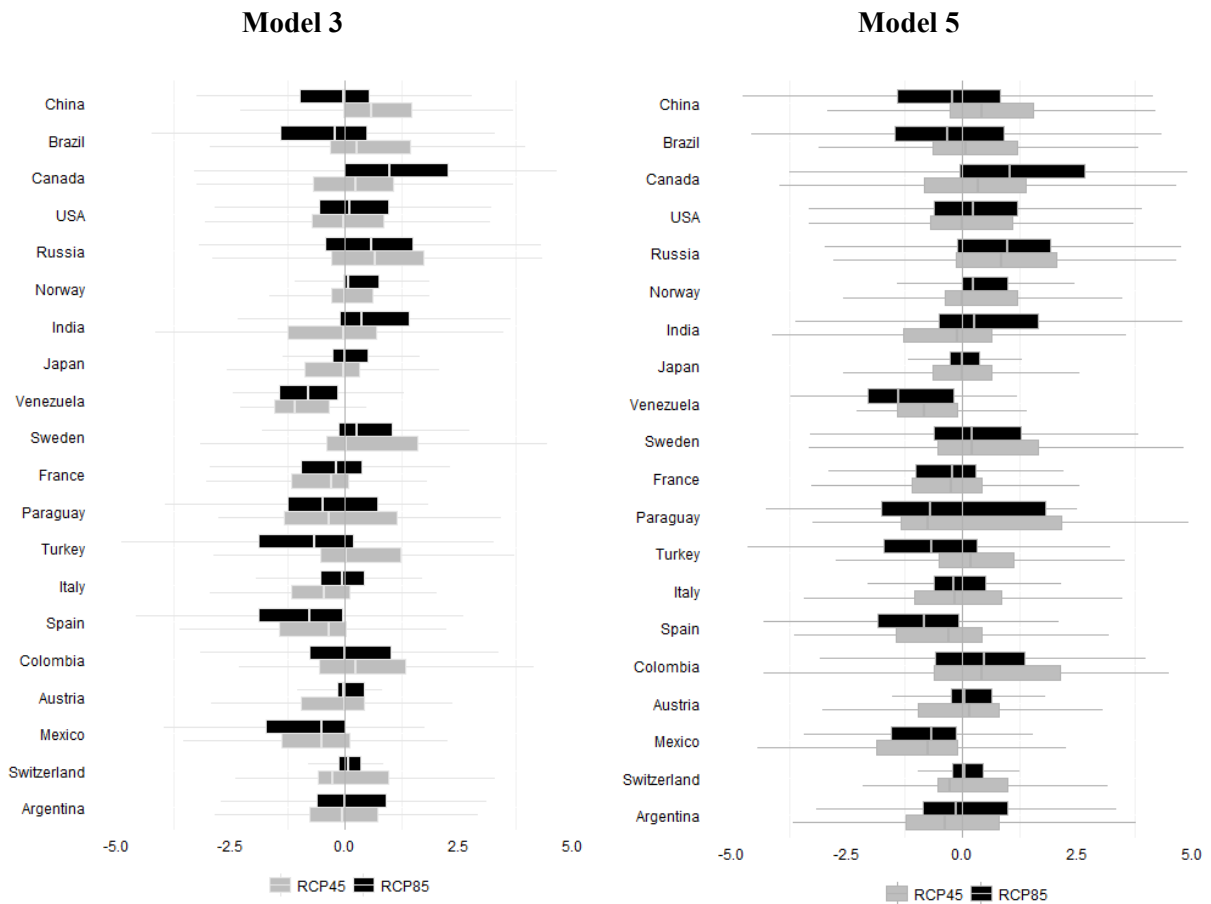


Figure A-1 Spatial distribution and GCMs uncertainty of climate change impacts on hydropower generation around 2050 in RCP 8.5 and RCP 4.5. Top 20 hydropower producer countries. Percentage changes in electricity generation relative to current levels (2006-2015 annual average). Comparison of model (3) and model (5) of Table S5.
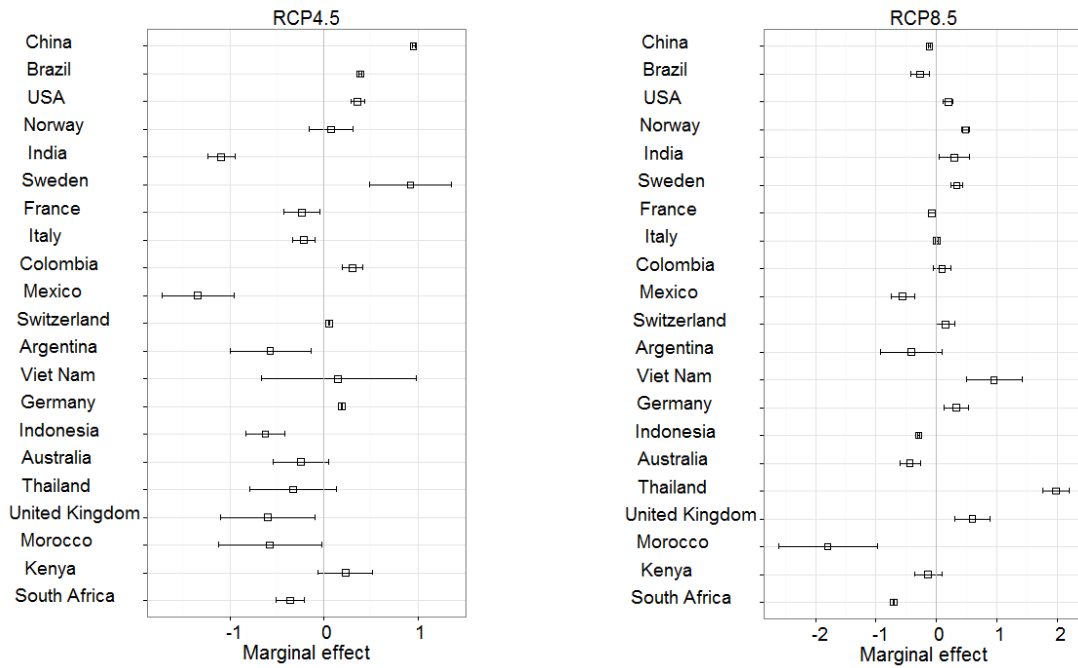
**Figure A-2 Statistical uncertainty at median climate of climate change impacts on hydropower generation around 2050 in RCP 8.5 and RCP 4.5 for the top 20 hydropower generators. Percentage changes in electricity generation relative to current levels (2006-2015 annual average) at the country level. Country-level impacts have been calculated as weighted average of impacts at the dam site with share of reservoir volume as weights.**
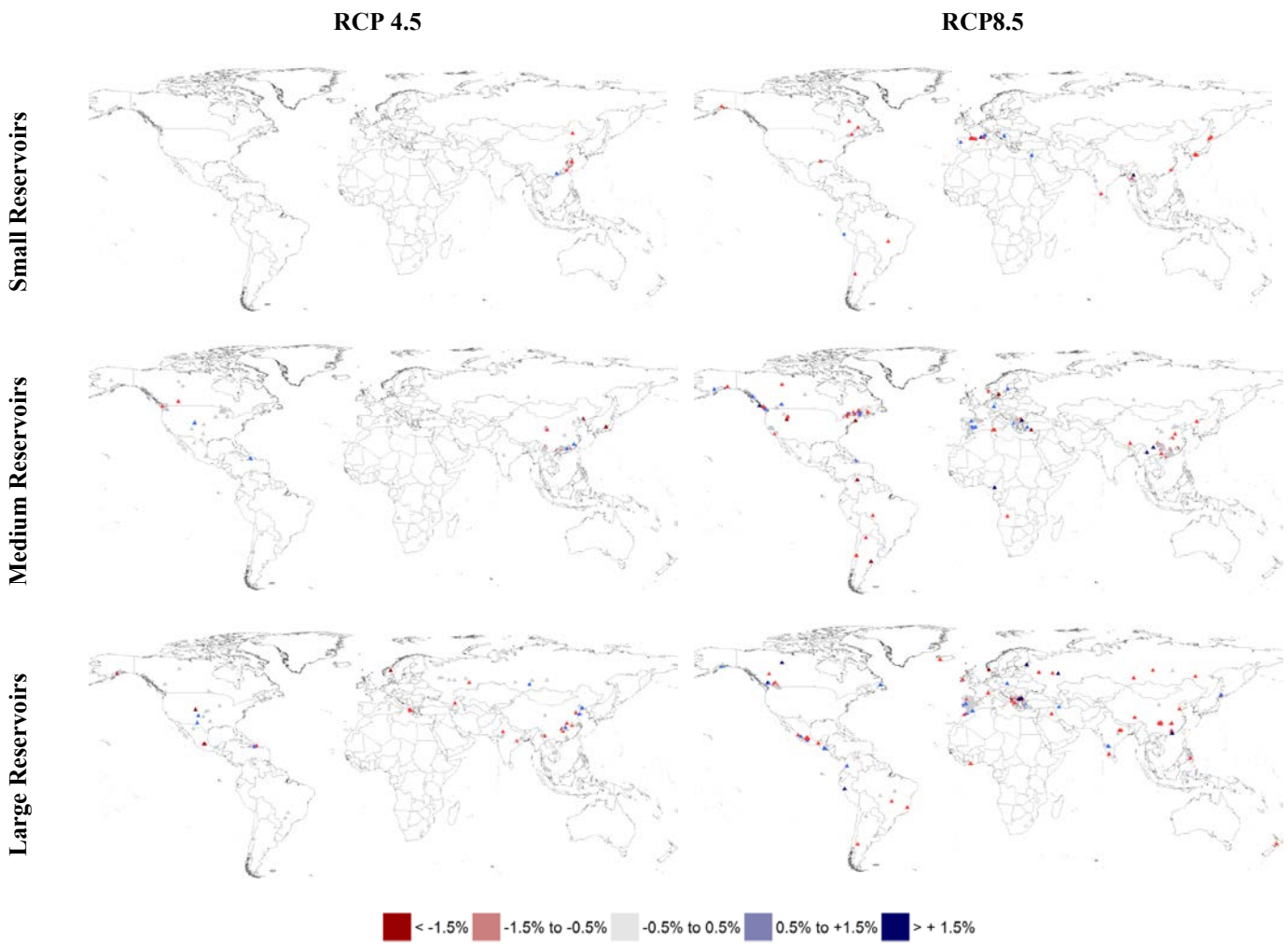
**Figure A-3 Climate change impacts in 2050 RCP 4.5 and RCP 8.5 as simulated by 5 different GCM models. Dam level Multi Model Median of the results calculated using the different climate models. Concordance 5 GCMs.**

**RCP 4.5**  **RCP8.5**

Small Reservoirs

Medium Reservoirs

Large Reservoirs

< -1.5%   -1.5% to -0.5%   -0.5% to 0.5%   0.5% to +1.5%   > + 1.5%
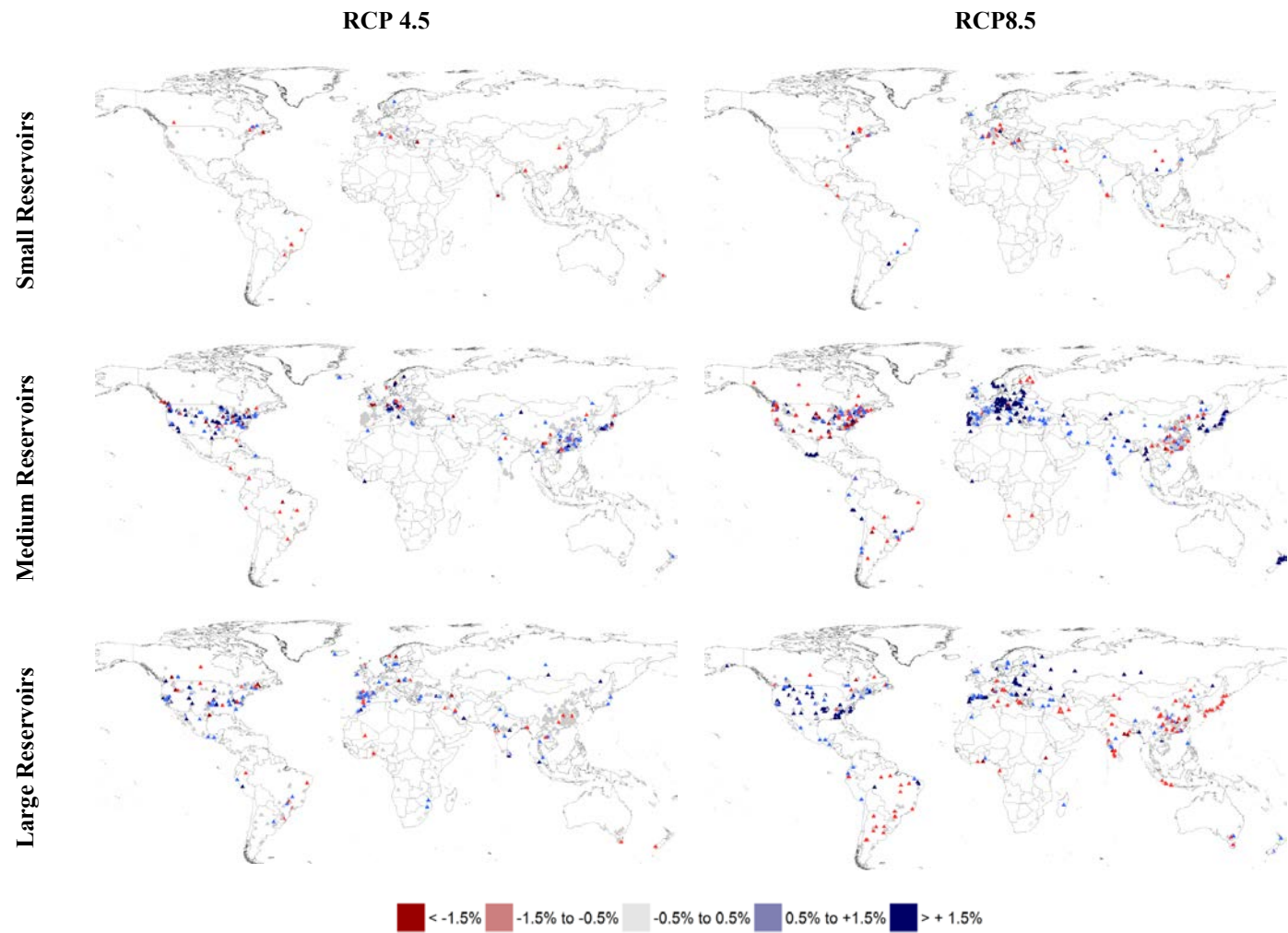
**Figure A-4 Climate change impacts in 2050 RCP 4.5 and RCP 8.5 as simulated by 5 different GCM models. Dam level Multi Model Median of the results calculated using the different climate models. Concordance 4 GCMs.**
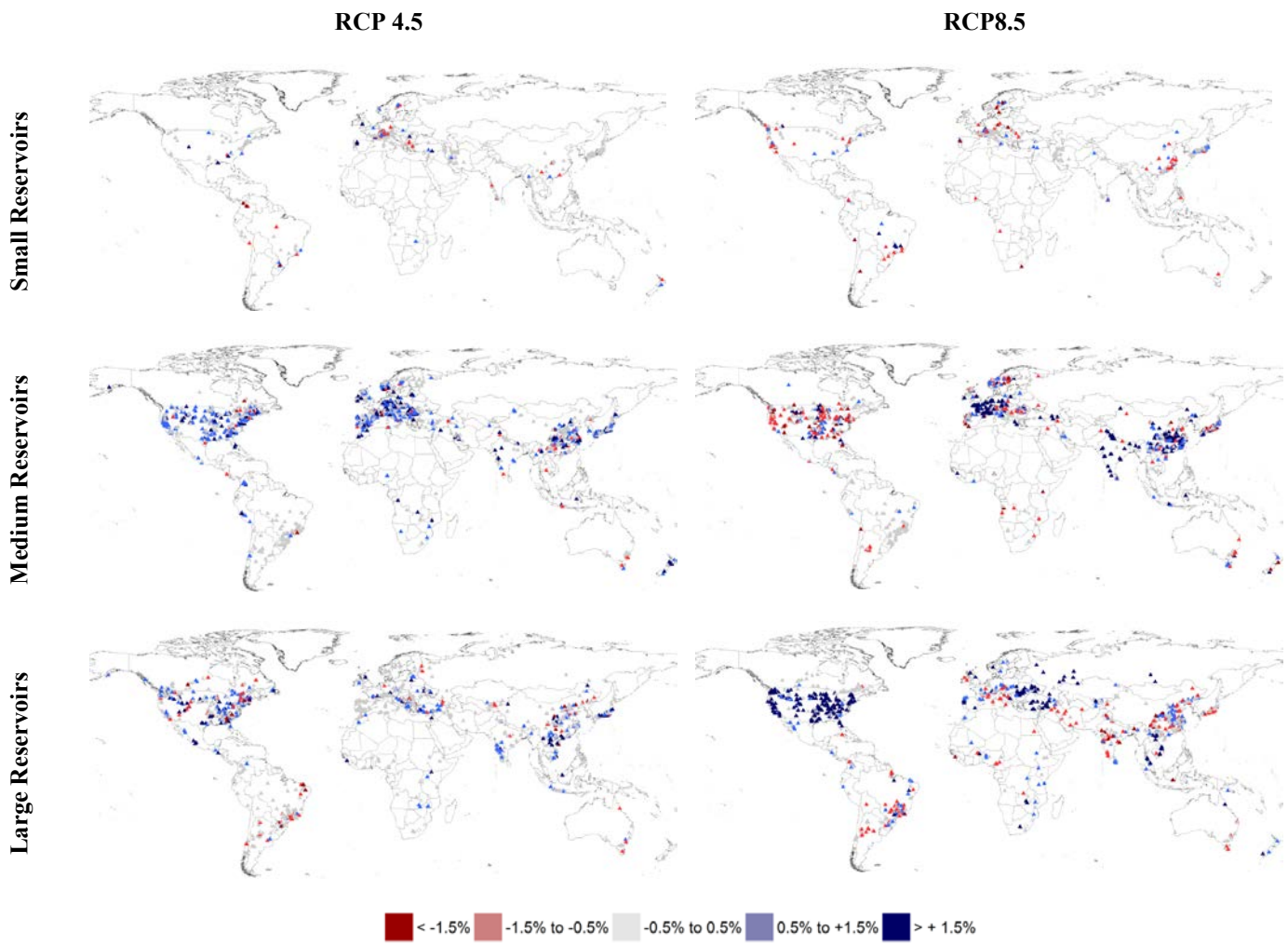
**Figure A-5 Climate change impacts in 2050 RCP 4.5 and RCP 8.5 as simulated by 5 different GCM models. Dam level Multi Model Median of the results calculated using the different climate models. Concordance 3 GCMs.**

# Annex B   Supplementary material for Chapter 3

Baseline

No Land use – RCP 4.5



No Land use – RCP 8.5

Governance Land use – RCP 4.5



Governance Land use – RCP 8.5

Extreme Land use – RCP 8.5
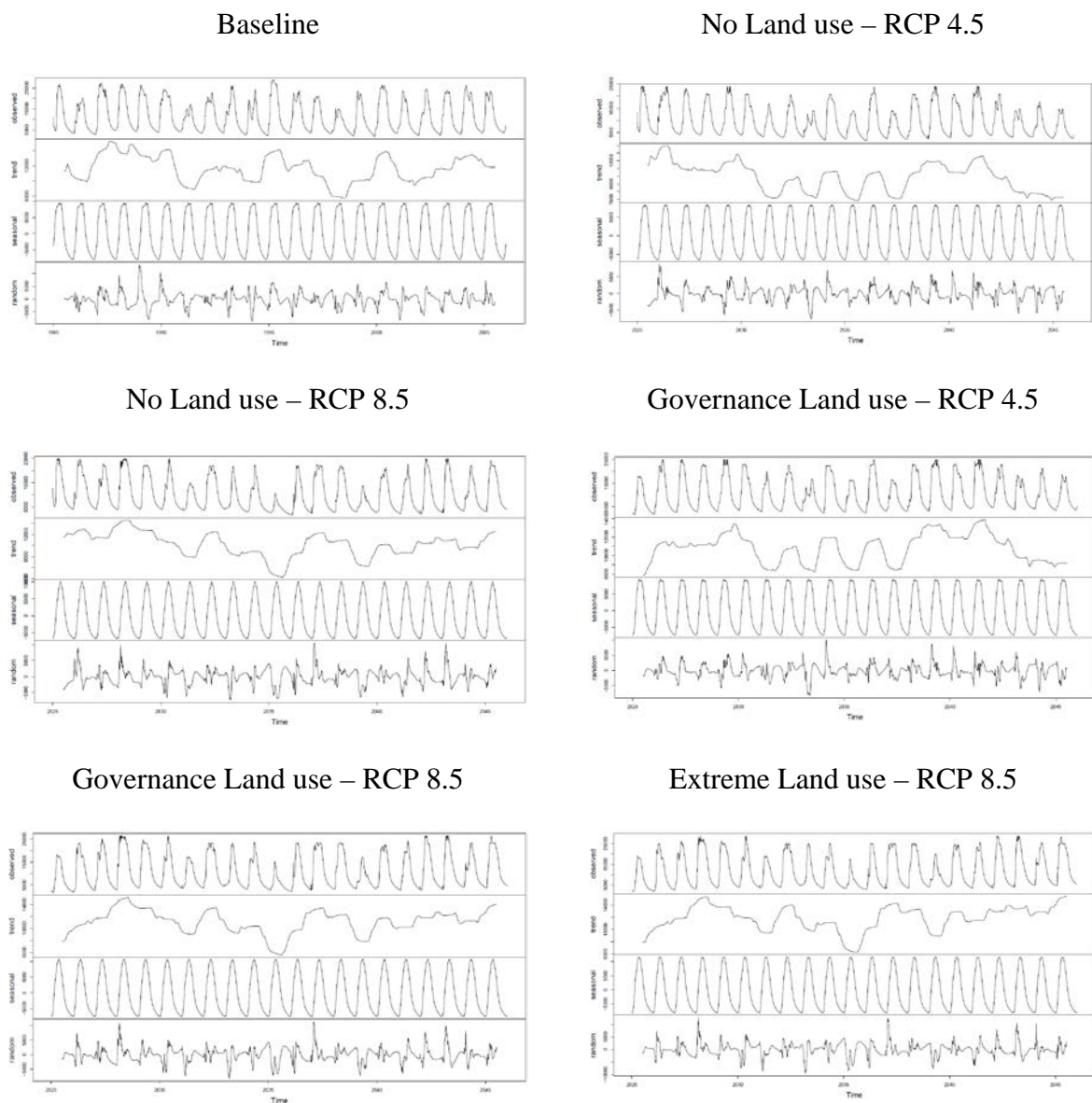


**Figure B-1 Simulated flows hydrographs and timeseries decomposition**

# Annex C   Supplementary material for Chapter 4

1. In this section we present the results of the calibration process for each of the counties producing the specific crop within the domain (total=49 counties):
- Soybean
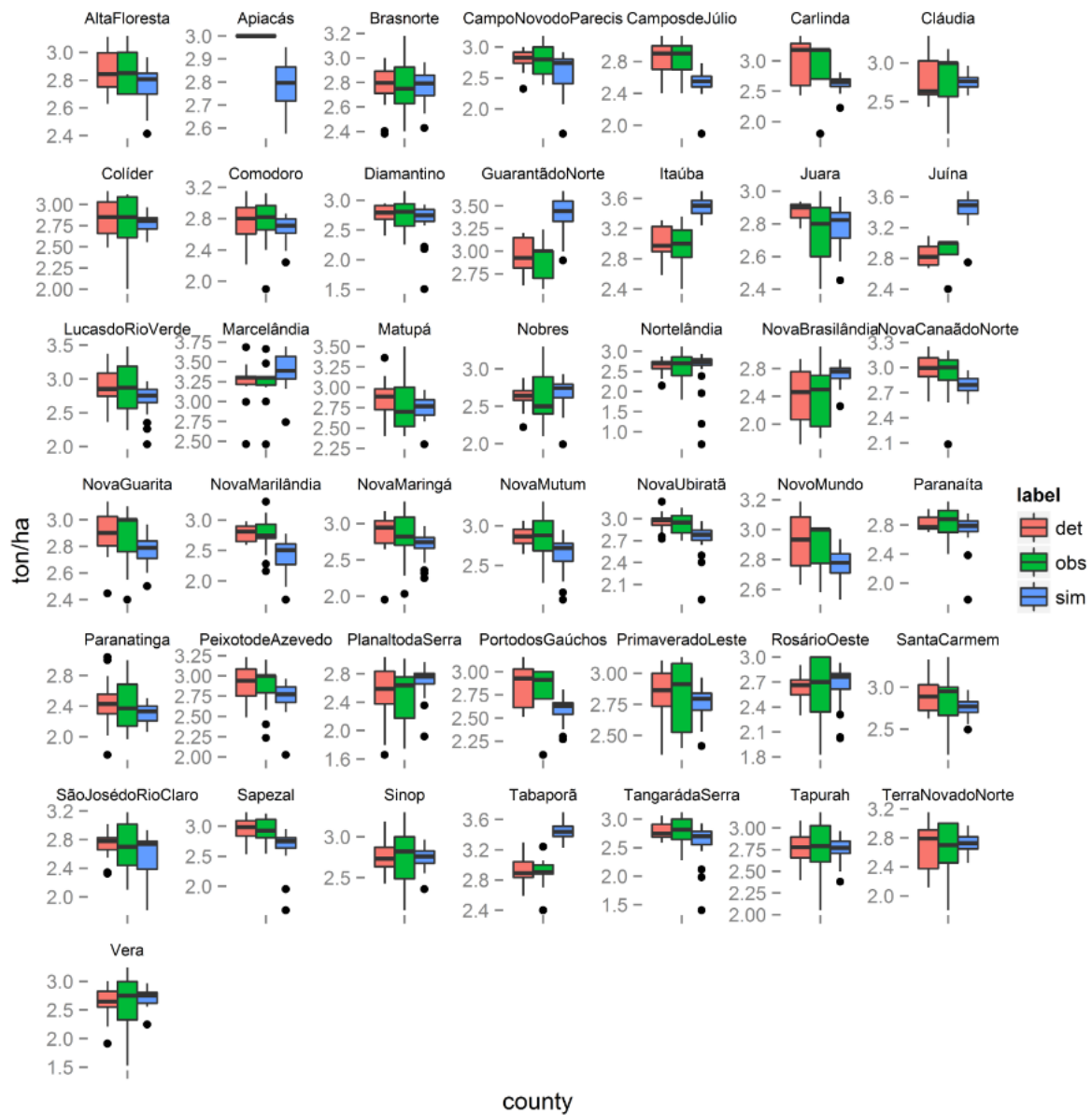


**Figure C-1 Calibration of the AquaCrop model for soybean simulation in the 43 counties where soybean was produced in the period into consideration (1991-2010). The boxplots refer to: observations (green), observations de-trended (light red), simulation (light blue).**

- Corn
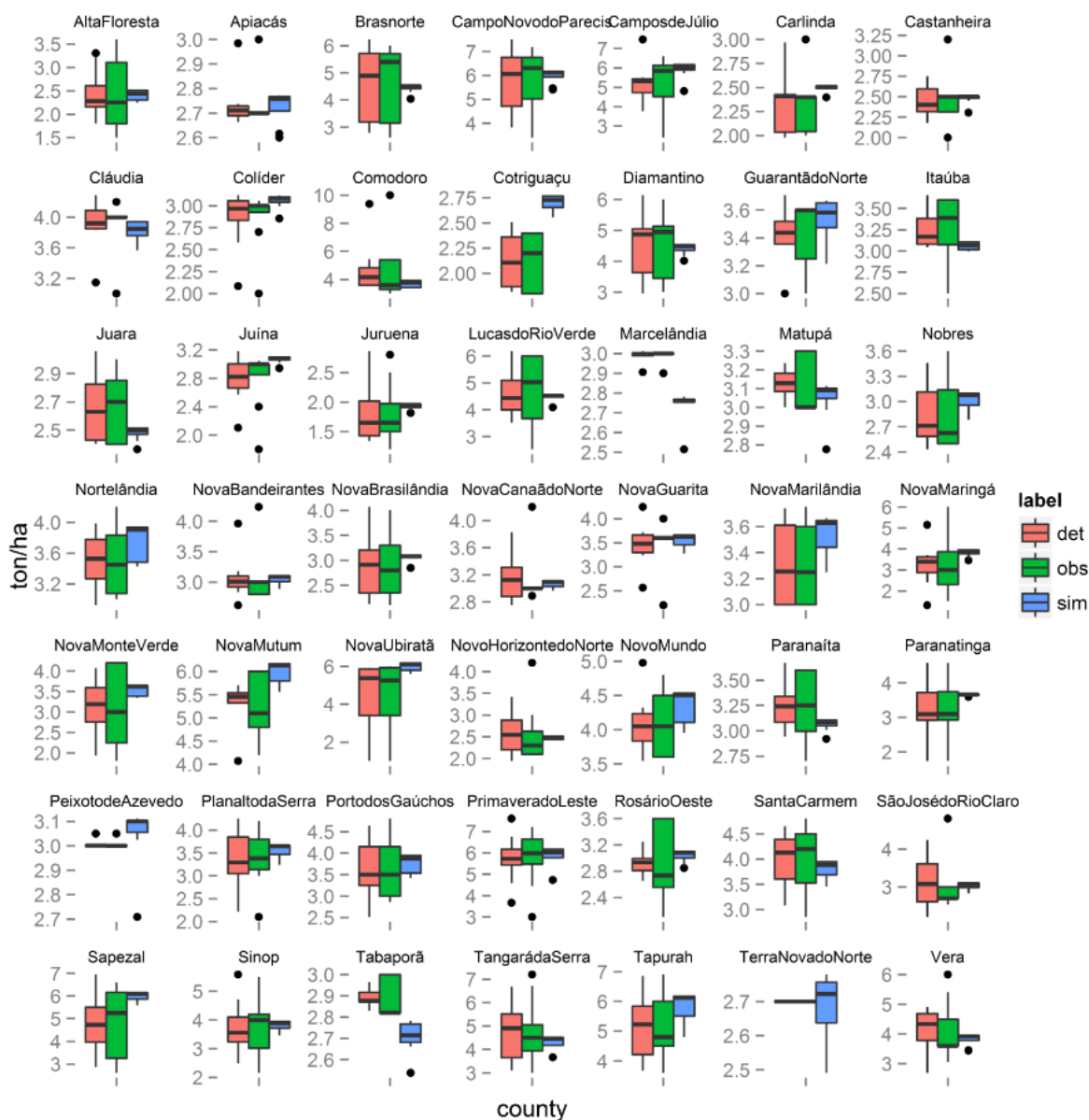


**Figure C-2 Calibration of the AquaCrop model for corn simulation in the 49 counties of the domain in the period into consideration (1991-2010). The boxplots refer to: observations (green), observations de-trended (light red), simulation (light blue).**

- Rice
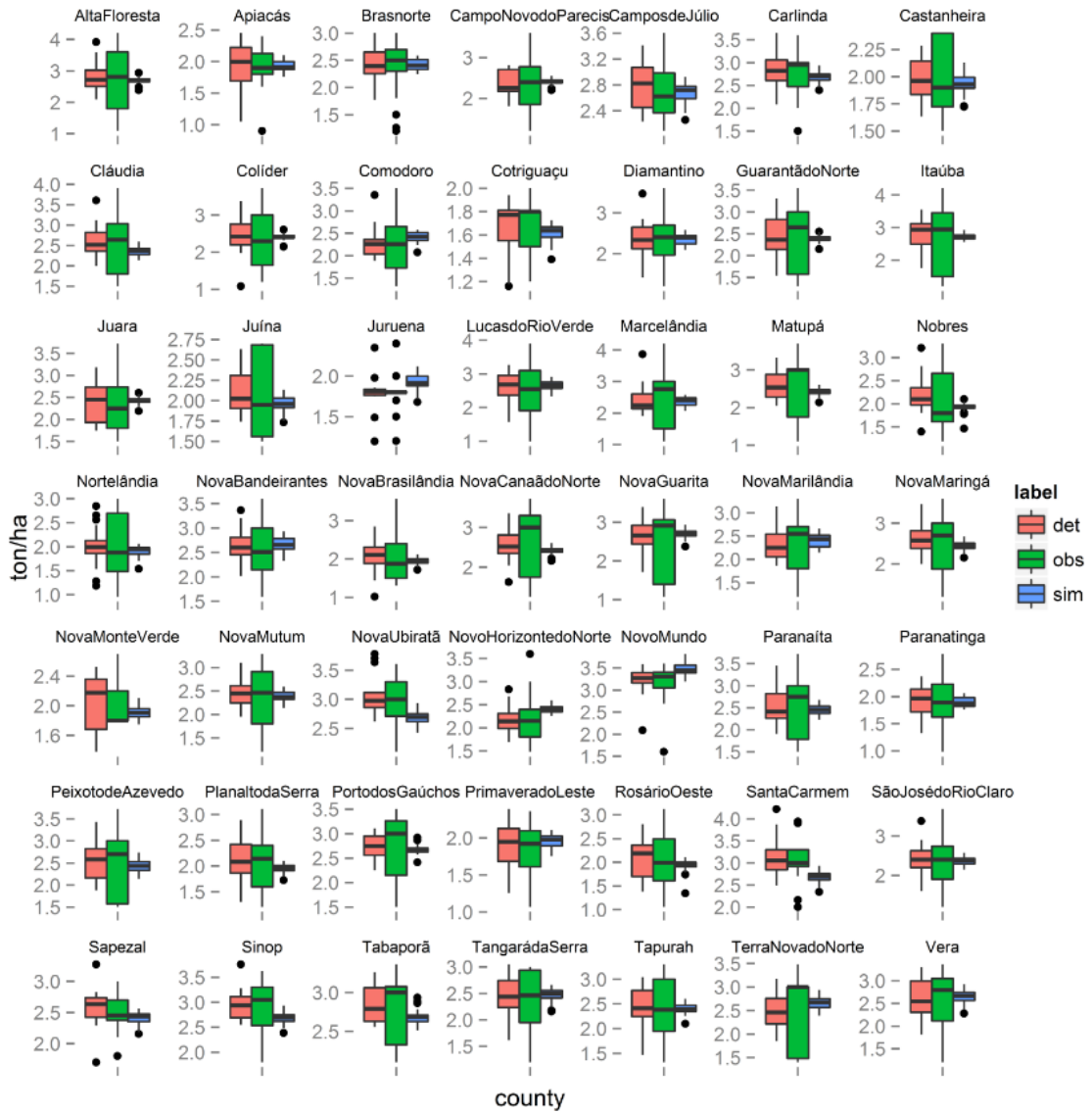


**Figure C-3 Calibration of the AquaCrop model for rice simulation in the 49 counties of the domain in the period into consideration (1991-2010). The boxplots refer to: observations (green), observations de-trended (light red), simulation (light blue).**

- Cotton
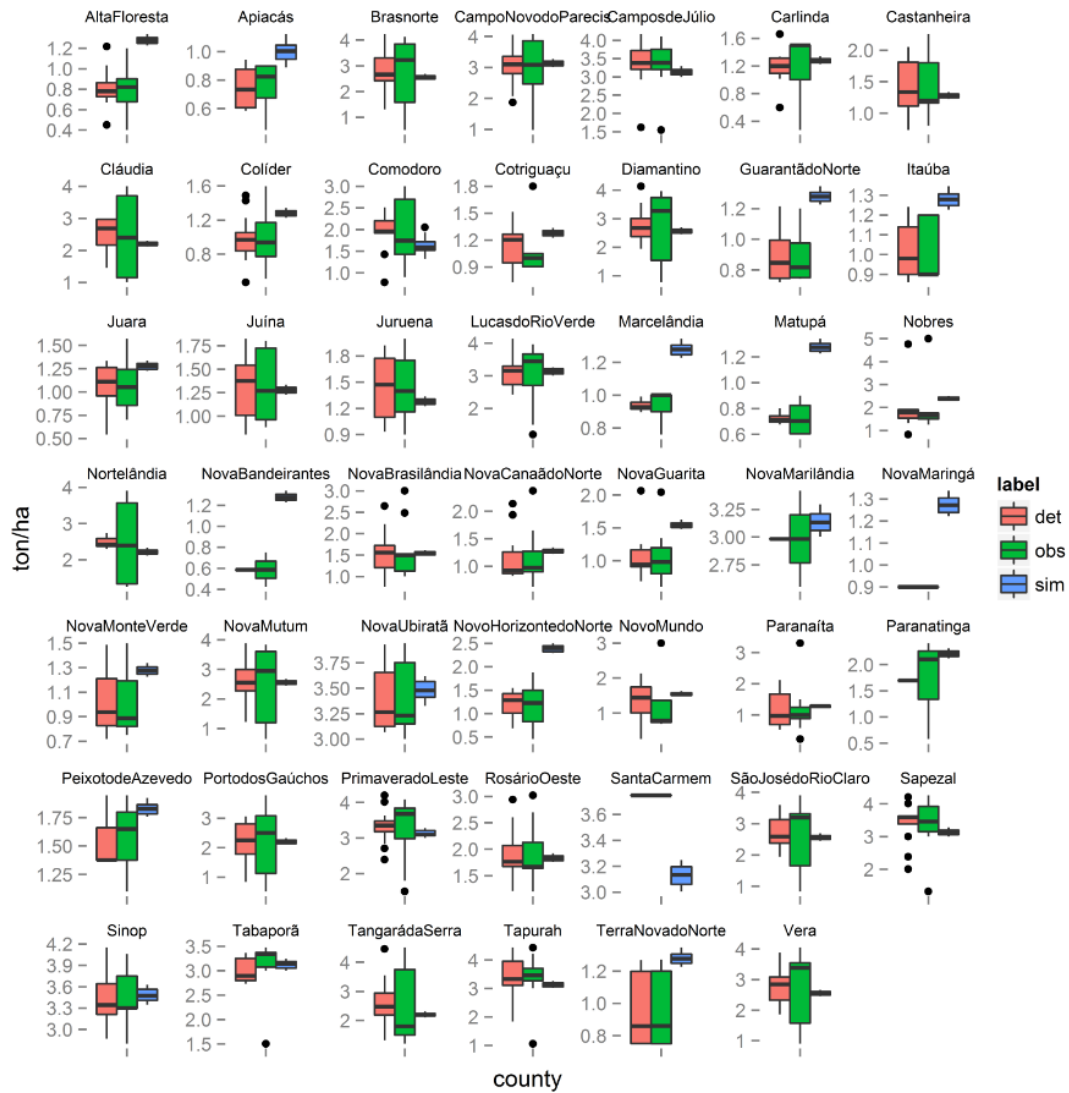


**Figure C-4 Calibration of the AquaCrop model for cotton simulation in the 48 counties where cotton was produced in the period into consideration (1991-2010). The boxplots refer to: observations (green), observations de-trended (light red), simulation (light blue).**

## 2. Crop Parameters

| Parameter | | Value | | | | | | | |
|---|---|---|---|---|---|---|---|---|---|
| | | Corn | | Soybean | | Rice | | Cotton | |
| | | FAO | EMBRAPA | FAO | EMBRAPA | FAO | EMBRAPA | FAO | EMBRAPA |
| **CROP PHENOLOGY** | | | | | | | | | |
| | **1.1 Threshold air temperatures** | | | | | | | | |
| Conservative | Base temperature, °C | 8 | 10 | 5 | 10 | 8 | 10 | 12 | 18 |
| Conservative | Cut off temperature, °C | 30 | 30 | 30 | 40 | 30 | 35 | 35 | 30 |
| | **1.2 Development of green canopy cover** | | | | | | | | |
| Conservative | Soil surface covered by an individual seedling at 90% emergence (cm2/plant) | 6.50 | | 5.0 | | 3.0 – 8.0 | | 5.0 - 7.0 | |
| Management | Number of plants per hectare | 50,000 – 100,000 | 40,000 – 80,000 (optimal 40000-55000) | 250,000 – 450,000 | 240,000 – 350,000 (optimal 300000-320000) | 300,000 – 1,500,000 | 800,000 – 1,200,000 | 60,000 – 150,000 | 80,000 +/- 25% |
| Management | Time from sowing to emergence (transplanting to recover for rice) (growing degree day) | 60 – 100 | | 150 – 300 | | 35 – 100 | | 10-80 | |
| Conservative | Canopy growth coefficient (fraction per growing degree day) | 0.012 – 0.013 | | 0.004- 0.005 | | 0.006 – 0.008 | | 0.006 – 0.008 | |
| Management | Maximum canopy cover (%) | 65 – 99 % | | ~100% | | ~100% | | ~100% | |
| Cultivar | Time from sowing (transplanting for rice) to start senescence (growing degree day) | Time to emergence + 1150 – 1500 | Time to emergence + 780 – 860 | Time to emergence + 1600 – 2400 | | Time to recover + 1000 – 1500 | | Time to emergence + 1000 – 1800 | |
| Conservative | Canopy decline coefficient (fraction per growing degree day) | 0.010 | | 0.015 | | 0.005 | | 0.002 - 0.003 | |
| Cultivar | Time from sowing (transplanting for rice) to maturity, i.e. length of crop cycle (growing degree day) | Time to emergence + 1450 – 1850 | | Time to emergence + 2000 – 3000 | | Time to recover + 1500 – 2000 | | Time to emergence + 1200 - 2000 | |
| | **1.3 Flowering** | | | | | | | | |
| Cultivar | Time from sowing (transplanting for rice) to flowering (growing degree day) | Time to emergence + 600 - 900 | | Time to emergence + 1000 – 1500 | | Time to recover + 1000 – 1300 | | Time to emergence + 450 - 700 | |
| Cultivar | Length of the flowering stage (growing degree day) | 150 - 200 | | 400 - 800 | | 300 - 400 | | 450 - 750 | |
| Conservative | Crop determinacy linked with flowering | Yes | | Yes | | Yes | | No | |
| | **1.4 Development of root zone** | | | | | | | | |
| Management | Minimum effective rooting depth (m) | 0.30 | | 0.30 | | 0.30 | | 0.30 | |

| Category | Description | | | | | | | |
|---|---|---|---|---|---|---|---|---|
| Management | Maximum effective rooting depth (m) | Up to 2.80 | | Up to 2.40 | | Up to 0.60 | | Up to 2.50 | |
| Conservative | Shape factor describing root zone expansion | 1.3 | | 1.5 | | 2.0 – 3.0 | | 1.5 | |
| **CROP TRANSPIRATION** | | | | | | | | |
| Conservative | Crop coefficient when canopy is complete but prior to senescence | 1.05 | 1.20 | 1.10 | 1.50 | 1.10 | 1.30 | 1.10 | 1.20 |
| Conservative | Decline of crop coefficient (%/day) as a result of ageing, nitrogen deficiency, etc. | 0.30 | | 0.30 | | 0.15 | | 0.30 | |
| Management | Effect of canopy cover on reducing soil evaporation in late season stage | 50 | | 25 | | 50 | | 60 | |
| **BIOMASS PRODUCTION AND YIELD FORMATION** | | | | | | | | |
| | **3.1 Crop water productivity** | | | | | | | |
| Conservative | Water productivity normalized for ETo and CO2 (gram/m2) | 33.7 | | 15.0 | | 19.0 | | 15.0 | |
| Conservative | Water productivity normalized for ETo and CO2 during yield formation (as percent WP* before yield formation) | 100 | | 60 | | 100 | | 70 | |
| | **3.2 Harvest Index** | | | | | | | |
| Cultivar | Reference harvest index (%) | 48 – 52 | | 40 | | 35 – 50 | | 25 – 40 | |
| Conservative | Possible increase (%) of HI due to water stress before flowering | None | | Small | | None | | Small | |
| Conservative | Excess of potential fruits (%) | Small | | Medium | | Large | | Large | |
| Conservative | Coefficient describing positive impact of restricted vegetative growth during yield formation on HI | Small | | None | | Small | | Moderate | |
| Conservative | Coefficient describing negative impact of stomatal closure during yield formation on HI | Strong | | Strong | | Moderate | | Small | |
| Conservative | Allowable maximum increase (%) of specified HI | 15 | | 10 | | 15 | | 30 | |
| **STRESSES** | | | | | | | | |
| | **4.1 Soil water stresses** | | | | | | | |
| Conservative | Soil water depletion threshold for canopy expansion - Upper threshold | 0.14 | | 0.15 | | 0.00 | | 0.20 | |
| Conservative | Soil water depletion threshold for canopy expansion - Lower threshold | 0.72 | | 0.65 | | 0.40 | | 0.70 | |
| Conservative | Shape factor for Water stress coefficient for canopy expansion | 2.9 | | 3.0 | | 3.0 | | 3.0 | |
| Conservative | Soil water depletion threshold for stomatal control - Upper threshold | 0.69 | | 0.50 | | 0.50 | | 0.65 | |
| Conservative | Shape factor for Water stress coefficient for stomatal control | 6.0 | | 3.0 | | 3.0 | | 2.5 | |
| Conservative | Soil water depletion threshold for canopy senescence - Upper threshold | 0.69 | | 0.70 | | 0.55 | | 0.75 | |

| | Parameter | | | | |
|---|---|---|---|---|---|
| Conservative | Shape factor for Water stress coefficient for canopy senescence | 2.7 | 3.0 | 3.0 | 2.5 |
| Conservative | Soil water depletion threshold for failure of pollination - Upper threshold | 0.80 (estimate) | 0.85 (estimate) | 0.75 (estimate) | 0.85 (estimate) |
| Cultivar / Environment | Vol% at anaerobiotic point (with reference to saturation) | Moderately tolerant to water logging | Moderately tolerant to water logging | | Moderately tolerant to water logging |
| **4.2 Air temperature stress** | | | | | |
| Conservative | Minimum air temperature below which pollination starts to fail (cold stress) (°C) | 10.0 (estimate) | 8.0 (estimate) | 8.0 | 15.0 (Estimate) |
| Conservative | Maximum air temperature above which pollination starts to fail (heat stress) (°C) | 40.0 (estimate) | 40.0 (estimate) | 35.0 | 40.0 to 45.0 (Estimate) |
| Conservative | Minimum growing degrees required for full biomass production (°C - day) | 12.0 (estimate) | 10.0 (estimate) | 10.0 (estimate) | Not considered |
| **4.3 Salinity stress** | | | | | |
| Conservative | Electrical conductivity of the saturated soil-paste extract: lower threshold (at which soil salinity stress starts to occur) | 1.7 | 5.0 | 3.0 | 7.7 |
| Conservative | Electrical conductivity of the saturated soil-paste extract: upper threshold (at which soil salinity stress has reached its maximum effect) | 10.0 | 10.0 | 11.3 | 26.9 |

Table C-1 Main parameters for the four crops considered in the analysis. FAO values are the standard values included in the AquaCrop model. Embrapa values are the site specific values that have been replaced to the standard ones.

3. Crop Characteristics:
- **Corn** (http://www.fao.org/nr/water/cropinfo_maize.html http://www.cnpms.embrapa.br/publicacoes/milho_6_ed/index.htm) (EMBRAPA & AGROCONSULT 2010) :
  - o Planting date:
    - First Yield: from September 1$^{st}$ to December 31$^{st}$;
    - Second Yield: from January 1$^{st}$ (or after soybean has been harvested) to February 28$^{th}$;
  - o Life cycle 125 days (FAO) – 120 (EMBRAPA Group II)

|  | Initial | Development | Midseason | Late season | Total |
|---|---|---|---|---|---|
| FAO - Stage (days) | 20 | 35 | 40 | 30 | 125 |
| EMBRAPA – Stage (Group II - days) | 10 | 45 | 40 | 25 | 120 |
| FAO - Root depth (m) | 0.30 | >> | >> | 1.00 | - |
| FAO - Crop coefficient (Kc) | 0.30 | >> | 1.20 | 0.5 | - |
| EMBRAPA - Crop coefficient (Kc) | 0.40 | 0.5 -> 0.8 | 1.20 | 0.8 -> 0.6 | - |
| FAO - Yield Response Factor (Ky) | 0.40 | 0.40 | 1.30 | 0.50 | 1.25 |

**Table C-2 Crop characteristics: Corn. FAO vs Embrapa**

- **Soybean** (http://www.fao.org/nr/water/cropinfo_soybean.html http://www.cnpso.embrapa.br/producaosoja/index.htm) (EMBRAPA & AGROCONSULT 2010):
  - o Planting date: from October 1$^{st}$ to December 31$^{st}$;
  - o Life cycle 85 days (FAO) – 125 (EMBRAPA)

|  | Initial | Development | Midseason | Late season | Total |
|---|---|---|---|---|---|
| FAO - Stage (days) | 15 | 15 | 40 | 15 | 85 |
| EMBRAPA – Stage (Group II - days) | 15 | 35 | 45 | 30 | 125 |
| FAO - Root depth (m) | 0.3 | >> | >> | 1.0 | - |
| FAO - Crop coefficient (Kc) | 0.5 | >> | 1.15 | 0.5 | - |
| EMBRAPA - Crop coefficient (Kc) | 0.4 -> 0.6 | 0.7 -> 1.0 | 1.2 -> 1.5 | 1.2 - > 0.8 | - |
| FAO - Yield Response Factor (Ky) | 0.2 | 0.8 | - | 1.0 | 0.85 |

**Table C-3 Crop characteristics: Soybean. FAO vs Embrapa**

- **Rice**
  ([http://sistemasdeproducao.cnptia.embrapa.br/FontesHTML/Arroz/ArrozTerrasAltasMatoGro](http://sistemasdeproducao.cnptia.embrapa.br/FontesHTML/Arroz/ArrozTerrasAltasMatoGro)
  [sso/pragas_metodos_controle.htm](http://sistemasdeproducao.cnptia.embrapa.br/FontesHTML/Arroz/ArrozTerrasAltasMatoGrosso/pragas_metodos_controle.htm))
  ([http://sistemasdeproducao.cnptia.embrapa.br/FontesHTML/Arroz/ArrozTerrasAltas/index.ht](http://sistemasdeproducao.cnptia.embrapa.br/FontesHTML/Arroz/ArrozTerrasAltas/index.ht)
  [m](http://sistemasdeproducao.cnptia.embrapa.br/FontesHTML/Arroz/ArrozTerrasAltas/index.htm)) (CROPWAT) (EMBRAPA & AGROCONSULT 2010):
  - o Transplanting date: from October $1^{st}$ (Mainly concentrated in November and December) to January $31^{st}$;
  - o Life cycle 150 days (30 nursery + 120 in the field) FAO – 120 (EMBRAPA)

| | Nursery | Initial | Development | Midseason | Late season | Total |
|---|---|---|---|---|---|---|
| FAO - Stage (days) | 30 | 20 | 30 | 40 | 30 | 150 (120) |
| EMBRAPA – Stage (Group II - days) | 15 | 45 | 35 | 25 | | 120 |
| FAO - Root depth (m) | | | | | | |
| FAO - Crop coefficient (Kc) | 1.05 | >> | 1.2 | 0.9 (0.6 dry) | - | |
| EMBRAPA - Crop coefficient (Kc) | 0.4 -> 0.6 | 0.8 -> 1.3 | 1.30 | 1.20 -> 0.6 | | |
| FAO - Yield Response Factor (Ky) | 1.0 | 1.09 | 1.32 | 0.50 | 1.10 | |

Table C-4 Crop characteristics: Rice. FAO vs Embrapa

- **Cotton** (http://www.fao.org/nr/water/cropinfo_cotton.html)
  (http://sistemasdeproducao.cnptia.embrapa.br/FontesHTML/Algodao/AlgodaoCerrado/)
  (EMBRAPA & AGROCONSULT 2010):
  - o Planting date: from December $1^{st}$ to January $31^{st}$;
  - o Life cycle 180 - 225 days (FAO) – 160 (EMBRAPA)

| | Initial | Development | Midseason | Late season | Total |
|---|---|---|---|---|---|
| FAO - Stage (days) | 30 | 50 | 55 | 45 | 180 |
| EMBRAPA – Stage (Group II - days) | 15 | 50 | 65 | 30 | 160 |
| FAO - Root depth (m) | 0.3 | >> | >> | 1.4 | - |
| FAO - Crop coefficient (Kc) | 0.35 | >> | 1.15-1.20 | 0.7-0.5 | - |
| EMBRAPA - Crop coefficient (Kc) | 0.3 -> 0.4 | 0.4 -> 1.10 | 1.20 | 1 - > 0.4 | - |
| FAO - Yield Response Factor (Ky) | 0.2 | 0.5 | - | 0.25 | 0.85 |

Table C-5 Crop characteristics: Cotton. FAO vs Embrapa